THE UNIVERSITY OF CHICAGO

FUNCTIONS OF BNIP3 IN NUTRIENT STRESS RESPONSES

A DISSERTATION SUBMITTED TO

THE FACULTY OF THE DIVISION OF THE BIOLOGICAL SCIENCES

AND THE PRITZKER SCHOOL OF MEDICINE

IN CANDIDACY FOR THE DEGREE OF

DOCTOR OF PHILOSOPHY

COMMITTEE ON CANCER BIOLOGY

BY

MAYA ZAFRIR SPRINGER

CHICAGO, ILLINOIS

DECEMBER 2019

TABLE OF CONTENTS

LIST OF FIGURES

LIST OF TABLES

ABBREVIATIONS

3-PG	3-Phosphoglycerate
AAR	Amino acid response
ASNS	Asparagine synthetase
AMPK	AMP-activated kinase
ATF4	Activating transcription factor-4
ATFS-1	Activating transcription factor associated with stress 1
ATG	Autophagy-related genes
BafA1	BafilomycinA1
BNIP3	BCL2/adenovirus E1B 19 kDa protein-interacting protein 3
BZIP	Basic leucine zipper
CRC	Colorectal cancer
CREB	cAMP response element-binding protein
CTH	cystathionine γ-yase
DCIS	Ductal carcinoma *in situ*
DFS	Disease-free survival
ECM	Extracellular matrix
EIF2α	Eukaryotic initiation factor 2-α
GCN2	General control non-derepressible 2
GEMM	Genetically engineered mouse model
HCC	Hepatocellular carcinoma
HIF1α	hypoxia-inducible factor-1 alpha
LC3	Microtubule-associated protein 1 light chain 3
LIR	LC3-interacting region
MTHFD2	Methylenetetrahydrofolate dehydrogenase (NADP+ dependent) 2
mTORC1	Mammalian target of rapamycin complex 1
NEAA	Non-essential amino acid
NSCLC	Non-small-cell lung cancer
OMM	Outer mitochondrial membrane
PanIN	Pancreatic intraepithelial neoplasia
PDAC	Pancreatic ductal adenocarcinoma
PE	Phosphoethanolamine
PHGDH	Phosphoglycerate dehydrogenase
PI3K	Phosphoinositol-3-kinase
PINK1	PTEN-induced putative kinase 1
PKM2	Pyruvate kinase isoenzyme type-M2
PSAT1	Phosphoserine aminotransferase 1
PSPH	Phosphoserine phosphatase
ROS	Reactive oxygen species
SHMT2	Hydroxymethyltransferase 2
TCA	Tricarboxylic acid cycle
TNBC	Triple-negative breast cancer

ACKNOWLEDGEMENTS

I would like to thank my advisor, Kay Macleod, for her support as my mentor for the past 6 years. My first interactions with Kay were in the lectures that she taught in my first year, where she welcomed my incessant questions about cancer with extremely detailed answers. In the laboratory, Kay has taught me the art of forming and testing hypotheses, with the ultimate goal of leading me to think independently, and confidently. In addition to extending her wealth of technical knowledge and resources to aid in my education and development as a scientist, Kay has been a source of motivation for me as I have encountered the inevitable ups and downs of research. No matter how despondent I became over an experimental result or difficulty, she was always at the ready, combatting my pessimism with encouraging words and the wise reminder that doing the work of science is hard, but worth it. Kay's pep talks have always helped to refocus my energy and reminded me that I am capable of seeing this through to the end.

The members of my thesis committee, Lev Becker, Geof Greene, and Mark Lingen, deserve many thanks for supporting me over the years. My project has seen some significant changes since it was first proposed, and they have been excellent sources of advice, criticisms, and encouragement throughout the process. Their congeniality and expertise made my committee meetings occasions to look forward to, where I could discuss my work with ease rather than anxiety. I thank them for always reminding me to see the big picture and keeping my eyes on the prize.

I would like to thank the core facilities at the University for their indispensible services, including those individuals who work at the DNA Sequencing Core, Light Microscopy Core, Human Tissue Resources Center, Biophysics Core, and Animal Resources Center. Without these resources and experts, much of my research would not have been possible—or would have been significantly more difficult to conduct.

The nature of research has meant that the lab has become my second home, and I am lucky to have shared this space with great labmates and friends. I joined the lab at a time when

solely women occupied it and it was truly an empowering, supportive environment. Lauren, Erin, Aparajita, Michelle, and Marina were a wonderful support system and we all managed to keep each other sane during work and after-hours or over coffee. Later, others joined the lab and more lifelong friends were made. Logan, Alex, Ivan, and Andy have become great friends, always sharing silly memes and moments, laughing, venting and commiserating with each other. Grazyna, our wonderful lab manager, joined our lab at perhaps the most stressful time in my graduate career and helped me immensely; she works tirelessly to make sure the lab runs smoothly, always with a sunny, supportive attitude.

My parents have always valued and supported my education from elementary school through graduate school. I am forever grateful to them for always supporting me in my academic pursuits, especially when it meant that I may not be at every family function or too distracted, stressed, or busy to chat on the phone. They have never once questioned my decision to go to graduate school. My siblings have likewise been sources of encouragement and strength, including my scientist big sister. I look forward to being able to spend more time with my nieces and nephews before they all grow up and are too cool for their nerdy aunt. My mother- and father-in-law deserve many thanks for their love and patience during this journey.

I am in gratitude to my best friend of 26 years, Lamise, who has borne witness to my interest in cancer research since we lost her mother to this disease during middle school. During the past 6 years, Lamise has been an inspiration to me, herself getting a PhD, getting married, and giving birth to and raising an extraordinary boy. Her rock-star Super-Doctor-Mom status has helped me realize what I myself am capable of and reminded me why I got into this field in the first place. I'm grateful to Lamise for always reminding me to breathe, planning de-stressing best friend activities at the spa, and letting me build nearly all of her IKEA furniture when I needed a win outside of the lab. Lamise is like my sister, and while I didn't end up curing cancer (yet), I hope I have made her proud.

Most of all, I thank David, my partner of 14 years, who has been there for me from the very beginning of this PhD. David has been my biggest cheerleader and support system, consistently believing in me when I didn't believe in myself. With him by my side, I learned how to persevere. With no questions asked, he has always brought a fresh perspective to me. He has listened to my presentations, let me blather on about exciting data, and allowed me to mourn appropriately when experiments failed, projects ended, and my research evolved. Together with our absolute angel of a dog, Lulu, David and his expert-level support skills have always been at the ready for me for the past 6 years—bringing me comfort, cuddles, and calm. David has centered me during an otherwise volatile stage of our lives. I truly would not have been able to make it through the trials and tribulations of grad school without a partner like him.

ABSTRACT

BNIP3 is a mitophagy receptor that targets mitochondria for degradation at the autophagolysosome. By mediating mitophagy, BNIP3 functions to decrease mitochondrial mass as an adaptive response to stress, namely hypoxia and nutrient starvation. This catabolic mechanism prevents the accumulation of damaging reactive oxygen species that are normally generated during mitochondrial respiration, thus functioning to maintain a healthy pool of mitochondria under nutrient stress. Evidence in the field has indicated a prognostic role for BNIP3 in hematological malignancies and cancers of the pancreas, breast, liver, colon, and stomach, with epigenetic silencing or deletion of BNIP3 observed in progression to invasive carcinoma. Importantly, loss of BNIP3 is associated with higher tumor grade, poor prognosis, and resistance to chemotherapy. Findings from our laboratory also support a tumor suppressor function for BNIP3 in mouse models of breast cancer, pancreatic ductal adenocarcinoma, and hepatocellular carcinoma. Work from our laboratory has also established a critical housekeeping function for BNIP3 in normal liver physiology and during fasting, with implications for systemic metabolism under nutrient deprivation. In addition to maintaining the integrity of the mitochondria in hepatocytes, BNIP3 also mediates downstream effects on oxygen consumption, gluconeogenesis, and lipid metabolism. The critical functions of BNIP3 in stress responses of the liver have implications for metabolic diseases, such as obesity, diabetes, steatohepatitis, and cancer.

The work in this thesis expands our understanding of how BNIP3 impacts cellular metabolism during nutrient stress to maintain mitochondrial integrity and energetic homeostasis, with implications for normal physiology and cancer. We describe a previously unknown function for BNIP3 in suppressing the nuclear transcription factor ATF4, the master regulator of the amino acid biosynthesis response, in response to nutrient starvation in the murine liver and human hepatocellular carcinoma cells. We demonstrate that this requires the mitochondrial

localization of ATF4 that is dependent on BNIP3, which functions to limit ATF4 nuclear localization and downstream transcriptional activities. Furthermore, this mechanism involves the tri-molecular interaction of ATF4, BNIP3, and LC3 at mitophagosomes and the turnover of ATF4 by mitophagy. Our studies reveal that this novel interaction bears functional consequences for mitophagy, mitochondrial stress responses, cellular metabolism, and cell growth. Together, these results establish an integral role for BNIP3 in regulating the amino acid stress response through a novel mitochondrial function for ATF4.

CHAPTER 1

INTRODUCTION

Autophagy and mitophagy: mediators of cellular homeostasis and stress responses

Macroautophagy, hereafter referred to as autophagy, is an evolutionarily conserved catabolic mechanism by which damaged or dysfunctional organelles, protein aggregates, and other cytoplasmic components are sequestered, degraded in the lysosome, and recycled.[1] In addition to maintaining basal cellular integrity, autophagy is upregulated during conditions of cellular stress, such as nutrient deprivation, hypoxia, oxidative stress, pathogenic infection, and cancer. [1] Over the past three decades, research in the field of autophagy has revealed a tightly regulated mechanism involving a relationship between nutrient-sensing proteins and many additional components that comprise the autophagic machinery (Figure 1.1). A group of over 30 highly conserved autophagy-related genes (Atgs) are essential for proper autophagic function.[2] Knocking out essential Atgs, such as Atg7 or Atg5, abrogates starvation-induced autophagy and results in the death of mouse neonates within one day of birth.[3,4] The nutrient- and stress-sensing kinases AMP-activated kinase (AMPK) and mammalian target of rapamycin complex 1 (mTORC1) can exert positive or negative regulation of the autophagy pathway.[1] Conditions of amino acid and growth factor starvation can inactivate mTORC1, which normally represses the autophagy pre-initiation ULK1/2 complex.[5] Similarly, low ATP/glucose deprivation drives activation of AMPK, which induces autophagy through stimulatory phosphorylation of the preinitiation complex.[5] The ULK1/2 complex goes on to activate the Class III phosphoinositol-3-kinase (PI3K) initiation complex composed of Beclin1, Vps34, and Atg14L.[6] This is followed by the formation of an isolation membrane, termed the phagophore.

Cargo that is to be degraded, such as aggregated proteins or dysfunctional organelles, are recruited to the phagophore, which elongates to form a double-membrane vesicle termed the autophagosome.[1] Two ubiquitin-like conjugation systems are essential for the recruitment

and lipid-conjugation of the adaptor protein, microtubule-associated proteins 1A/1B light chain 3B (LC3), to the autophagosome membrane, as well as overall autophagosome formation.[1] The first conjugation reaction involves activation of Atg12 by Atg7, which is transferred to Atg10, and finally conjugated to Atg5. Eventually, a tri-molecular complex is formed with Atg16L, forming the Atg5-Atg12-Atg16L complex.[1,7] This complex is required for the second conjugation reaction involving LC3, which undergoes covalent attachment to phosphatidylethanolamine (PE); this conjugated form is termed LC3-II.[7] LC3-II integrates into the inner and outer membrane surface of the developing autophagosome in addition to recruiting cargo.[8,9] Eventually, the mature autophagosome fuses with the lysosome, where the sequestered cargo is degraded by acidic lysosomal hydrolases. The degraded byproducts include amino acids, sugars, nucleotides, and fatty acids, which are released into the cytoplasm for future biosynthetic reactions and/or catabolized for energy production (Figure 1.1).[10] Autophagy can be experimentally inhibited by addition of BafilomycinA1 (BafA1), which prevents lysosomal acidification and blocks fusion of autophagosomes with lysosomes, and also allows for experimental assessment of autophagic flux.[11]

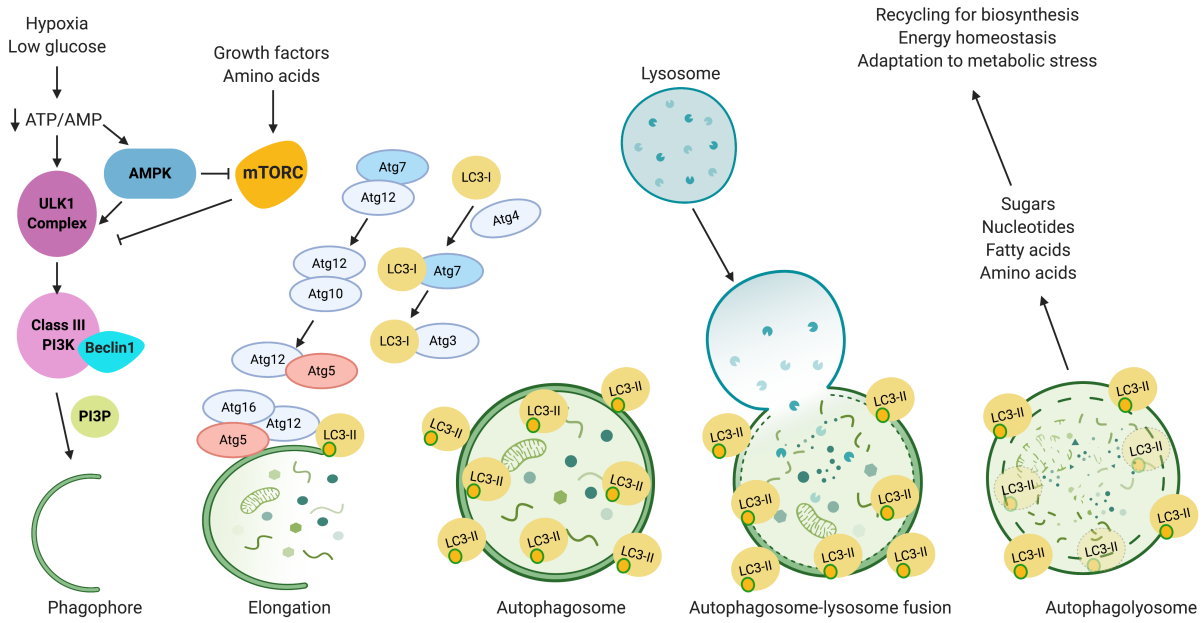

Figure 1.1 Autophagy: a tightly regulated catabolic mechanism. When nutrients are abundant, mTORC inhibits autophagy. Autophagy is induced under nutrient stress, such as depletion of amino acids or growth factors, or by hypoxia or low glucose, which stimulates AMPK and inhibits mTORC activity. Stimulation of AMPK results in activation of the ULK1 complex, which activates the Class III PI3K/Beclin1 complex, which generates PI3P and results in the formation of the phagophore isolation membrane. Elongation of the phagophore is mediated by two conjugation reactions. The first reaction results in formation of the Atg5-Atg12-Atg16 complex, which goes on to complete the second reaction involving conjugation of LC3-I to PE, forming LC3-II. LC3-II decorates the phagophore membrane and aids in closure of the autophagosome around cargo that is to be degraded. The autophagosome fuses with the lysosome, forming the autophagolysosome, which goes on to degrade the sequestered cargo through the catalytic activity of lysosomal hydrolases. The degraded byproducts include amino acids, sugars, nucleotides, and fatty acids, which are released into the cytoplasm for future biosynthetic reactions and/or catabolized for energy production.

Autophagy has emerged as a crucial factor in cancer development. Autophagy functions in coping with cellular stressors common to oncogenic transformation and tumor progression, such as oxidative stress, metabolic stress/nutrient deprivation, and hypoxia.[12] Given the dynamic process of tumorigenesis, autophagy plays a context-dependent role in cancer, switching from tumor-suppressor in early stages to tumor- and metastasis-promoter as cancers progress.[12,13] For example, autophagy increases in response to oxidative stress, limiting genomic instability and suppressing transformation.[14] Beclin1, which is frequently monoallelically deleted in human breast and ovarian cancers, functions as a haploinsufficient tumor suppressor by inducing autophagy to limit metabolic and genotoxic stress and Beclin1$^{+/-}$ mice have a high incidence of spontaneous tumors.[15–17] Similarly, mice with liver-specific deletion of essential autophagy genes *Atg5* or *Atg7* develop benign hepatomas.[18] In early tumors, autophagy limits pro-inflammatory (and therefore pro-tumorigenic) necrosis in metabolically-stressed tumor cells that are otherwise deficient in apoptotic function.[13]

While autophagy serves a tumor-suppressive function during transformation and tumor initiation, it is tumor-promoting at later stages of cancer. During tumor invasion, autophagy enables cells to survive detachment from the extracellular matrix (ECM), thereby evading anoikis and likely fueling metastatic dissemination.[19] In a study from our laboratory, autophagy was not required for primary tumor growth in the 4T1 orthotopic model of murine breast cancer, but was required for promoting metastasis through focal adhesion disassembly by targeted degradation of paxillin.[20] As a tumor progresses and encounters increasing intrinsic and microenvironmental stressors, such as hypoxia, autophagy upregulation enables tumor cells to cope by recycling nutrients, such as amino acids, and maintaining energy balance.[21]

Observations in several genetically engineered mouse models (GEMMS) of cancer support a role for autophagy in promoting tumorigenesis.[21] In KRAS^{G12D}-driven lung tumors, deletion of Atg7 prevented progression to carcinoma, and mice instead developed benign oncocytomas characterized by an accumulation of abnormal mitochondria.[22] Similar results

were observed in Atg7$^{-/-}$-BRAF^{V600E}-driven lung-tumors, with tumor-derived cell lines exhibiting impaired mitochondrial respiration and an inability to cope with nutrient starvation compared to those derived from autophagy-competent tumors.[23] Other studies in pancreatic ductal adenocarcinoma (PDAC) have supported this tumor-promoting function of autophagy through maintenance of mitochondrial function and metabolism.[24–26]

It is difficult to determine what aspect of autophagy is required for driving tumor growth, as the majority of studies have examined general autophagy inhibition through targeting of essential Atgs. In recent years, autophagy has become an attractive therapeutic target in cancer.[27] In addition to drugs that directly inhibit autophagy, such as the lysosomal inhibitor hydroxychloroquine, many commonly used chemotherapeutic agents also induce autophagy downstream of their primary mechanism of action. In order to achieve better clinical outcomes, further mechanistic and *in vivo* studies are required to fully elucidate the role of autophagy in tumorigenesis. Given the wealth of evidence that proper mitochondrial functioning is critical to sustaining tumor growth in the context of autophagy, and the observations indicating that dysfunctional mitochondria accumulate in many of these models, increasing studies in cancer are examining the role of mitophagy, a more selective form of autophagy.[28,29]

Mitochondria are highly active and multifaceted organelles, contributing to the generation of intracellular ATP through oxidative phosphorylation, fatty acid oxidation, and the tricarboxylic acid (TCA) cycle, and additional functioning in calcium homeostasis, apoptosis, and biosynthesis of macromolecules.[30] As such, mitochondrial activities can lead to the excessive production of reactive oxygen species (ROS) and oxidative damage to mitochondrial proteins and mtDNA. Such mitochondrial dysfunction can eventually lead to mitochondrial depolarization, which if unchecked, may result in dwindling ATP stores, accumulation of ROS, loss of mitochondrial membrane polarization, and cell death.[31] Mitophagy is a selective form of autophagy by which mitochondria are targeted for degradation at the autophagolysosome. This process plays a critical role in cellular homeostasis through the elimination of dysfunctional

mitochondria, and the reduction of mitochondrial mass as an adaptive response to oxidative and nutrient stress.[8] While this mechanism utilizes the general autophagy machinery, mitophagy also requires the interaction of specific mitochondrial adaptor molecules, or receptors, with LC3-II on the phagophore membrane. There are multiple mechanisms by which mitochondria are targeted for degradation at the autophagosome but the most well-studied pathways are PINK1/Parkin-induced mitophagy and the BNIP3/ NIX- and FUNDC1-dependent pathways.[32,33]

The PINK1/Parkin pathway specifically functions to eliminate depolarized mitochondria and maintain mitochondrial and cellular integrity.[33] Following loss of mitochondrial membrane potential, PINK1 (PTEN-induced putative kinase-1), a serine/threonine kinase, accumulates at the outer mitochondrial membrane (OMM), where it phosphorylates ubiquitin on mitochondrial proteins to recruit autophagy cargo adaptors that bind directly to LC3 at the autophagosome.[33] PINK1 also recruits and phosphorylates the cytosolic E3 ubiquitin ligase Parkin, which conjugates ubiquitin chains to specific substrates at the OMM, including VDAC, Miro, and mitofusin-2, which are further phosphorylated by PINK1 to amplify the signal to induce mitphagy.[33,34] Both PINK1 and Parkin are necessary for the recruitment of cargo adaptors such as OPTN, NDP52, and p62/Sqstm1, which have LC3-interacting region (LIR) motifs that interact with processed LC3 (LC3-II) at nascent phagophores, thereby specifically targeting depolarized mitochondria for degradation at the lysosome.[33]

BNIP3: a stress-induced mitophagy receptor

BCL2/Adenovirus E1B 19kDa Interacting Protein 3 (BNIP3) is a stress-induced mitophagy receptor that, unlike PINK1/Parkin, does not require membrane depolarization to target mitochondria to the autophagosome for degradation. NIX (also known as BNIP3L) is a structurally related mitophagy receptor that is also upregulated in response to stress and developmental signals, namely red blood cell maturation.[35] BNIP3 (and NIX) was originally reported to be a member of the BH3-only family of pro-apoptotic proteins, involved in

programmed cell death.[36,37] However, the BH3 domain is poorly conserved and redundant for function, and BNIP3 is expressed at high levels in normal tissues such as the heart, muscle, and liver, in the absence of cell death.[38–40] As part of its discovery in a yeast-two hybrid study, BNIP3 was found to heterodimerize with Bcl2- and later, Bcl-X_L, which occurs through an interaction with the first 49 amino acids at the N-terminus.[41–43]Additionally, BNIP3 interacts with Opa1, a regulator of mitochondrial fusion and cristae structure, to promote mitochondrial fragmentation that precedes apoptosis.[44] Through its C-terminal transmembrane domain (TMD), BNIP3 forms a detergent-resistant homodimer that integrates into the outer mitochondrial membrane (OMM), with only ten amino acids extending into the intermembrane space (Figure 1.2A).[39,45] In addition to dimerization, the TMD is required for mitochondrial localization of BNIP3.[42] The cytosolic amino terminus of BNIP3 possesses a highly conserved LIR motif that is required for binding to LC3-II at nascent phagophores (Figure 1.2B). Mutation of a critical tryptophan residue in the LIR motif (W18A) specifically abrogates the interaction of BNIP3 and LC3, preventing mitophagy.[46] Phosphorylation of key serine/threonine residues near the LIR motif can modulate the interaction with LC3 through an as-yet unknown mechanism.[47]

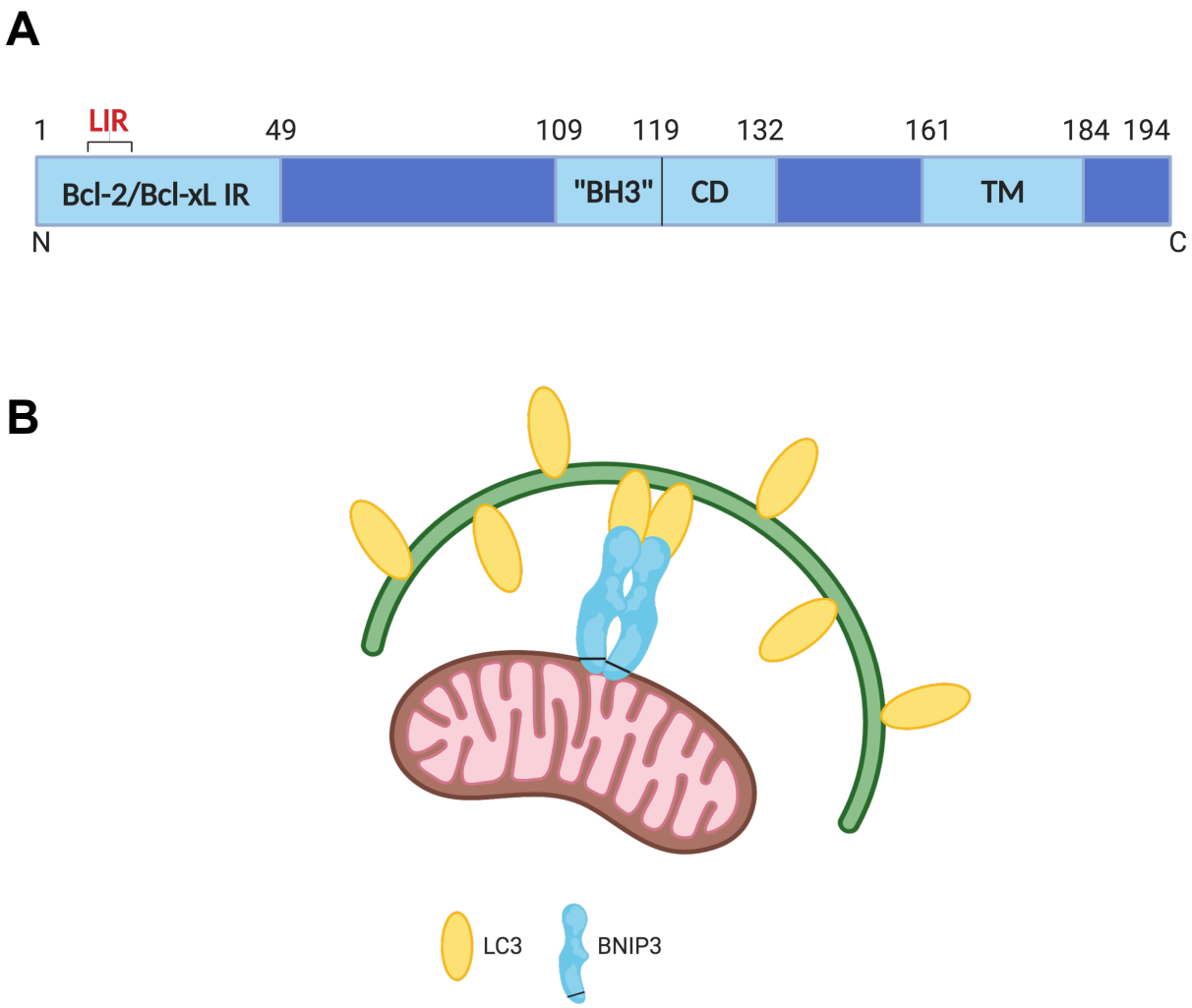

Figure 1.2: BNIP3 mediates mitophagy through binding of LC3. A) Schematic of the functional domains in BNIP3 B) BNIP3 integrates as a dimer into the outer mitochondrial membrane (OMM) through its C-terminal transmembrane domain. It interacts with LC3 on nascent phagophores via an LC3-interacting region (LIR) motif at its cytosolic N-terminus.

Unlike Parkin/PINK1-mediated mitophagy, which specifically targets depolarized mitochondria, BNIP3-mediated mitophagy functions primarily during conditions of hypoxia and nutrient stress, thereby reducing mitochondrial mass as an adaptive response. Hypoxia is a key energy stressor that induces BNIP3 transcriptional upregulation, as BNIP3 is a direct target of hypoxia-inducible factor-1 alpha (HIF1α.)[48] BNIP3 is also transcriptionally regulated by other stress-related proteins that are frequently deregulated in cancer, including Rb/E2F, NF-κB, FoxO3, PPARα, oncogenic Ras, GR, and p53.[49–55] Early work from our laboratory identified BNIP3 as a target of pRb/E2F-mediated transcriptional repression that functions to inhibit hypoxia-induced autophagic cell death in mouse embryonic fibroblasts, mouse fetal liver, and tumor cell lines.[49] A subsequent study from our laboratory also indicated that BNIP3 is superinduced by starvation in the murine liver; this finding and its functional significance will be expanded upon later in this chapter.[38] Hypoxia and nutrient deprivation are microenvironmental cues prominently featured in metabolic tissues as well as tumors. Therefore, altered BNIP3 levels and subsequent mitophagy are crucial factors in the normal physiology of metabolic tissues and in numerous human cancers.[28,34,38,49, 56]

Autophagy, mitophagy, and mitochondrial function in the liver

The liver is the central metabolic organ regulating systemic metabolism and energy homeostasis, controlling levels of glucose, lipid, and amino acids via tightly regulated signaling pathways.[57] As such, metabolic disorders including fatty liver disease and steatohepatitis, diabetes, and obesity exhibit dysfunction of autophagy in the liver.[58] Given the liver's nutrient-sensitive status and high metabolic demands, both autophagy and mitophagy play critical roles in its response to starvation and maintenance of mitochondrial function. Indeed, the liver is the principal site of starvation-induced autophagy in adult organisms.[59] During the first 4-6 hours of starvation, mTOR is inactivated and autophagy is induced, whereby hepatic protein is degraded to generate amino acids that may then feed into the TCA cycle to generate ATP and maintain

energetic homeostasis.[31] In mice, it was shown that during starvation, the autophagic degradation of liver proteins to amino acids contributes to blood glucose regulation through conversion of amino acids to glucose via gluconeogenesis.[59] In addition to protein catabolism, other forms of autophagic degradation are activated in response to nutrient deprivation. The liver is able to generate glucose from intracellular glycogen stores through glycophagy, another selective form of autophagy.[31] Through an additional selective form of autophagy, termed lipophagy, triglycerides stored in lipid droplets are degraded to generate free fatty acids, (FFA), which may then go on to generate energy via fatty acid oxidation in the mitochondria.[60,61]

The liver is a mitochondria-rich organ responsible for maintaining organismal energy homeostasis, and as such, the maintenance of mitochondrial quality and number is paramount to sustained metabolic capacity. Mitophagy plays a particularly important housekeeping function in the liver, as well as in the response to starvation. Defects in hepatic mitophagy may play a role in the development of mitochondrial dysfunction and metabolic disorders such as obesity, hepatic steatosis, and diabetes.[31,58,61] However, it is unclear to what extent these defects are a result of or are causal factors participating in the etiology of these disorders.

Much of the work from our laboratory has focused on the role of BNIP3-mediated mitophagy in the mouse liver and its implications for metabolic diseases and cancer.[38] Our initial work showed that BNip3 is constitutively expressed at markedly higher levels in the murine liver than other tissues, owing in large part to the mitochondria-dense nature of this metabolic organ and indicative of its important housekeeping functions.[38] BNip3 was transcriptionally superinduced in the liver upon fasting in wild-type mice and functioned to maintain mitochondrial integrity and efficient metabolism under nutrient stress.[38] In contrast, constitutive whole-body knock-out of BNip3 in mice resulted in defective mitophagy, resulting in the accumulation of dysfunctional mitochondria in hepatocytes.[38] In response to fasting, these mice also exhibited defective gluconeogenesis, and reduced oxygen consumption.[38] Furthermore, BNip3 null livers exhibited lipid accumulation due to increased lipid synthesis and decreased mitochondrial β-

oxidation. This lipid accumulation was observed under normal fed conditions and was drastically elevated upon fasting, indicating that BNip3 plays a broad role in regulating lipid metabolism that is attuned to nutrient supply. Owing to defects in mitophagy and the accumulation of lipid, BNip3 null livers also exhibited increased generation of ROS and inflammation, and developed steatohepatitis.[38] This function of BNip3 in the liver has clinical ramifications for metabolic diseases, namely nonalcoholic steatohepatitis (NASH), the prevalence of which has increased due to the rise in obesity and type 2 diabetes.[62] Furthermore, NASH is a major risk factor for the development of hepatocellular carcinoma (HCC), indicating a role for mitophagy and BNIP3 in the etiology of cancer.[62]

The role of mitophagy and BNIP3 in cancer

Given the plethora of studies linking autophagy to tumor initiation and progression, it is perhaps unsurprising that the more selective process of mitophagy is of relevance to cancer. Maintenance of mitochondrial fitness and homeostasis is critical to efficient energy metabolism and macromolecule biosynthesis in the context of rapidly dividing cancer cells.[30] This is assured through mechanisms acting in concert including mitochondrial proteostasis, fusion and fission, biogenesis, and mitophagy.[63] Key players in mitophagy, including *PARK2* (Parkin), *BNIP3*, and *NIX*, are deleted or epigenetically silenced in various human tumors, largely indicating a tumor suppressor function for mitophagy.[32] *PARK2,* the gene encoding Parkin, maps to a site commonly deleted in breast, lung, ovarian, and bladder cancers.[56] Similarly, *PARK6* (PINK1), expression is downregulated in ovarian cancer and glioblastoma, with loss-of-function mutations also observed in neuroblastoma.[64]

Studies in mice are consistent with a tumor suppressor function for the Parkin/PINK1 pathway. *Parkin*-null mice were shown to develop spontaneous HCC, and were sensitized to ionizing-radiation-induced tumorigenesis through promotion of the Warburg effect.[65,66] Loss of PINK1 or Parkin was shown to promote mutant-*Kras*-driven PDAC in mice, and low *PARK2*

expression was associated with poor prognosis in pancreatic cancer patients.[67] NIX has also been implicated in tumor suppression through induction by p53 under hypoxia.[68] However, a more recent study indicated an oncogenic function for NIX-mediated mitophagy in promoting murine PDAC through driving glycolysis and enhanced redox capacity, with increased NIX expression found to be associated with significantly worse survival in pancreatic cancer patients.[29]

Studies of BNIP3 in cancer indicate that it may function as a tumor suppressor, although some evidence implies a context-dependent tumor-promoting role. Early work examined BNIP3 expression in breast cancer cell lines and in patient tumors.[69–72] In murine breast cancer cell lines, knockdown of BNIP3 expression resulted in increased primary tumor growth and metastasis to the liver, lung, and bone following orthotopic transplantation in mice.[69] One study of patient breast tumors found that cytoplasmic BNIP3 expression was elevated in ductal carcinoma *in situ* (DCIS) and invasive carcinoma relative to normal breast.[70] Nuclear BNIP3 expression was also observed in these tumors; expression in DCIS was associated with increased risk of recurrence and shorter disease-free survival (DFS), while nuclear BNIP3 in invasive tumors was associated with longer DFS and better prognosis. [70] Published work from our laboratory supports a tumor suppressor function for BNip3 in the PyMT murine model of breast cancer, whereby BNip3-mediated mitophagy prevented the accumulation of dysfunctional mitochondria and damaging ROS.[28] In contrast, BNip3 null primary tumors progressed rapidly with metastases to the lung, exhibiting increased mitochondrial mass and excess ROS, which stimulated HIF1α expression and transcription of tumor-promoting genes involved in the Warburg effect and angiogenesis.[28] Furthermore, these findings bore clinical significance, with analysis of patient samples indicating that BNIP3 deletion is predictive of progression to metastasis in triple-negative breast cancer (TNBC) patients.[28]

In other studies, BNIP3 was shown to be epigenetically silenced via hypermethylation of a CpG island in its promoter in hematopoietic cancers as well as several solid tumor types,

including HCC, PDAC, gastric cancer, and colorectal cancer (CRC). [73–78] Treatment of cancer cell lines with the methyltransferase inhibitor 5-aza-2'-deoxycytidine restored expression of BNIP3 and sensitized cells to hypoxia-induced cell death.[74,75,77,79]In PDAC, loss of BNIP3 expression is a late event that occurs upon progression to invasive cancer, and is correlated with poor prognosis and chemoresistance to gemcitabine.[77] An unpublished study from our laboratory supports a tumor suppressor function for BNip3 in the Pdx1-Cre;LSL-$KRAS^{G12D}$ mouse model of PDAC. Loss of BNip3 resulted in significantly reduced overall survival compared to wild-type mice. BNip3 null- Pdx1-Cre;LSL-$KRAS^{G12D}$ mice exhibited markedly accelerated pancreatic intraepithelial neoplasia (PanIN) formation and progression to invasive PDAC, in addition to increased metastasis compared to age-matched BNip3-wild-type mice. In other unpublished work from our laboratory, we have shown that BNip3 suppresses tumor growth in a carcinogen-induced mouse model of HCC, through a mechanism involving suppression of lipogenesis that can be therapeutically targeted by treatment with a fatty acid synthase inhibitor.

A non-mitophagy pro-survival function has also been proposed for BNIP3 in glioma and glioblastoma. One study has shown that overexpression of NLS-tagged BNIP3 in glioblastoma cells results in nuclear translocation and transcriptional repression of TRAIL-induced apoptosis by preventing transcription of death receptor-5 (DR5).[80] Patient glioblastoma tumors also exhibited increased nuclear BNIP3 staining associated with decreased DR5 expression. Another study indicated that BNIP3 may negatively regulate expression of apoptosis-inducing factor (AIF) in gliomas, although the significance of this is unclear as the role of AIF in apoptosis remains controversial.[81,82] Challenging this role as a transcriptional repressor, another group has shown that BNIP3 may impact global transcriptional upregulation by binding to and activating the histone acetyltransferase p300 in cardiomyocytes, but these effects were not assessed in a tumor model or cancer cell lines.[83] It is possible that BNIP3 plays a tumor suppressor role only in certain contexts, tissue types, or tumor stages or may promote growth

through non-mitophagy pathways that remain to be elucidated. BNIP3 is tightly transcriptionally upregulated in response to numerous types of stress and data from our own laboratory also indicates that it is rapidly turned over at the protein level (at the proteasome and through autophagy), a characteristic that is typical of many stress responsive proteins.[84] Understanding other cellular stress response pathways may further reveal novel functions for BNIP3 in physiology and disease.

ATF4: transcriptional master regulator of cellular stress responses

Activating transcription factor-4 (ATF4, also known as CREB2) is a member of the ATF/cAMP responsive element binding protein (CREB) family of basic leucine zipper (bZIP) transcription factors characterized by a common consensus binding site at cAMP responsive elements (CRE).[85] ATF4 functions as a heterodimer with other transcription factors in the ATF/CREB, FOS/JUN, and bZIP protein families.[85,86] ATF4 activity is potently induced in response to intrinsic and extrinsic stressors, including ER stress, oxidative stress, hypoxia, and amino acid deprivation.[85–87] This stress-induced signaling pathway is termed the integrated stress response (ISR) and consists of multiple arms of induction that impinge on activation of eurkaryotic initiation factor 2α (eIF2α), the master regulator of protein translation (Figure 1.3). In response to dietary amino acid depletion, the amino acid response (AAR) pathway is rapidly activated, beginning with the detection of uncharged tRNAs by the general control non-derepressible 2 (GCN2) kinase, which goes on to phosphorylate eIF2α on Ser51.[87] In response to ER stress, oxidative stress, or hypoxia, the activation of eIF2α is mediated by activated protein kinase R (PKR)-like endoplasmic reticulum kinase (PERK).[86] While there are other kinases that may activate eIF2α, the focus of this chapter will be on the PERK and GCN2 arms of the ISR. The phosphorylation of eIF2α goes on to repress global protein translation in order to conserve resources while upregulating the translation of select mRNAs, including ATF4.[88,89]

To cope with acute stress, ATF4 is rapidly upregulated at the translational level and activates expression of adaptive genes to promote cell survival or, under the context of prolonged stress, cell death.[86] As part of the unfolded protein response (UPR) during ER stress, ATF4 induces expression of ER chaperones such as *BiP*, and with the ATF4 binding partner (and transcriptional target) CHOP (also know as DDIT3), also coordinates ER-stress-induced death.[90,91] In response to fasting or ER stress in the liver, ATF4 was shown to upregulate expression of the metabolic regulator and hormone *FGF21.*[92–94] Other ATF4 targets that are induced by the ISR include proteins involved in antioxidant defense and redox balance, such as cystathionine γ-yase (*CTH*) and heme oxygenase-1 (*HO1*).[95–98] In response to prolonged stress, ATF4 was shown to directly induce the expression of genes involved in autophagy, including *ULK1* and *LC3* and indirectly upregulate *ATG5* via the ATF4-target *CHOP*.[99–103] Given the growth-promoting and growth-suppressive effects of autophagy, ATF4 thus plays a context-dependent function in directing cell survival or cell death in response to acute and prolonged stress, respectively. As autophagy itself plays a critical role in the recycling of amino acids, ATF4 effectively coordinates amino acid homeostasis in response to amino acid depletion through direct anabolic and indirect catabolic mechanisms.[102,104]

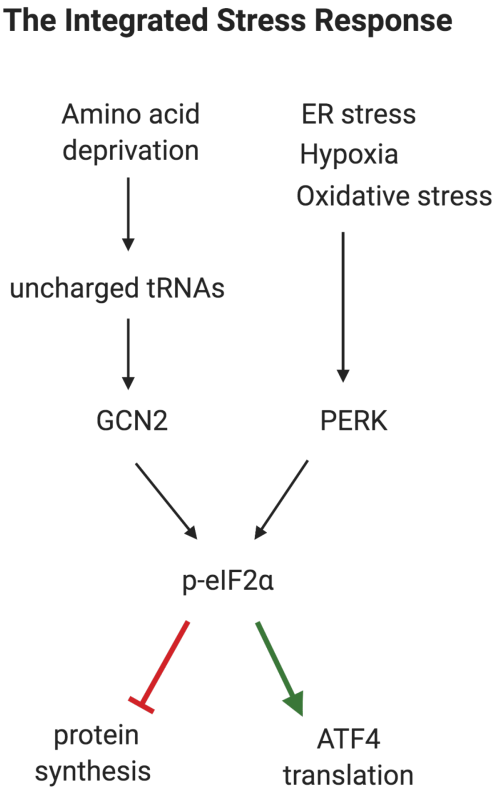

Figure 1.3. The integrated stress response. Schematic depicting the two arms of the integrated stress response (ISR). In response to amino acid deprivation, the accumulation of uncharged tRNAs activates GCN2 kinase. ER stress, hypoxia, and oxidative stress activate PERK. GCN2 or PERK may then phosphorylate eIF2α, which inhibits general protein synthesis while upregulating translation of ATF4, the major effector of the ISR.

The role of ATF4 as a mediator of the AAR is perhaps one of its best-characterized functions. In concert with a number of heterodimerization partners, ATF4 transcriptionally activates an acute, adaptive response via a CCAAT-enhancer binding-protein (C/EBP)-activating transcription factor response element (CARE) that is composed of half sites for C/EBP and ATF family members. [87,105] ATF4 gene targets that are activated as part of the AAR include amino acid transporters and metabolic enzymes involved in the biosynthesis of non-essential amino acids (NEAAs), as well as other transcription factors that may act as heterodimerization partners and/or as counter-regulatory signals for ATF4, including ATF3, CHOP, and C/EBPβ.[87,98,106–108] Genes encoding key amino acid transporters that are activated by ATF4 include cationic amino acid transporter 1 (*CAT1*), system A neutral amino acid transporter 2 (*SNAT2*), and cysteine/glutamate transporter (*xCT,* also known as *SLC7A11*).[87] ATF4 also activates expression of metabolic enzymes involved in the generation of most NEAAs including phosphoserine aminotransferase 1 (PSAT1) and asparagine synthetase (ASNS), which are involved in the biosynthesis of serine and asparagine, respectively.

ASNS is a canonical target of ATF4, and catalyzes the generation of asparagine from aspartate through the amino group donor, glutamine (generating glutamate in the process, and thus also feeding back into the TCA cycle).[109] ASNS is induced by the GCN2- eIF2α-ATF4 pathway in response to amino acid deprivation, and by the PERK- eIF2α-ATF4 pathway following hypoxia or ER stress as part of the UPR.[110] The rapid induction of ASNS by ATF4 has been extensively examined, illustrating the importance of ATF4 in mediating a swift response to stress. Binding to the *ASNS* promoter occurs within 30-45 minutes of amino acid depletion, and remains elevated for 4-6 hours, followed by a decline in ATF4 protein levels. [111] ASNS plays a critical role in tumor progression, and this will be expanded upon later in this chapter.

As part of the stress response to amino acid deprivation, ATF4 upregulates other metabolic enzymes involved in the biosynthesis of serine and glycine.[109,112] The *de novo* serine synthesis pathway begins with the glycolytic intermediate 3-phosphoglycerate (3-PG), which is

converted to serine through a series of enzymatic reactions with phosphoglycerate dehydrogenase (PHGDH), phosphoserine aminotransferase 1 (PSAT1), and phosphoserine phosphatase (PSPH).[113] Serine is an allosteric activator of pyruvate kinase isoenzyme type-M2 (PKM2), and in the absence of exogenous serine, PKM2 activity is significantly reduced to allow for accumulation of glycolytic intermediates (3-PG and NAD^+) that then feed into the serine synthesis pathway downstream of GCN2-ATF4.[113] In addition to its role in protein synthesis, serine is also used in the generation of phospholipids and ceramides, the major components of cell membranes.[114,115] Serine is converted to glycine by hydroxymethyltransferase 2 (SHMT2) in the mitochondria.[113] Glycine is a source of carbon units for one-carbon metabolism, a pathway occurring in the mitochondria that generates numerous intermediates, such as nucleotides and glutathione, and is required for the biosynthesis of the major macromolecules that sustain cell growth and proliferation and maintain redox balance.[113] The genes encoding these four enzymes have been shown to be ATF4 targets in a variety of systems.[112,113,116] Thus, through the action of ATF4 in response to exogenous depletion of amino acids such as serine, the ISR is critical for generating the biosynthetic intermediates required to maintain homeostatic functions (Figure 1.4). ATF4 was also shown to be induced independent of any stress by mTORC1 to drive expression of methylenetetrahydrofolate dehydrogenase (NADP+ dependent) 2 (*MTHFD2)* downstream of serine/glycine synthesis, and was required for *de novo* purine synthesis in normal and cancer cell lines.[117] Recent work has highlighted the importance of ATF4 activity and serine/glycine metabolism in cancer, and will be addressed later in this chapter.

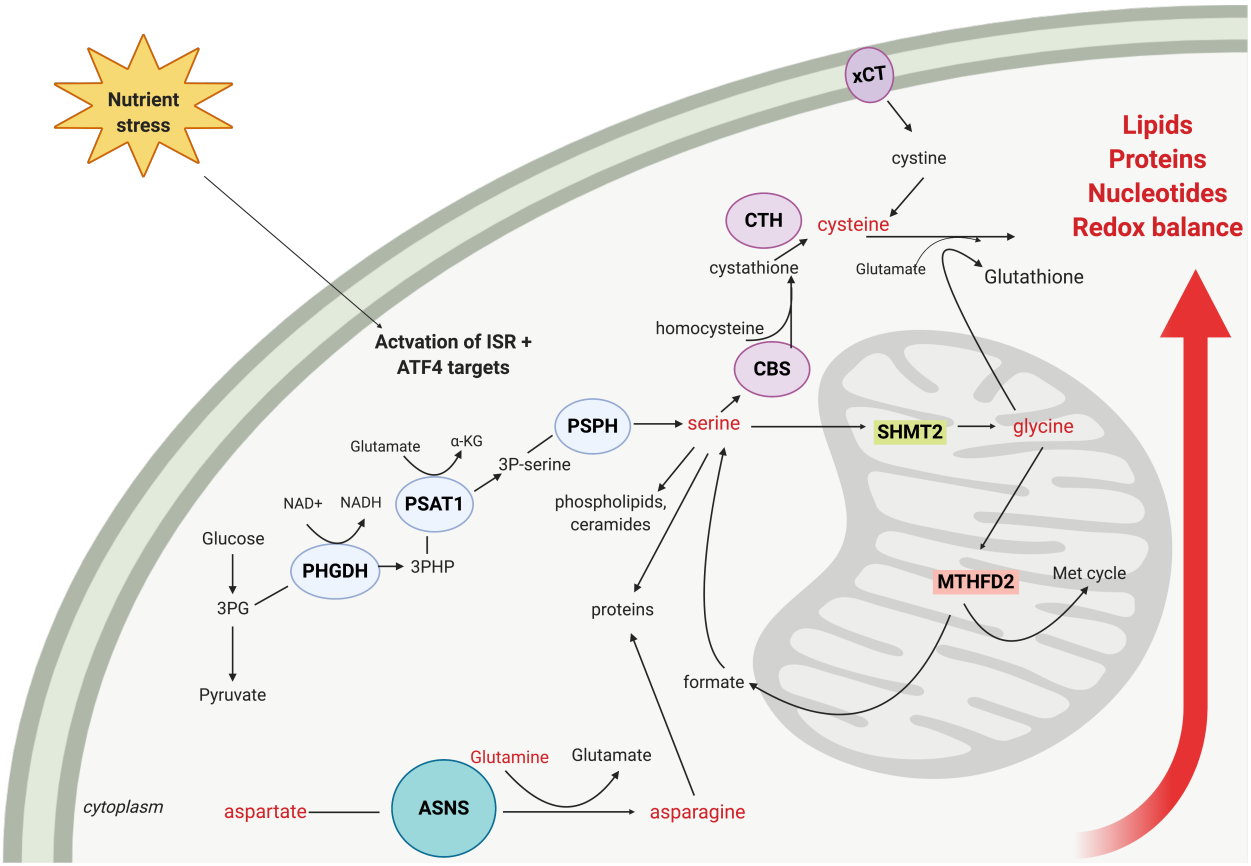

Figure 1.4: The *de novo* serine/glycine synthesis pathway. In response to activation of the ISR, ATF4 is translationally upregulated and activates transcription of PHGDH, PSAT1, PSPH, SHMT2, CBS, CTH, xCT, and MTHFD2. The glycolytic intermediate 3PG is converted to serine through a series of enzymatic reactions with PHGDH, PSAT1, and PSPH. In addition to its role in protein synthesis, serine is also used in the generation of phospholipids and ceramides.. Serine is converted to glycine by SHMT2 in the mitochondria. Through the action of CBS, CTH, and xCT, serine and glycine are also both involved in the synthesis of glutathione. Glycine is a source of carbon units for one-carbon/folate metabolism, a pathway involving MTHFD2 that generates numerous substrates required for the biosynthesis of the major macromolecules (lipids, proteins, and nucleotides) that sustain cell growth and proliferation and maintain redox balance.

Emerging functions for ATF4 in the mitochondrial stress response

As the key organelles responsible for generating energy and metabolic intermediates to sustain organismal homeostasis, proper mitochondrial functioning is important for preventing many diseases. The downstream consequences of mitochondrial stress include loss of mitochondrial membrane integrity and membrane potential, dysfunctional mitophagy, defects in metabolic function, loss of mitochondrial proteostasis and compromised mitochondrial protein translation.[118,119] The collective cytoprotective mechanism that is initiated in response to these mitochondrial insults is characterized by the production of mitochondrial chaperones and proteases and is termed the mitochondrial unfolded protein response (UPR^{mt}), and may also be activated by some of the same stressors that induce the more general ISR, including mitochondrial toxins that inhibit respiratory chain function.[119–121] While first described in mammalian cells as part of the response to mtDNA depletion by exposure to ethidium bromide, the mechanism of the UPR^{mt} has been extensively studied in *C. elegans*.[122,123] As the mitochondrial genome consists of only 13 genes, mitochondria must communicate with the nucleus, which encodes the majority of mitochondrial proteins, to induce signals aimed at coping with mitochondrial stress and restoring proper function.[119] This coupling of mitochondrial dysfunction to nuclear transcription that bears functional consequences for mitochondrial function is called mitonuclear communication, and it is critical for regulating the UPR^{mt}.[119]

Recently, ATF4 has been suggested to function as the mammalian homolog of the bZIP activating transcription factor associated with stress-1 (ATFS-1), which is the principal mediator of the UPR^{mt} in worms.[124,125] ATFS-1 participates in the mitonuclear response to mitochondrial proteotoxic stress by virtue of its nuclear localization sequence and mitochondrial targeting sequence (MTS). Under basal conditions in the absence of stress, ATFS-1 is imported into the mitochondrial matrix, where the MTS is cleaved and the protein is degraded.[126] In response to mitochondrial dysfunction, ATFS-1 instead accumulates in the cytosol and traffics to the nucleus, where it activates a cytoprotective transcriptional response, thus initiating the

UPR^{mt}.[121,126] The mitochondrial import efficiency of ATFS-1 was shown to regulate the extent of its nuclear activity in response to mitochondrial stress.[126] The genes activated by ATFS-1 include mitochondrial chaperones and proteases, ROS-detoxifying enzymes, and mitochondrial import machinery.[121] The proteostatic effects of ATFS-1 also function to limit mitochondrial metabolism by transcriptionally repressing OXPHOS and TCA cycle genes at both nuclear and mitochondrial promoters, while activating glycolysis.[116] Mitochondrial function, the UPR^{mt}, and mitophagy have been shown to be disrupted in aging and neurodegenerative diseases, such as Alzheimer's disease.[127–129] Mitophagy and mitochondrial biogenesis were also recently shown to be coordinately induced during aging in *C. elegans*, and the worm homolog of BNIP3, *dct-1,* was a major mediator promoting lifespan as part of the mitochondrial stress response.[129]

Sorrentino *et al.* recently investigated mitochondrial proteostasis in a worm model of amyloid-β proteotoxicity.[127] In response to amyloid plaque aggregation, *atfs-1* was required for mediating the mitochondrial stress response, including induction of the UPR^{mt} and of mitophagy genes such as *dct-1*.[127] Upon silencing of *atfs-1,* basal and maximal respiration was also reduced, despite compensatory elevation in OXPHOS protein expressions. Genetic or pharmacological induction of the UPR^{mt} also induced mitophagy and respiration genes, reduced plaque aggregation, and resulted in a marked increase in worm health and lifespan.[127] Of note, these positive effects of UPR^{mt} induction were attenuated by silencing of *dct-1*, indicating the importance of mitophagy in the mitochondrial stress response in Alzheimer's disease. NAD$^+$-boosting compounds, such as nicotinamide riboside (NR), have been shown to beneficially induce mitophagy and the UPR^{mt} in a manner involving *atfs-1* and *dct-1* in this system and in other models of neurodegenerative diseases.[127,130]

Recent work indicates that other bZIP proteins, such as ATF4, ATF5, and CHOP, function as mammalian orthologs of ATFS-1 under certain contexts.[119,121,124,125,131,132] ATF4 in particular has several target genes in common with ATFS-1, including *ATF5, CHOP, FGF21, and ASNS,* as part of the ISR.[124,133–135] A recent study has implicated ATF4 in mediating a

mitochondrial stress response in mammalian cells. Using a multi-omics approach in HeLa cervical cancer cells, Quiros and colleagues found that treatment with different mitochondrial stressors promoted mitochondrial proteostasis through the decrease of mitochondrial ribosomal proteins, as well as the activation of the ISR transcriptionally mediated by ATF4.[124] ATF4 upregulated the expression of genes to rewire cellular metabolism, chiefly those involved in amino acid biosynthesis.[124] Of note, key enzymes involved in the serine biosynthesis (*PSAT1, PSPH,* and *PHGDH*), cysteine biosynthesis (*CTH*), and *ASNS* were upregulated at the transcript and protein levels in response to mitochondrial stress.[124] Consistent with these findings, one of the most upregulated metabolites in these cells was serine, while levels of aspartic acid was significantly decreased, consistent with increased conversion to asparagine through *ASNS*.[124] This study provided a critical link between mitochondrial dysfunction and amino acid biosynthesis, mediated by ATF4 in cancer cells.

Another recent study in mammalian cells revealed that mitochondrial dysfunction induced by respiratory chain inhibitors resulted in depletion of mtDNA and induced an ATF4-mediated increase in serine synthesis and transsulfuration.[132] In certain cell types tested, treatment with respiratory chain inhibitors rendered them serine-dependent and inhibited their growth, a phenotype that was reversible with supplementation of 1C metabolites.[132] However, precisely how ATF4 is induced by mitochondrial stress in mammalian cells remains to be elucidated. It is unknown whether BNIP3-mediated mitophagy might interplay with the UPR^{mt} in mammalian cells under nutrient stress, although ATF4 has been shown to induce expression of Parkin in response to ER stress and mitochondrial stress.[136] Elucidating such a mechanism could prove relevant for treating diseases characterized by mitochondrial dysfunction, including metabolic diseases, neurodegenerative disorders, aging, and cancer.

The role of ATF4 in cancer

Much of the recent work examining ATF4 has been performed in cancer cell lines and mouse models. The majority of these studies have established a tumor-promoting role for the transcription factor, although some evidence indicates that ATF4 has a tumor-suppressive function in certain contexts.[137,138] ATF4 is upregulated or overexpressed in mouse and human tumors and cell lines.[139–141] In a study from Ye *et al*., induction of ATF4 was shown to be required for proliferation and survival of tumor cells in the context of nutrient deprivation. [141] Knockdown of ATF4 expression in tumor cell lines induced a cytoprotective autophagic response and apoptosis under NEAA deprivation, a phenotype that could be reversed by addition of asparagine or ASNS expression. Of note, GCN2 activation was required for induction of a pro-survival autophagy response under amino acid depletion, independent of ATF4 (which can also induce autophagy). This pro-survival AAR via the GCN2- eIF2α-ATF4 pathway was also activated in response to glucose deprivation, through indirect depletion of amino acid pools as they are used as an alternative fuel source.[141] These findings were confirmed *in vivo*, with abrogation of ATF4 or GCN2 expression significantly blunting growth of human fibrosarcoma xenografts.[141] In a recent study, Zhang *et al*. showed that the ATF4-mediated AAR was upregulated in response to autophagy deficiency, thereby promoting increased amino acid uptake from the extracellular microenvironment to compensate for loss of amino acids that would otherwise be generated through catabolism via autophagy.[142] This mechanism rendered autophagy-deficient tumor cells reliant on the activation of the AAR in response to deprivation of glutamine.[142] This finding bears clinical significance, as it indicates that concomitant inhibition of ATF4-mediated AAR may be required when therapeutically targeting autophagy.

Numerous studies have specifically focused on ASNS as the major downstream effector of ATF4. A recent study from Gwinn *et al.* highlighted the significance of amino acid homeostasis and ASNS in KRAS-driven non-small-cell lung cancer (NSCLC). In NSCLC cell lines, oncogenic KRAS induced transcriptional upregulation of ATF4 by NRF2 downstream of

PI3K-AKT.[143] Under glutamine withdrawal, this increased pool of ATF4 mRNAs was upregulated at the translational level via the canonical GCN2-eIF2α pathway, going on to activate pro-survival amino acid biosynthesis genes and sustaining tumor growth.[143] ASNS was shown to be the rate-limiting factor for the anti-apoptotic and growth-promoting effects of this mechanism. Consequently, dual treatment with an AKT inhibitor and L-asparaginase effectively halted tumor progression in NSCLC xenograft mouse models.[143] Other studies have confirmed the significance of increased asparagine levels and ASNS in solid tumor progression as a potential therapeutic vulnerability, with implications for targeting ASNS activity with L-asparaginase therapy and/or dietary restriction of asparagine.[144–148]Indeed, L-asparaginase has been successfully used as a chemotherapeutic agent to treat childhood acute lymphoblastic leukemia for several decades, although the significance of its mechanism of action had not been fully appreciated until recently.[110,149]

Other work has established a pro-survival function for ATF4 via the *de novo* synthesis of serine and glycine to fuel tumor growth. Through the coupling of enhanced glycolysis observed in rapidly proliferating tumor cells with serine/glycine synthesis, substrates for the TCA cycle and 1C metabolism are generated, facilitating the production of macromolecules essential for increasing cellular biomass.[113,114] As such, certain genes encoding enzymes involved this pathway have been found to be amplified in cancer and correlate with poor prognosis, such as *PHGDH* in breast cancer and melanoma.[150,151] Another study showed that via NRF2, which is frequently deregulated in NSCLC, ATF4 promoted serine synthesis to supply nucleotides and glutathione to fuel tumor growth, with PHGDH, PSAT1, and SHMT2 overexpression linked to higher tumor grade and poor outcome in patients.[116,150,151] Serine synthesis gene transcription was also shown to be upregulated by ATF4 via an epigenetic mechanism involving the histone lysine demethylase KDM4C, which regulated expression of ATF4 and directly interacted with it to transcriptionally upregulate global AAR genes.[152] Studies continue to reveal additional functions for serine in metabolism and mitochondrial function, particularly in cancer cells. Serine

levels and reduced serine-derived ceramides have also been linked to defects in mitochondrial dynamics and lipid metabolism, with serine deprivation leading to reduction of fatty acid oxidation, increased mitochondrial fragmentation and depolarization, and reduced cell proliferation in cancer cell lines.[115]

Cancer cells encounter a variety of stressors over the course of tumor development and metastasis. A critical step in the metastatic cascade is the avoidance of anoikis, a specialized form of apoptotic cell death that occurs following detachment from the ECM. In a study from Dey *et al*., the UPR arm of the ISR was induced following matrix detachment and found to be required for preventing anoikis in fibrosarcoma and CRC cell lines.[96] ATF4, in conjunction with its binding partner NRF2, activated a cytoprotective transcriptional program characterized by upregulation of autophagy and antioxidant genes, in particular *HO1*, which proved essential for coping with the oxidative stress that is normally induced by matrix detachment.[96] ATF4-mediated anoikis resistance was sufficient to promote lung colonization in experimental metastasis assays *in vivo.*[96] Accordingly, analysis of human lung cancer specimens and patient data revealed that high HO-1 expression was associated with metastasis and reduced overall survival.[96]

ATF4 is turned over at the proteasome by phosphorylation of its β-TrCP domain by the Skp-Cullin-F box (SCF) ubiquitin ligase complex containing the beta-transducin repeat containing E3 ubiquitin protein ligase (β-TrCP).[153] Therefore, in addition to its activation by the ISR, increased ATF4 activity in tumors may occur as a therapeutic consequence, as in the case of Bortezomib, a proteosomal inhibitor. In response to treatment with Bortezomib, MCF7 breast cancer cells exhibited stabilized ATF4 protein levels due to inhibition of its proteosomal degradation, while PERK- eIF2α was not activated despite induction of ER stress.[103] ATF4 went on to promote a pro-survival autophagic response via induction of LC3 expression, thereby fueling Bortezomib resistance.[103] ATF4 was later shown to bind to CRE sites in the LC3

promoter, upregulating its expression in response to ER stress and severe hypoxia, and promoting survival of breast cancer cells.[154]

In another study, the regulation of ATF4 stability by p62-mediated polyubiquitination (independent of its autophagy function) was found to play a non-cell autonomous role in the progression of prostate cancer.[155] Tumor stromal cells that were deficient in p62 promoted resistance to glutamine deprivation through a mechanism involving the stabilization of ATF4 protein via an interaction with β-TrCP.[155] Subsequent generation of asparagine via ASNS promoted increased glucose flux to the TCA cycle in the absence of glutamine, and asparagine was secreted to fuel proliferation in the neighboring tumor cells.[155] β-TrCP-mediated destabilization of ATF4 was also shown to be promoted by mTORC1, which went on to repress SIRT4 (an ATF4 target).[138] In this context, the activity of ATF4 was tumor-suppressive, as ATF4 regulates SIRT4 expression, which goes on to inhibit glutamate dehydrogenase activity and subsequent conversion of glutamate to α-ketoglutarate, thus inhibiting glutamine anaplerosis to the TCA cycle and limiting cell proliferation.[138]

Another study implicated ATF4 in tumor suppression in a model of MYCN-amplified neuroblastoma, whereby glutamine deprivation downstream of MYC induced ATF4 induction of the pro-apoptotic genes PUMA, NOXA, and TRB3, in a manner that could be targeted with ATF4 agonists or glutaminolysis inhibitors.[137] Paradoxically, oncogenic MYC has also been shown to induce tumor cell survival via ATF4 by activating PERK and GCN2.[156,157] ATF4 and MYC were found to share common promoter binding sites of genes involved in protein synthesis, and the authors postulated that ATF4 negatively regulated these genes to limit the accumulation of proteotoxic stress as a survival mechanism for rapidly proliferating tumors.[157] There are likely additional modes of induction for ATF4 and other factors that interplay, such as tumor type, tumor stage, type of stress and duration, that dictate the various downstream consequences for cell proliferation and survival.

Summary

Numerous mechanisms are employed in normal physiology and in malignant cells to cope with external stressors. Autophagy and the more selective mitophagy are highly conserved catabolic processes that turnover cytoplasmic components at the lysosome in response to stressors such as starvation and hypoxia. BNIP3 is the principal mediator of stress-induced mitophagy, playing an adaptive role in preserving mitochondrial function and metabolic homeostasis in the liver. BNIP3 is a putative tumor suppressor in human cancers and is silenced or deleted in progression to invasive carcinoma. Rapidly proliferating tumor cells may elicit and eventually co-opt other stress response pathways, such as the ISR, to fuel their continued growth despite accumulating extrinsic stressors. ATF4 is the master transcriptional regulator of cellular stress responses and a mediator of the ISR in response to ER stress, hypoxia, oxidative stress, and amino acid depletion. ATF4 has been recently implicated in coordinating a cytoprotective mechanism in response to mitochondrial stress that results in metabolic rewiring and induction of amino acid biosynthesis.

The work in this thesis explores the convergence of two pathways involved in modulating the cellular stress response to starvation. Specifically, I describe the finding that BNIP3 suppresses the amino acid stress response under fasting in the murine liver via a mechanism involving ATF4 transcriptional activation of amino acid biosynthesis genes (Chapter 3). Furthermore, I demonstrate that this involves an interaction between BNIP3 and ATF4 at mitochondria that functions to suppress ATF4 nuclear localization and subsequent target gene expression in murine hepatocytes and in human liver cancer cells (Chapter 4) and that this involves an interaction with LC3 at mitophagosomes with functional consequences for cellular stress responses, cellular metabolism and cell growth (Chapter 5). Together, these findings demonstrate an integral role for BNIP3 in regulating the amino acid stress response through a novel mitochondrial function for ATF4 in mitophagy.

CHAPTER 2

MATERIALS AND METHODS

Chemicals

BafilomycinA1 (BafA1) was purchased from Sigma Aldrich and used at a final concentration of 100 nM. Glucagon was purchased from Sigma Aldrich and used at a final concentration of 1 μM.

Mice

For these studies, two strains of mice were used: wild-type (WT) and whole body BNip3 null, maintained on a C57Bl/6J background. Mice were housed in an environmentally controlled, specific pathogen-free animal barrier facility and provided water and standard chow *ad libitum.* All work presented here was approved by the University of Chicago Institutional Animal Care and Use Committee under protocol 71155.

Genotyping

Mice were weaned and had their tail tips snipped for genotyping at 3 weeks of age by technicians at the University of Chicago Animal Resource Center. Tail tips were digested overnight at 55 °C in tail lysis buffer (100 mM Tris pH 8.0, 5 mM EDTA pH 8.0, 0.2% SDS, 200 mM NaCl,100 nM proteinase K). Genomic DNA was isolated by isopropanol precipitation, resuspended in nuclease-free deionized water, and used in subsequent genotyping analysis. The following primers were used to detect the WT and BNip3 null alleles, respectively: WT intron 2, 5'-TGTGGCTGAGAGTCAGTGGTC-3'; GT2, 5'- TTGCAAGTCTAGGAGTCAGTT-3'; NTKV, 5'- GTGGATGTGGAATGTGTGCG 3'. These primers generate a 435 bp product for the WT allele and a 220 bp product for the BNip3 null allele.

Immunohistochemistry

Mouse tissues were harvested at experimental endpoints, rinsed in PBS, and fixed in 10% neutral buffered formalin (NBF) for 24 hours and then transferred to 70% ethanol until further processing. For mouse tissues and for banked human tumors, all paraffin-embedding, sectioning, hemotoxylin and eosin staining, and immunohistochemistry was performed by the Human Tissue Resource Center at the University of Chicago. Briefly, the paraffin-embedded sections were incubated in two washes of xylenes and rehydrated in successive dilutions of ethanol. Endogenous peroxidase activity was quenched by incubation in a methanol/hydrogen peroxide solution. Epitope retrieval was carried out by boiling slides in citrate buffer. Sections were then incubated in appropriate primary antibody followed by biotinylated secondary antibody with avidin-biotin signal amplification. Proteins were visualized by DAB HRP substrate (Vector Laboratories). Tumor section staining was scored by a pathologist.

Primary mouse hepatocyte isolation and culture

Primary hepatocytes were isolated from anesthetized mice using a modified two-step non-recirculating perfusion method. While mice were anesthetized with isoflurane, the portal vein (PV) was cannulated using a 23-gauge needle and pre-warmed Hank's Balanced Salt Solution (HBSS, 5 mM glucose, 0.5 mM EGTA, 25 mM HEPES pH 7.4) was perfused at a flow rate of 2 mL/min. Successful cannulation was confirmed upon immediate blanching of the liver, followed by cutting of the inferior vena cava (IVC) and increasing of the flow rate to 8 mL/min. Approximately 50 mL of HBSS was perfused through the liver, for approximately 6 minutes. During this time, the IVC was periodically clamped for 5-second intervals, ensuring proper flow of the solution through the liver. Pre-warmed digestion medium (low-glucose DMEM, Gibco), supplemented with 15 mM HEPES, 100 U/mL penicillin and 0.1 mg/mL streptomycin (Pen/Strep), and 100 U/mL type IV collagenase (Worthington) was then perfused at 8 mL/min for approximately 8 minutes or until the liver appeared fully digested, with periodic clamping of the IVC to aid in digestion and maximize cell yield. Digestion was considered complete upon

loss of liver elasticity and little to no change in liver size upon IVC clamping. The digested liver was excised and transferred to a culture dish containing 20 mL of the digestion medium, and gently ripped and shaken using forceps to release the cells. The remainder of the procedure was performed in a tissue culture hood. Cells were gently triturated 3 times using a 25 mL pipet and filtered through a 74 μM fine mesh stainless steel strainer (Dual Manufacturing). Cells were centrifuged at 50 g for 2 minutes at 4 °C followed by three washes with 25 mL of cold isolation medium (high glucose DMEM supplemented with 1 mM sodium lactate, 2 mM L-glutamine, 15 mM HEPES, 0.1 μM dexamethasone, 1X Pen/Strep, and 10% fetal bovine serum). Following the final wash, the pellet was resuspended in 25 mL of isolation medium and the viability and total yield were assessed by 0.4% trypan blue exclusion and counting using a hemocytometer. Hepatocytes were diluted to 3 x 10^5 cells/mL and approximately 4.5 x 10^5 cells were added per well of 6 well tissue culture plates. Tissue culture plates (overlayed with glass coverslips if being used for immunofluorescence) were previously coated with 5 μg/cm^2 rat tail collagen (type I, BD) in 0.02N acetic acid, dried, and sterilized in a hood under UV light for at least 4 hours, and washed with sterile PBS prior to plating hepatocytes. Cells were evenly distributed by shaking of the plates gently in a linear fashion. Following a 1 hour incubation in a tissue culture incubator (37 °C, 5% CO_2), media were aspirated and replaced with fresh, pre-warmed isolation medium, followed by an additional 4 hours of incubation. After this recovery period, the medium was replaced with serum-free culture medium (low-glucose DMEM supplemented with 10 mM sodium lactate, 2 mM L-glutamine, 5 mM HEPES, 10 nM dexamethasone, and 1X Pen/Strep). For starvation experiments used for qPCR, cells were incubated overnight in HEPES-buffered Kreb's Ringer solution (KRH, 115 mM NaCL, 0.5 mM KCl, 0.1 mM $CaCl_2$, 0.1 mM KH_2PO_4 , 1.2 mM $MgSO_4$, 2.5 mM Na-HEPES) and 1 μM glucagon (KRHg). For experiments requiring exogenous overexpression, adenoviruses encoding empty vector (EV), WT-BNIP3, or W18A-BNIP3 were added a dose of 2.9 x 10^{10} viral particles in 1 mL of media. For experiments

involving immunofluorescence or western blots, viral media was aspirated the next morning, and wells were washed 2X with PBS followed by incubation in experimental media conditions.

Whole cell protein extraction

For harvesting of cells, plates were washed in ice-cold DPBS followed by scraping in 1mL of DPBS containing protease inhibitors (0.5 mM PMSF, 1 µg/mL aprotinin, 1 µg/mL leupeptin, 1 mM Na_3VO_4). Cells were pelleted at 3000xg for 3 minutes at 4°C and resuspended in RIPA lysis buffer (10 mM Tris-HCl pH 8.0, 150 mM NaCl, 1% sodium deoxycholate, 0.1% SDS, 1% Trition X-100) containing protease and phosphatase inhibitors (Roche PhosSTOP inhibitor cocktail tablet). Samples were incubated on ice for 15 minutes with vortexing every 5 minutes, and centrifuged at full speed for 15 minutes at 4 °C. The supernatant was transferred to fresh, pre-chilled Eppendorf tubes and protein concentration was measured on a NanoDrop spectrophotometer and stored frozen at -80 °C.

Mitochondrial and nuclear protein fractionation

Plates were washed and scraped as described above for whole cell extraction. Biochemical fractionation was carried out using the Cell Fractionation Kit (Abcam, cat # ab109719). Cells were pelleted at 300g for 5 min at 4 °C and resuspended in 2mL of 1X Buffer A (with protease and phosphatase inhibitors) and counted using a Countess. Cells were pelleted and resuspended in Buffer A at a concentration of $6.6x10^6$ cells/mL based on the cell counts. These volumes were used for the remainder of the extraction protocol.To extract cystolic proteins, an equal volume of Buffer B was added and samples were incubated at room temperature for 7 minutes on a shaker. Samples were pelleted at 5000g for 1 min at 4 °C and the supernatants containing the cytosolic fractions were removed. Pellets were resuspended in equal volumes of Buffer A and Buffer C to extract mitochondrial proteins, and incubated for 10 minutes at room temperature on a shaker. Samples were pelleted at 5000g for 1 minute and the supernatants containing the mitochondrial fraction were transferred to new tubes, leaving

behind the nuclear fraction in the pellet. The supernatants were centrifuged again at 10000g for 1 minute to pellet any remaining nuclear proteins, and transferred to fresh tubes. The nuclear pellets were resuspended in 100uL of Buffer A and sonicated briefly for 5 sec at 10% amplitude using a Branson probe sonicator to shear DNA and allow for accurate pipetting. Mitochondrial and nuclear fraction protein concentration was measured using a NanoDrop. Samples were prepared for western blot analysis using the provided 5X sample buffer and boiled for 10 minutes. To determine fraction enrichment, Tom20 was used as a mitochondrial marker and Parp1 was used as a nuclear marker.

Immunoprecipitation

Cells were transiently transfected and/or treated prior to protein extraction as described above. Following scraping and centrifugation, cell pellets were resuspended in 150μL NP-40 IP lysis buffer (50 mM Tris-HCL pH 7.5, 150 mM NaCL, 1 mM EDTA, 1% Igepal, 0.01% β-mercaptoethanol), and sonicated at 10% power for 5 sec using a Fisher Sonic Dismembrator Model 500 while keeping samples cold in an ethanol-ice bath. Samples were incubated on ice for 5 minutes and centrifuged at full speed for 15 minutes at 4 °C. The supernatant was transferred to fresh, pre-chilled Eppendorf tubes and protein concentration measured as above. For immunoprecipitation of exogenously-expressed GFP-tagged proteins, 25 μL GFP-Trap or agarose control-Trap magnetic beads (Chromotek) were washed twice in 500 μL IP lysis buffer using a magnetic bead rack, followed by resuspension in 1 mL IP lysis buffer and addition of 1.5 mg protein lysate. Lysates were incubated on beads for 1 hr at 4 °C on a rotator followed by three 1 mL washes with IP lysis buffer using a magnetic bead rack. Beads were transferred to a fresh Eppendorf tube for the final wash and resuspended in 50 μL 2x sample loading buffer (1:2:2 10x SDS:5xBPB:ddH2O) and boiled for 10 minutes. Supernatant containing denatured IP lysate was transferred to a fresh tube and frozen at -80 °C.

Western blot

Protein samples were denatured by boiling for 5 min with SDS reducing sample buffer (400 mM Tris pH 6.8, 10% SDS, 500 mM β-mercaptoethanol) and sample loading dye (60% glycerol and bromophenol blue). The amount of protein loaded per sample varied depending on the proteins being probed, but typically 75 µg was loaded onto SDS-PAGE gels, followed by transfer to nitrocellulose (0.2 µm pore, GE Healthcare) or PVDF (0.45 µm pore, GE Healthcare) membranes. Membranes were blocked in 5% nonfat milk in TBS/0.05% Tween (TBST) for 30 minutes at room temperature with shaking and incubated with primary antibodies overnight at 4 °C on a rocker, in 5% BSA/TBST for antibodies from Cell Signaling Technology and in 5% nonfat milk/TBST for all others. The next day, membranes were washed 3 times with TBST and incubated with HRP-conjugated secondary antibody (Dako) in 5% nonfat milk/TBST for 2 hours at room temperature on a shaker. Membranes were washed 3 times in TBST and proteins were visualized by chemiluminescence and exposure on X-ray film.

Chromatin immunoprecipitation (chIP) and qPCR

All chIP assays were performed using whole mouse liver harvested from BNip3 null or wild-type mice fasted for 24 hours and intraperitoneally injected with glucagon at a dose of 200 mg/kg. Following mouse euthanasia and liver harvesting, livers were processed and chromatin extracted according to the protocol for the SimpleChIP Plus Enzymatic Chomatin IP Magnetic Bead Kit from Cell Signaling Technology (cat#9005). Briefly, fresh liver was finely minced and cross-linked at RT in 1% formadehyde in PBS and protease inhibitor cocktail (PIC) for 20 min and quenched in glycine for 5 min. Tissue was disaggregated using a dounce homogenizer and nuclei were extracted using the proprietary buffers provided in the kit. Micrococcal nuclease was used for digestion of chromatin for 20 min at 37 °C with frequent mixing and the reaction was stopped by addition of 0.5M EDTA and placing samples on ice. Nuclei were pelleted and sonicated for a total of three 15-20 sec intervals using a Fisher Scientific Sonic Dismembrator

Model 500 at the lowest amplitude setting. Lysates were clarified by sonication and the resultant supernatant was aliquoted in microcentrifuge tubes and stored at -80 °C. A small aliquot was used for analysis of chromatin digestion and determination of concentration according to the manufacturer's protocol. Using this concentration, 10 µg chromatin from each sample were immunoprecipitated with 2.5 µL (0.17 µg) ATF4 antibody (CST) or control rabbit IgG according to the kit protocol. IP samples as well as an aliquot of total input chromatin were eluted and DNA was purified using the provided spin columns. qPCR was performed on purified DNA using Perfecta Sybr Green Fastmix (Quantabio) using the following primers directed to the promoters of ATF4 target mouse genes of interest:

Atf3: 5'-TGAGTGAGACTGTGGCTGGGA-3'; 3'-ATTGGTAACCTGGAGTTAAGCGGG-5'

Fgf21: 5'-TTCAGACCCCTGTTGGAAAG-3'; 3'-CACACTTGGCAGGAACCTGAAT-5'

For Asns, we used a commercial EpiTect chIP qPCR Assay (Qiagen), catalog# GPM1051843(-)18A, RefSeq Accession no: NM_012055.2 (-)18Kb.

For Ppargc1a, we used a commercial EpiTect chIP qPCR Assay (Qiagen), catalog# GPM1051240(-)01A, RefSeq Accession no: NM_008904.1 (-)01Kb.

A StepOne Plus thermocycler (Applied Biosystems) was used for qPCR and the signal relative to the total input chromatin was calculated using the following equation: percent input = 2% x $2^{(C[T]2\%\text{Input Sample} - C[T]\text{ IP Sample})}$, where C[T] = C_T = Threshold cycle of PCR reaction.

Immunofluorescence

Hepatocytes were seeded onto collagen-coated glass-coverslips in 6-well tissue culture plates as previously described. Wells were treated with full media or KRH supplemented with 1 µM glucagon (KRHg) for 6 hours, with the addition of 100 nM bafilomycin A1 or DMSO vehicle for the final 4 hours of incubation. At experimental endpoint, media were aspirated and wells washed in DPBS followed by fixation in 4% paraformaldehyde (PFA) for 20 minutes at RT. Wells were washed 3 times in DPBS followed by permeabilization in ice-cold 100% methanol for

5 minutes at -20 °C. Coverslips were washed with TBST 3 times and blocked in 10% goat serum in PBS for 30 minutes. Coverslips were incubated with primary antibodies in 10% goat serum in PBS overnight at 4 °C. The next day, wells were washed in TBST for 3x5 minutes, followed by incubation in appropriate fluorescent secondary antibodies in 10% goat serum/PBS for 1 hour at RT, protected from light. Wells were washed in PBS, rinsed in ddH_2O, and mounted onto slides with 18 µL ProlongGold containing DAPI. Slides were allowed to cure for 24 hours in the dark at room temperature, with subsequent storage at 4 °C.

Confocal microscopy

Fixed slides were imaged on an Olympus DSU Spinning Disk Confocal microscope in the Integrated Microscopy Core Facility at the University of Chicago. All images were collected using a 100X oil-immersion objective. Ten representative images per sample were obtained and images were background subtracted and thresholded using ImageJ software.

ImageJ quantification of colocalization

For quantification of colocalization (overlap) between two channels, a macro was generated in ImageJ to automatically subtract background, threshold each channel, and select the cell of interest in each image. The JACoP plugin was then used to calculate the M1 and M2 coefficients, representing the overlap between two channels. Averages and SEM were then calculated for each set of images.

Target	Clone #	Species	Company	Catalog #	Dilution for IHC	Dilution for WB	Dilution for IF
ATF4	D4B8	rabbit	Cell Signaling	11815S	1:25	1:250-1:500	1:200
ATF4	EPR18111	rabbit	Abcam	ab184909		1:1000	1:400
BNIP3	D7U1T	rabbit	Cell Signaling	44060	1:100	1:500	
GFP	D5.1	rabbit	Cell Signaling	2956S		1:250-1:500	
HA	C29F4	rabbit	Cell Signaling	3724S		1:2000	
HA	7C9	rat	Chromotek	7C9-100			1:1000
Lamp1	1D4B	rat	Abcam	ab25245			1:200
LC3B	E5Q2K	mouse	Cell Signaling	83506			1:400
Tomm20	--	mouse	Abcam	ab56783		1:500	1:100

Table 2.1 Antibodies and usage information

Cell culture

Human cell lines (293T and HepG2) were cultured in Dulbecco's Modified Essential Medium (DMEM) supplemented with 10% fetal bovine serum (FBS) and 1% penicillin/streptomycin. Cultures were maintained in a humidified CO_2 incubator at 5% CO_2 and 37 °C. For lentivirally-transduced HepG2ΔBNIP3 cells over-expressing EV, WT, or W18A-BNIP3, media were supplemented with 500 μg/mL hygromycin.

Generation of CRISPR/Cas9 BNIP3-KO cell lines

We genetically deleted the BNIP3 locus in HepG2 and HEK-293T cells. BNIP3-CRISPR/Cas9 and HDR plasmids were purchased from Santa Cruz Biotechnology (sc-400985 and sc-400985-HDR). HepG2 and 293T cells were transfected with 2 μg of each plasmid using Lipofectamine 3000 at a ratio of 2:1 Lipofectamine to DNA. After 24 hrs of transfection, media was changed and dual fluorescence of GFP and RFP was confirmed using the Incucyte S3 imaging system. Cells were selected 48-72 hours post-transfection with 0.5-2.0 μg/mL puromycin and seeded sparsely onto 15cm plates for clonal outgrowth. Single clones were isolated using cloning cylinders, expanded in 6-well plates, and further expanded onto 10cm plates. At confluence, plates were placed in a hypoxia chamber (1% O_2) for 16-24 hrs and protein was extracted as described previously. Lysates were run on western blots and probed for BNIP3 to confirm 100% deletion of the BNIP3 gene and absence of BNIP3 protein, compared to control untransfected parental cells. The HepG2 clones with successful deletion of BNIP3 were further transfected with Cre recombinase to remove the puromycin resistance genes and RFP, both of which were flanked by loxP sites introduced by the CRISPR plasmids. RFP-negative clones were selected once more using cloning cylinders and confirmed by western blot.

We genetically deleted the LC3 locus in HEK-293T cells using plasmids from Santa Cruz Biotechnology (sc-417828 and sc-417828-HDR). Transfection and selection of clones was

performed as described above. At confluence, clones were treated with 100 nM BafA1 for 4 hours, followed by protein extraction. Lysates were run on western blots and probed for LC3 to confirm 100% deletion of the LC3 gene and absence of the protein, compared to control untransfected parental cells.

Cloning

Site-directed mutagenesis was used for the generation of pLVX-IRES-hygro-HA-BNIP3 plasmids expressing different mutant forms of BNIP3. Primers were designed using the NEBaseChanger website and the primers were manufactured by Lifetechnologies. The recommended annealing temperatures were used in conjunction with the Q5 Site-Directed Mutagenesis Kit (New England BioLabs).

Growth curves

Human cell lines were seeded at a density of $4x10^4$ cells per well in 6 well plates. Each genotype was seeded in duplicate for each day of counting. The next day (D1), culture medium was changed. On D2 through D7, each well was rinsed in PBS, trypsinized, and resuspended in media for counting by hemacytometer.

Transient transfections

For the transient transfection of human cell lines, including HEK-293T cells, cells were seeded onto 10 cm plates at a density of 0.8×10^6 cells. The next day, 5 µg of pLVX-IRES-hygro-HA-BNIP3 plasmid (for other plasmids, 10 µg was added) and Lipofectamine 2000 reagent were added in a 1:1 ratio in 3 mL of Opti-MEM media and allowed to incubate for 5 minutes at room temperature.

Stable transfections

For the generation of HEK-293T-BNIP3-KO cells stably overexpressing ATF4-GFP, cells were transfected with 10 µg of pCMV3-ATF4-GFPSpark plasmid (Sino Biologicals) with

Lipofectamine 2000 in a 1:1 ratio and selected in 250 µg/mL hygromycin. Clones were expanded and screened for expression of ATF4-GFP by western blot. A positive clone was used for subsequent immunoprecipitation experiments.

Lentivirus production and transduction

The pLVX-IRES-hygro lentiviral vector expressing either empty vector (EV), WT-BNIP3, or W18A-BNIP3 was transfected into HEK-293T cells overnight using the fourth-generation Lenti-X Packaging Single Shot (Clontech). Lentivirus particles were collected 24 hours post-transfection and media containing the particles was centrifuged to pellet any contaminating cells and passed through a 0.45 µm pore filter. Lentiviral-containing media was frozen at -80 °C and/or immediately used in transduction of HepG2 target cells (a clone previously deleted for BNIP3 by CRISPR, followed by removal of the puro and RFP cassette by Cre recombinase). For infection, 500 µL of lentivirus was added to target cells in media containing 8 µg/mL polybrene. Cells were transduced for 24 hours, followed by removal of viral media and washing with PBS and replacement with normal growth media. After 24 hours of growth post-transduction, cells were selected in 500 µg/mL hygromycin to generate stable lines. Clones were picked from stable lines as previously described to ensure equal expression of WT-BNIP3 and W18A-BNIP3.

RNA extraction

Cells in a 6-well plate were washed twice with 2mL of DPBS followed by addition of 1mL Trizol. Wells were incubated for 5 minutes at RT and collected in eppendorf tubes. At this step, samples could be frozen at -80 °C or immediately extracted for RNA. For extraction, 200uL of chloroform was added to each sample, followed by vigorous shaking for 15 seconds and incubation for 3 minutes at RT. Tubes were centrifuged at 12,000xg, 15 min, at 4 °C. The aqueous upper phase (~400 µL) was transferred into a fresh tube, followed by addition of 1 volume of 70% EtOH (~400uL) and vigorous shaking. Samples were incubated for 5 minutes

and then applied to RNasy columns. The remainder of the extraction was performed according to the RNeasy Mini kit protocol (Qiagen), and included on-column DNaseI digestion. RNA was eluted in 50 µL of RNase-free water, concentrations were measured using the NanoDrop Spectrophotometer, and samples were stored at -80 °C.

RT-PCR

To make cDNA, 1-2 µg of RNA was reverse transcribed using the High Capacity RNA-to-cDNA kit (Applied Biosystems). The concentration of cDNA was measured by NanoDrop and samples were stored at -20 °C.

Quantitative PCR

For gene expression analysis, we performed quantitative real-time PCR on 250 ng of cDNA per sample using Taqman gene-specific fluorogenic probes (Applied Biosystems). qPCR was performed on a StepOne Plus thermocycler (Applied Biosystems). Samples were assayed in triplicate and normalized to their respective endogenous control (ACTB). Gene expression levels were quantified using the $\Delta\Delta C_T$ method and relative expression of each sample was normalized to a control and/or untreated sample.

Analysis of Oxygen Consumption Rates

For HepG2s and primary hepatocytes, cells were seeded in Seahorse XF96 microplates at a density of $2x10^4$ and $0.75x10^4$ cells/well, respectively. For primary hepatocytes, the plates were pre-coated with collagen as previously described. The next day, the cellular mito stress test was performed according to the manufacturer's protocol using the Seahorse XF96 analyzer in the Biophysics Core at the University of Chicago. Briefly, 2X DMEM base media was used to make 1X DMEM supplemented with 4.5 g/L glucose, 2mM glutamine, and 1mM sodium pyruvate, with a pH adjusted to 7.35. Cells were rinsed with PBS prior to addition of 175uL of 1X DMEM and the plate was incubated in the absence of CO_2 for approximately 1 hour. Data were

normalized by cell number using Hoechst 33342 nuclear counterstain and fluorescence quantification using a microplate reader. Normalized OCR data was then analyzed using Agilent Seahorse Wave software.

^{13}Carbon-flux metabolomics

HepG2 cells were plated such that they were at 70-90% confluent on the day of extraction. Two tracing experiments were conducted, both in triplicate, for each cell line (EV, WT-BNIP3, W18A-BNIP3). Prior to labeling, cells were cultured in sodium-pyruvate-free media for 24 hours. The DMEM used for both experiments was glucose-, glutamine-, and sodium pyruvate-free and was supplemented with 5% dialyzed FBS. For glucose labeling, media were supplemented with 4.5 g/L [U-^{13}C] D-glucose (Sigma) and 4 mM unlabeled L-glutamine and cells were labeled for 24 hours. For glutamine labeling, media were supplemented with 4 mM [U-^{13}C] L-glutamine (Sigma) and 4.5 g/L unlabeled D-glucose and cells were labeled for 6 hours. At the time of harvest, plates were placed on ice, media were aspirated quickly and cells were scraped in 0.5 mL ice-cold 80% methanol and placed in Eppendorf tubes on dry ice. The tubes were subjected to 3 rounds of alternating freeze/thaw cycles between liquid nitrogen and a 37 °C waterbath. Samples were the centrifuged at 14000 rpm for 10 minutes at 4 °C. Supernatants were transferred to new tubes and pellets were stored at -80 °C. The supernatants were then shipped on dry ice to the UT Southwestern Medical Center Metabolomics Facility for analysis of metabolic flux by mass spectrometry.

Statistics

Data were plotted and analyzed using Graphpad Prism software and presented as the mean ± SEM. Statistical significance was determined using unpaired, two-tailed Student's t-test for comparisons of two groups, while 1-way ANOVA was used to comparisons of > two groups. *p<0.05, **p<0.01, ***p<0.001, ***p<0.0001.

CHAPTER 3

BNIP3 SUPPRESSES THE AMINO ACID STRESS RESPONSE UNDER FASTED CONDITIONS IN THE MURINE LIVER VIA ATF4

Introduction

Mitophagy plays an important role in reducing mitochondrial mass in response to nutrient deprivation, thereby preventing the accumulation of harmful reactive oxygen species (ROS) normally generated during mitochondrial metabolism and maintaining a healthy pool of mitochondria. This mechanism also functions to reduce the inefficient consumption of otherwise scarce nutrients during starvation. BNIP3 is a mitophagy adaptor that localizes to the outer mitochondrial membrane, where it engages with LC3 on nascent phagophores, targeting mitochondria for degradation at the autophagolysosome.[39] BNIP3 is constitutively expressed in certain tissues, including the heart, skeletal muscle, and liver.[40] Our laboratory has previously used the murine liver as a model system to study the function of BNIP3 in mitophagy and metabolism. We have shown that upon fasting in wild-type mice, BNip3 is transcriptionally superinduced and functions to maintain mitochondrial integrity and efficient metabolism.[38] In contrast, BNip3 null mice exhibit defects in mitophagy in hepatocytes, resulting in the accumulation of dysfunctional mitochondria, defective glucose output, and reduced oxygen consumption.[38] Furthermore, BNip3 null livers have increased lipid accumulation due to increased lipid synthesis and decreased fatty acid oxidation, and these mice go on to develop steatohepatitis.[38] This study indicated a broader role for BNIP3 in regulating liver metabolism, potentially extending beyond its known function in mitophagy.

In this chapter, we sought to understand the consequences of BNip3 loss on hepatic metabolism from previous unbiased transcriptomic profiling of livers from wild-type and BNip3 null mice in the fed and fasted states. Our findings led us to investigate a novel function for

BNip3 in suppressing the transcriptional regulation of amino acid biosynthesis in response to nutrient stress, mediated by the nuclear transcription factor ATF4.

Unbiased transcriptomic profiling revealed upregulation of pathways involved in amino acid biosynthesis in livers of BNip3 null fasted mice

Previously, our laboratory investigated the effects of loss of BNip3 on the liver transcriptome in whole body BNip3 null mice compared to wild-type mice in the fed and fasted states. This was accomplished using an Illumina Mouse Ref8 v2 microarray, followed by Ingenuity Pathway Analysis to identify gene ontology (GO) terms representing the most significantly deregulated pathways between wild-type and BNip3 null mice. This study concluded that loss of BNip3 significantly impacted gene expression patterns in the liver specifically in the fasted state. The most differentially regulated genes were those involved in amino acid biosynthetic and other metabolic pathways (Figure 3.1). While it is unsurprising that the hepatic fasted state induces gene pathways involved in amino acid metabolism, BNIP3 and its role in mitophagy have not been previously linked to the regulation of amino acid homeostasis. While the vast majority of work in the field suggests that the primary function of BNIP3 is to regulate stress-induced mitophagy, we cannot exclude the possibility that other unknown functions of BNIP3 explain the differences observed between livers from fasted BNip3 null and wild-type mice.

The microarray results indicated a role for BNip3 in the suppression of genes involved in amino acid biosynthesis in the liver of fasted mice. We next sought to examine the specific genes that were upregulated in the livers of BNip3 null fasted mice. As BNip3 is predominantly a mitochondrial protein and lacks a DNA-binding domain, we hypothesized that it may be altering the activity of a transcription factor involved in amino acid homeostasis. The major transcriptional mediator of amino acid biosynthesis under conditions of cellular and microenvironmental stress is ATF4.[87] Of note, the most significantly upregulated gene in the

BNip3 null fasted liver was *Asns* (fold-change: 6.4), the enzyme mediating the conversion of aspartate to asparagine, and a well-characterized canonical gene target of ATF4 (Table 3.1).[110,111] Other significantly upregulated gene targets included *Ddit4, Slc7a2, Cth, Aass, and Ppargc1α*, which have each also been identified as transcriptional targets of ATF4 and/or are involved in amino acid metabolism.[87,108,133,158,159]

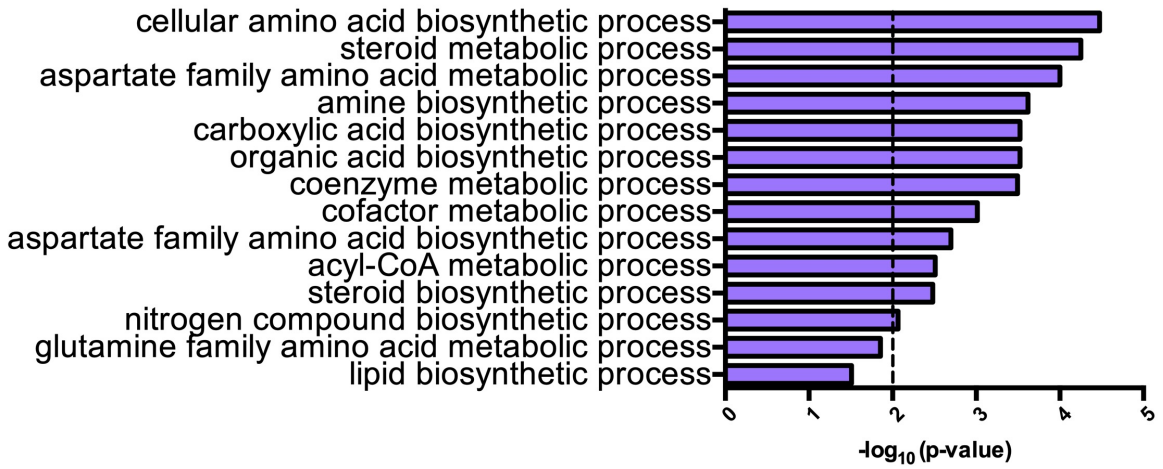

Figure 3.1 Summary of significantly upregulated gene pathways in BNip3 null mouse livers in the fasted state. Ingenuity pathway analysis was used to identify the gene ontology (GO) terms representing the most significantly upregulated gene pathways in the livers of BNip3 null 24-hr fasted and glucagon-injected mice. Data in this figure were generated by Michelle Boland.

Probeset ID	SYMBOL	p-value(BNip3 null vs. Wt)	qvalue(p-value(BNip3 null vs. Wt))	Fold-Change
ILMN_2643513	Asns	2.36E-05	0.00102904	6.34788
ILMN_2657685	Aass	4.05E-06	0.000487277	2.17499
ILMN_2733193	Cth	1.83E-07	0.000186522	2.14877
ILMN_2993109	Ddit4	0.000349488	0.00472442	1.77524
ILMN_2710139	Ppargc1a	9.05E-06	0.000627133	1.7718
ILMN_2642349	Slc7a2	1.01E-06	0.00022081	1.69734

Table 3.1 Top upregulated genes in livers from BNip3 null fasted mice identified by Illumina Mouse Ref8 v2 microarray are ATF4 target genes. List of several of the most significantly upregulated genes in BNip3 null fasted mice identified by transcriptomic analysis. These genes shared a common transcriptional regulator, ATF4.

BNip3 is necessary and sufficient to suppress expression of ATF4 target genes in the murine liver following fasting

To confirm that the top differentially expressed genes identified in the microarray were indeed altered, we performed qPCR analysis on RNA harvested from the livers of fed and fasted wild-type and BNip3 null mice. We confirmed that the expression of these genes was significantly upregulated in the livers of fasted BNip3 null mice compared to wild-type mice (Figure 3.2), indicating that BNip3 is required for suppression of these known ATF4 target genes.

In complementary studies, we utilized a technique to isolate primary hepatocytes from BNip3 mouse liver, allowing us to conduct *in vitro* genetic and microenvironmental manipulation of hepatocytes, which comprise approximately 80% of the liver.[57] These hepatocytes were infected with adenoviruses delivering empty vector (EV) or HA-tagged human BNIP3-WT, and incubated in either full culture media or KRH starvation buffer supplemented with glucagon (KRHg) to mimic the fasted state (see Chapter 2: Materials and Methods). Exogenous overexpression of BNIP3-WT resulted in significantly decreased expression of ATF4 target genes, including additional known targets *ATF3* and *FGF21*, in response to starvation compared to BNip3 null hepatocytes expressing EV (Figure 3.3).[87,93,107] Together, these experiments indicate that BNip3 is both necessary and sufficient for the suppression of ATF4 target gene expression in response to nutrient stress in the liver both *in vivo* and *in vitro*.

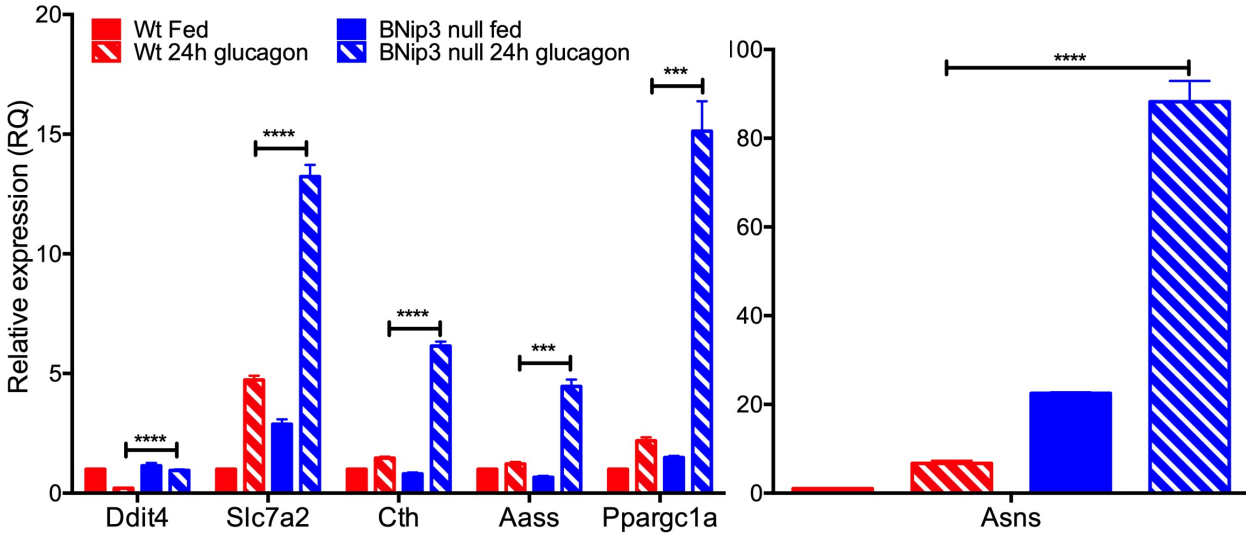

Figure 3.2 Loss of BNip3 results in increased expression of ATF4 target genes in the murine liver following fasting. Quantitative PCR of ATF4 target genes on cDNA from livers of fed and 24h fasted/glucagon-injected wild-type or BNip3 null mice. Normalized to levels of β-actin. Gene expression was relative to WT Fed. (*p<0.05, **p<0.01, ***p<0.001, ****p<0.0001). Data in this figure were generated in cooperation with Lauren Drake.

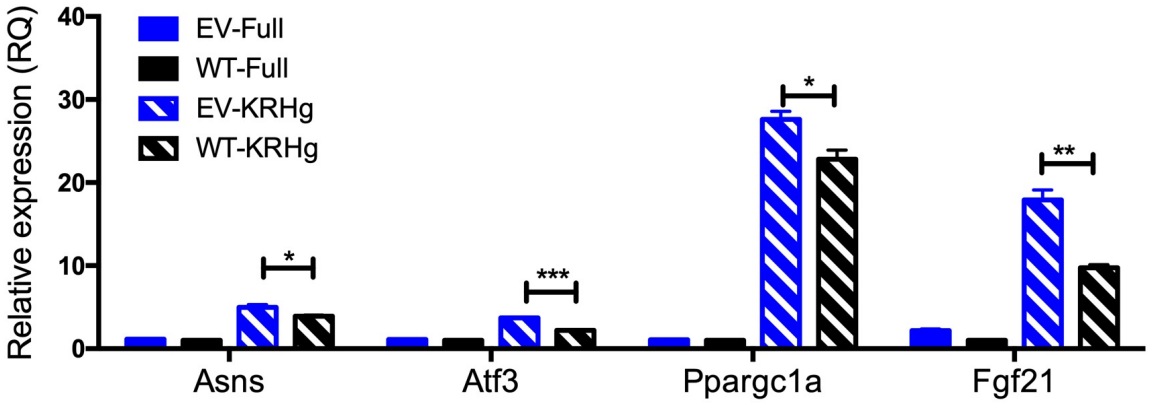

Figure 3.3 Overexpression of BNIP3 rescues suppression of ATF4 target genes in primary murine hepatocytes. Quantitative PCR of ATF4 target genes on cDNA from primary BNip3 null hepatocytes infected with control or overexpressing BNIP3-WT, and incubated in ± KRHg for 16 hrs. Normalized to levels of mouse β-actin. Gene expression was relative to WT Fed. (*p<0.05, **p<0.01, ***p<0.001)

Loss of BNip3 results in increased promoter occupancy of ATF4 on target loci

To investigate the hypothesis that BNip3 is involved in suppressing the transcriptional activity of ATF4 during fasting, we performed chromatin immunoprecipitation (chIP) using an antibody against ATF4 on livers harvested from wild-type and BNip3 null mice in the fasted state. Following chIP, qPCR was performed using primers directed to the promoters of *Asns* and *Ppargc1α,* two of the differentially expressed genes identified in the microarray and known to be regulated by ATF4, and to *Atf3* and *Fgf21,* two additional known targets of ATF4 that we previously observed to be upregulated in BNip3 null livers by qPCR (data not shown). For all four promoter loci, we observed significantly increased binding of ATF4 to the chromatin harvested from BNip3 null livers, indicating that loss of BNip3 plays a role in modulating the promoter occupancy of known ATF4 target genes (Figure 3.4). Given the established role of ATF4 as the master transcriptional regulator of amino acid biosynthesis pathways and our transcriptomic results implicating BNip3 in the regulation of these and other metabolic pathways in response to fasting, we concluded that BNip3 acts to suppress the expression of genes involved in amino acid biosynthesis through a mechanism involving ATF4.

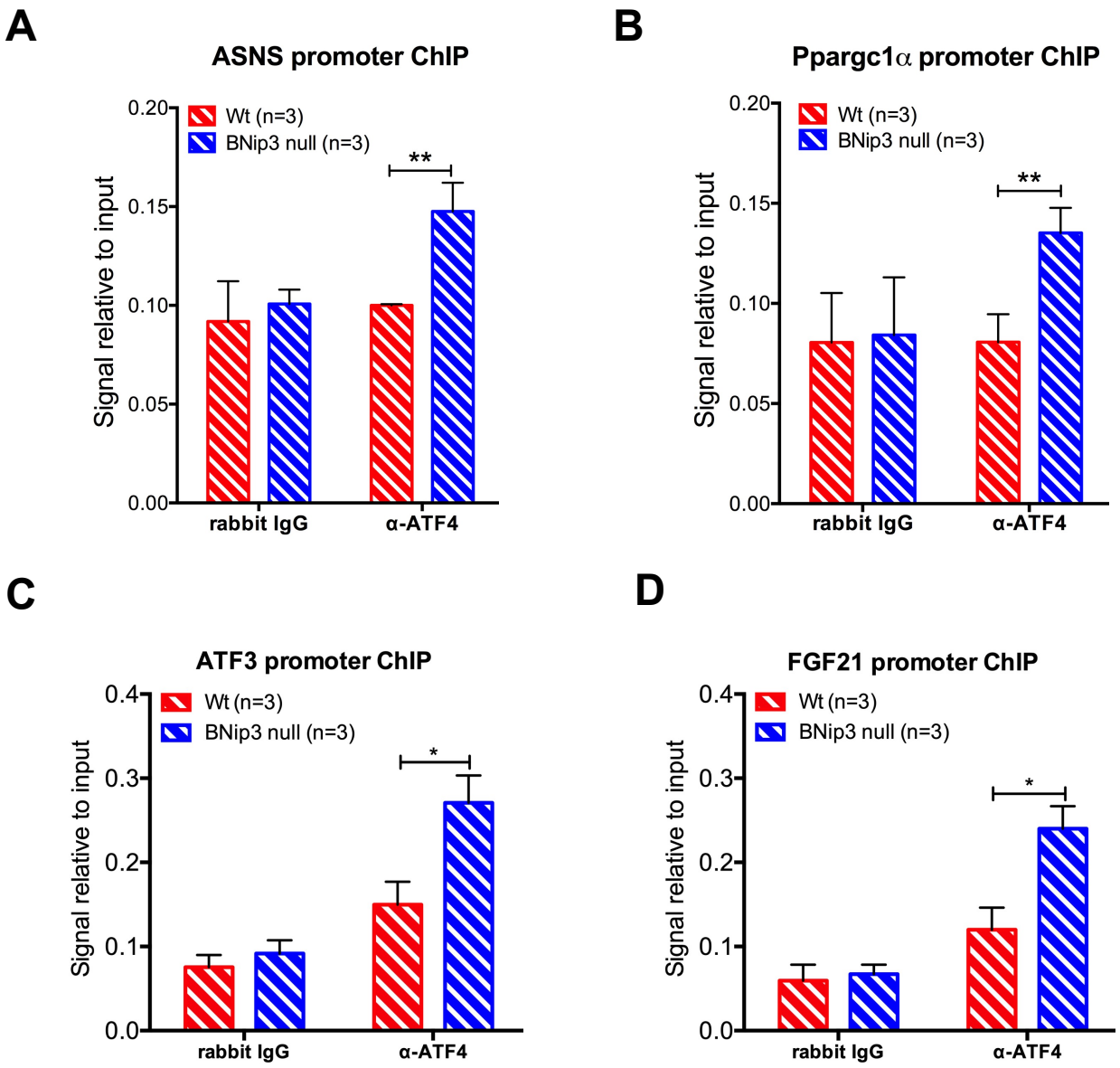

Figure 3.4 BNip3 null livers from fasted mice exhibit increased promoter occupancy by ATF4 on target loci. Chromatin immunoprecipitation-qPCR of ATF4 on target genes from the livers of BNip3 null and wild-type mice following glucagon injection and 24 hr fasting. A) ASNS B) PPARGC1A C) ATF3, and D) FGF21 chIP-qPCR. Data represents an n of 3 mice per group. **(**$p<0.05$, **$p<0.01$)

Conclusions

In this chapter, we identified a novel role for BNip3 in amino acid biosynthesis during the fasted state in the murine liver. We examined previously acquired data from a gene microarray comparing the liver transcriptome from fasted BNip3 null and wild-type mice and found that the most significantly altered genes were enriched in amino acid biosynthesis pathways. Further examination of the differentially expressed genes revealed several transcriptional targets involved in the amino acid biosynthesis response mediated by the transcription factor ATF4. These included the most significantly altered gene, *Asns*, a well-established transcriptional target of ATF4, and *Ddit4, Slc7a2, Cth, Aass, and Ppargc1α.* In qPCR validation experiments, we confirmed that these genes were significantly upregulated in whole liver from fed and fasted BNip3 null mice compared to wild-type mice. Additionally, we showed that exogenous overexpression of BNIP3 in cultured primary hepatocytes from BNip3 null mice suppressed ATF4 target gene expression in response to starvation, compared to EV controls. The degree of induction of certain genes, namely *Asns,* was lower in hepatocytes than in the whole fasted liver, which could be a reflection of the differences between *in vitro* and *in vivo* systems we employed.

Finally, we observed significantly increased promoter occupancy by ATF4 on target loci from the liver chromatin of fasted BNip3 null mice compared to WT mice. Together, these data indicate that BNip3 expression is associated with suppression of the amino acid biosynthesis response to nutrient starvation in a manner involving ATF4-mediated transcription. While numerous studies have established a role for ATF4 in mediating the response to amino acid deprivation, no such studies have examined a function for BNIP3 in this process. Prior to our observations, limited studies have implicated BNIP3 in transcriptional regulation and ATF4 had not been previously linked to mitophagy.[80,82,83] However, mitochondrial dysfunction was shown to induce the cytoprotective UPR^{mt} and mitophagy in worms, involving homologs of ATF4 and BNIP3, and induction of amino acid biosynthesis has been observed in response to

mitochondrial dysfunction in worms and mammalian cells. Our findings suggest a broader role for BNIP3 in modulating a key homeostatic mechanism in the response to fasting in the liver, possibly involving stress-induced mitochondrial-to-nuclear communication with ATF4. Mitochondria are major biosynthetic hubs for macromolecule biosynthesis and BNIP3 plays a crucial function in maintaining mitochondrial integrity in the fasted liver. Evidence from our laboratory also indicates that BNIP3 may also positively regulate general autophagy, and thus loss of BNIP3 may result in decreased amino acid generation through catabolism. Indeed, a study has linked defective autophagy to induction of and reliance on the ATF4-mediated AAR in response to amino acid deprivation.[142] Thus, it is possible that enhancing amino acid biosynthnesis could be an adaptive response to the inhibiton of BNIP3-mediated mitophagy. In the next chapter, we investigated the mechanism of BNIP3-mediated suppression of amino acid biosynthesis in the murine liver and a human liver cancer cell line and identified a novel function for ATF4.

CHAPTER 4

BNIP3 INTERACTS WITH ATF4 AT MITOCHONDRIA IN THE MURINE LIVER AND HUMAN HEPATOCELLULAR CARCINOMA CELL LINES UNDER FASTED CONDITIONS

Introduction

In the previous chapter, I described my findings indicating a role for BNip3 in altering the transcriptional activity of ATF4 in the liver during the fasted state. There are several mechanisms by which BNip3 could be suppressing ATF4, but several lines of evidence directed our attention to the altered subcellular localization of ATF4. First, previous work from our laboratory and others has shown BNIP3 to be localized primarily to the mitochondria. One laboratory has reported to observe nuclear BNIP3 *in vitro,* but this was accomplished using exogenous overexpression of NLS-tagged BNIP3.[80,82] Our group has been unable to detect endogenous BNip3 in the nucleus of hepatocytes and other cell types under a variety of conditions *in vitro* (data not shown). In addition, BNIP3 lacks a nuclear localization signal and DNA-binding domain nor does it possess kinase or other enzymatic activity. Therefore, we hypothesized that ATF4 transcriptional activity was not likely being suppressed directly in the nucleus by BNip3, nor by BNip3-mediated post-translational modification. Instead, we postulated that BNip3 was suppressing the action of ATF4 through an interaction outside of the nucleus at the mitochondria. This interaction could be direct or indirect, involving other proteins in a complex. ATF4 has not previously been observed to localize at the mitochondria, with the majority of studies having examined its function as a nuclear transcription factor. [86,87] However, mitochondrial localization for other related proteins, including ATF2, ATF5, and CREB, have been recently described.[131,160,161]

While ATF4 lacks a mitochondrial targeting sequence, its homolog ATFS-1 in *C. elegans* has a well-described role in the response to mitochondrial stress and can localize to the

mitochondria as well the nucleus to regulate the mitochondrial unfolded protein response (UPR^{mt}).[18] In addition, this process involves the coordinate activation of ATFS-1 and DCT-1, the worm homolog of BNIP3[127] More recently, omics studies have indicated an analogous role for ATF4 in mediating a mamalian UPR^{mt}.[124] However, this study did not examine a role for ATF4 at the mitochondria and instead focused on its function in nuclear transcription.

With these lines of evidence in mind, we hypothesized that the suppression of ATF4 target genes could be mediated by altered localization of ATF4 from the nucleus to the mitochondria in a BNIP3-dependent matter. We investigated a novel mitochondrial interaction between BNIP3 with ATF4 in primary hepatocytes, identified an interaction domain on BNIP3, and determined the downstream consequences of this interaction on transcription of ATF4 target genes under basal and starvation conditions. To extended our studies to the cancer setting, we validated the functional effects of the BNIP3-ATF4 interaction in HepG2s, a human liver cancer cell line.

Loss of BNip3 alters the subcellular localization of ATF4 in hepatocytes in the fed and fasted states

To investigate the effects of BNip3 loss on ATF4 localization in a physiological setting, we performed immunofluorescence staining for endogenous ATF4 on isolated primary murine hepatocytes from wild-type and BNip3 null mice. Strinkingly, wild-type fed hepatocytes exhibited predominantly nuclear ATF4 with some ATF4 in the mitochondria, while fasted wild-type hepatocytes exhibited almost exclusively mitochondrial ATF4. In contrast, ATF4 was largely nuclear in BNip3 null fed and fasted hepatocytes, indicating a defect in both basal and stress-induced localization of ATF4 due to loss of BNip3.

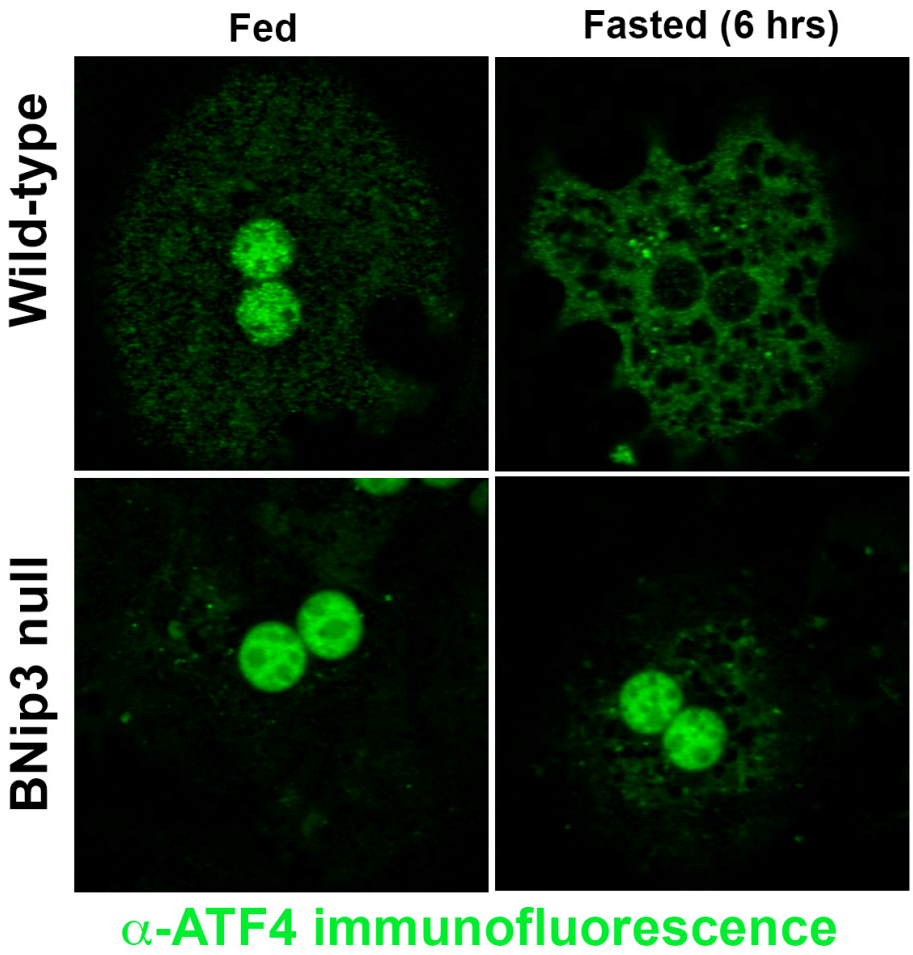

Figure 4.1 ATF4 localizes to the mitochondria in WT fed and fasted hepatocytes, but remains predominantly nuclear in KO hepatocytes. Immunofluorescence for endogenous ATF4 in wild-type and BNip3 null hepatocytes following incubation in full or starvation (KRHg) media.

HA-BNIP3 coimmunoprecipitates with ATF4-GFP in 293T cells

The preceding experiments established that in primary mouse hepatocytes, BNip3 is required for mitochondrial localization of ATF4 in response to fasting, such that BNip3 null hepatocytes exhibit predominantly nuclear ATF4 regardless of nutrient status. In order to determine whether BNIP3 directly interacts with ATF4, we utilized HEK-293T cells in which BNIP3 was genetically deleted by CRISPR gene editing approaches (293T-ΔBNIP3)and then engineered to over-express exogenous ATF4-GFP with either HA-BNIP3 or FLAG-NIX (a BNIP3-related protein). HA-BNIP3 coimmunoprecipitated efficiently with ATF4-GFP whereas FLAG-NIX did not (Figure 4.2) indicating a specificity to the interaction of BNIP3 with ATF4. Of note, the HA-BNIP3 monomer interacted more efficiently with ATF4 than did the HA-BNIP3 dimer (Figure 4.2).

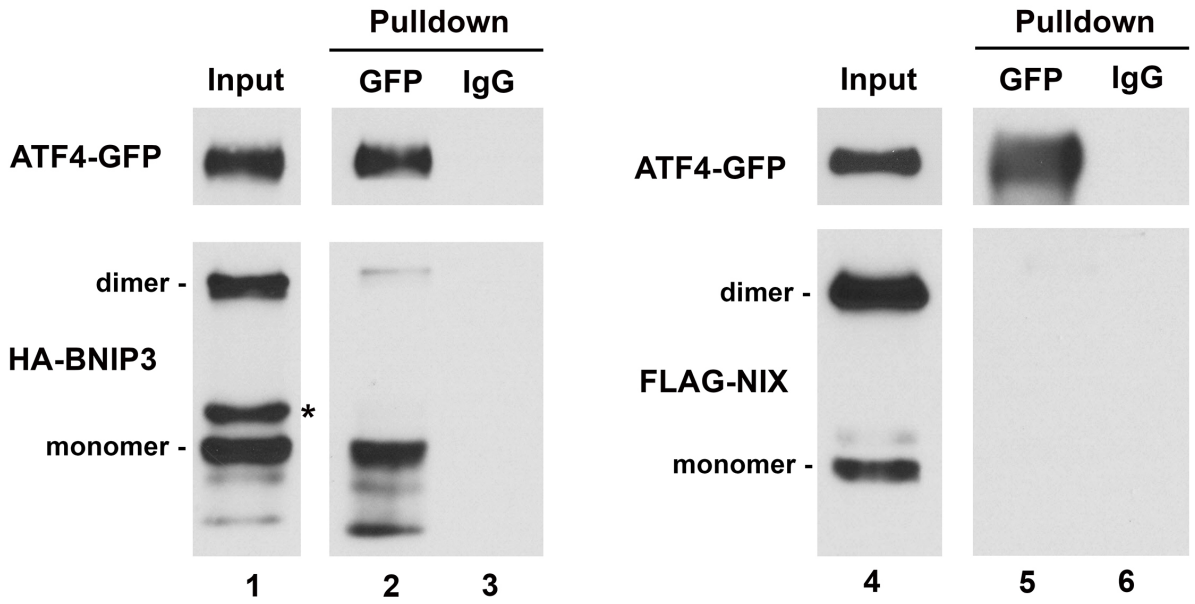

Figure 4.2 BNIP3 monomer coimmunoprecipitates with ATF4 in 293T cells. Coimmunoprecipitation in cells transiently co-expressing ATF4-GFP and HA-BNIP3 or ATF4-GFP and FLAG-NIX. The monomer of BNIP3 interacts with ATF4 while NIX does not.

The amino terminus of BNIP3 is required for coimmunoprecipitation with ATF4

To map the region of BNIP3 required for interaction with ATF4, we generated a panel of HA-BNIP3 mutants using site-directed mutagenesis targeting defined regions of the protein (Figure 4.3A). ATF4-GFP was stably overexpressed by transfection in 293T-ΔBNIP3 cells, as described above and then transiently transfected with exogenous HA-tagged BNIP3-WT, BNIP3-W18A, BNIP3-ΔN1-49, BNIP3-ΔBH3, BNIP3-ΔTM, or BNIP3-C8-NIX, in which the final 8 amino acids of the C-terminus of BNIP3 were substituted with those of NIX. These particular mutants were generated because they target known interactions and/or functional domains of BNIP3 (Chapter 1). We then performed pulldown experiments of ATF4-GFP using GFP-trap beads followed by western blot analysis for HA to assess how the different mutations/deletions in BNIP3 affected interaction with ATF4. While BNIP3-WT monomer came down strongly with ATF4-GFP, BNIP3-W18A and ΔN1-49-BNIP3 exhibited the least amount of pull-down (Figure 4.3B), indicating that a region in the amino-terminus of BNIP3 is required for mediating the interaction with ATF4. A single point mutation, BNIP3-W18A, was sufficient to significantly reduce pull-down with ATF4-GFP. Of note, BNIP3-W18A is also unable to bind to LC3 and is deficient at promoting mitophagy, as will be discussed in the next chapter. In conclusion, these experiments indicate that the region of BNIP3 required for interaction with ATF4 maps around amino acid W18 and thus overlaps with the region of BNIP3 required for interaction with LC3. Given these results, the following studies utilized overexpression of EV, BNIP3-WT, and BNIP3-W18A to dissect the functional significance of the BNIP3-ATF4 interaction.

A

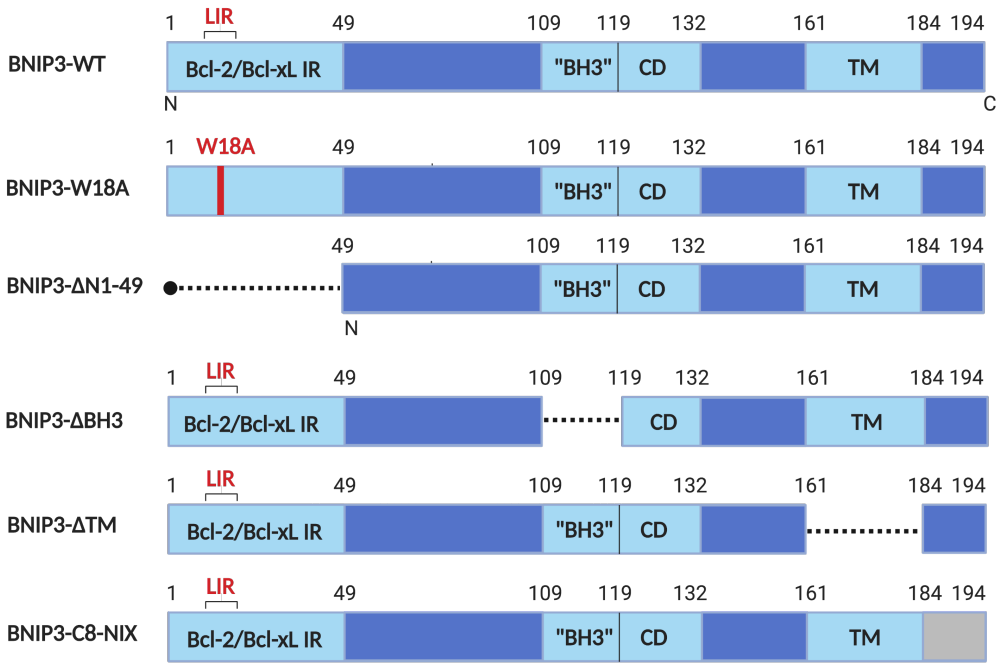

B

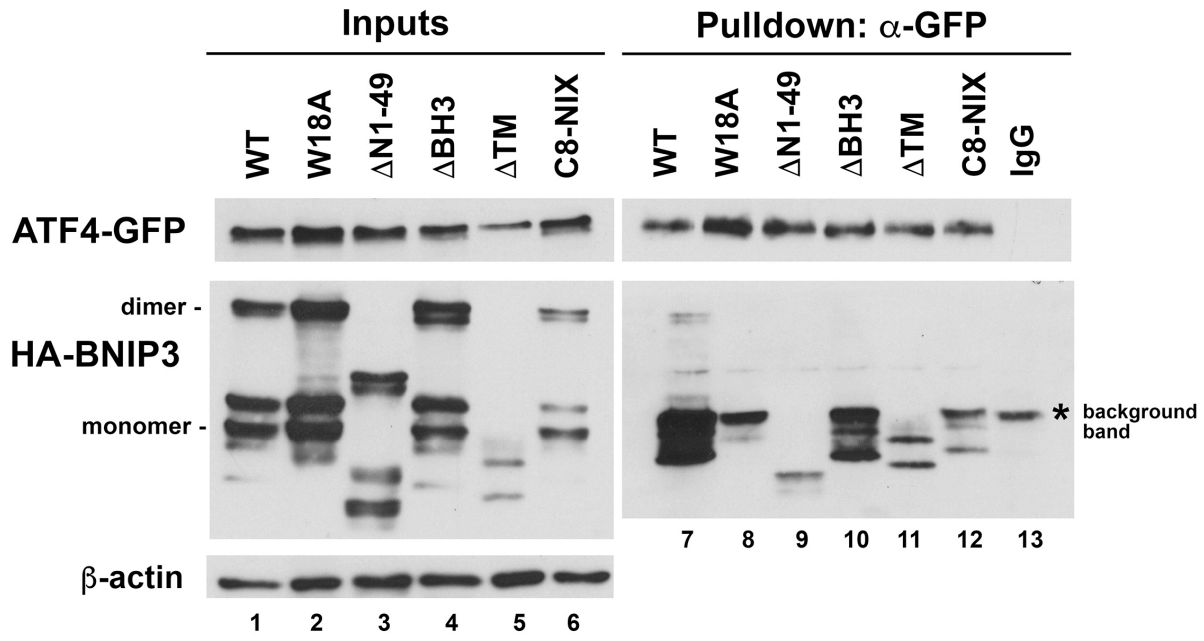

Figure 4.3 The amino terminus of BNIP3 is required for coimmunoprecipitation with ATF4. A) Schematic of BNIP3 structure and mutations/deletions generated by site-directed mutagenesis. B) Coimmunoprecipitation in cells stably over-expressing ATF4-GFP and transiently over-expressing a panel of HA-BNIP3 mutants.

Overexpression of BNIP3-WT in BNip3 null hepatocytes promotes mitochondrial localization of ATF4

Having established that BNIP3 interacts with ATF4 *in vitro*, we next investigated how this interaction affected the subcellular localization of endogenous ATF4 in BNip3 null primary mouse hepatocytes overexpressing EV, BNIP3-WT, or BNIP3-W18A. Using immunofluorescence and confocal microscopy, we observed that in cells overexpressing BNIP3-WT, ATF4 was predominantly non-nuclear, with the majority of signal overlapping with the mitochondrial marker Tom20 (Figure 4.4). Consistent with our previous finding that BNIP3 requires a functional LIR motif to bind ATF4 (Figure 4.3), hepatocytes expressing BNIP3-W18A did not exhibit altered localization of ATF4. In these cells, as in BNip3 null hepatocytes expressing EV, ATF4 was almost exclusively nuclear, indicating that the ability of BNIP3 to interact with ATF4 and/or LC3 is required for ATF4 to localize to mitochondria. These effects were enhanced by treatment of cells with the autophagy inhibitor BafilomycinA1 (BafA1) and KRHg starvation buffer, with increased levels of ATF4 accumulating at mitochondria under these conditions, indicating that ATF4 may be turned over at mitochondria by mitophagy in a BNIP3-dependent manner. We also observed that BNIP3-WT expression promoted the localization of ATF4 to specific mitochondria near the perinuclear region, and that ATF4 was not detected at all mitochondria in the cell. Of note, while some non-nuclear signal was observed under starvation conditions in EV and BNIP3-W18A expressing cells, this signal did not appear to overlap with mitochondria, based on statistical colocalization analysis (Figure 4.4C).

A

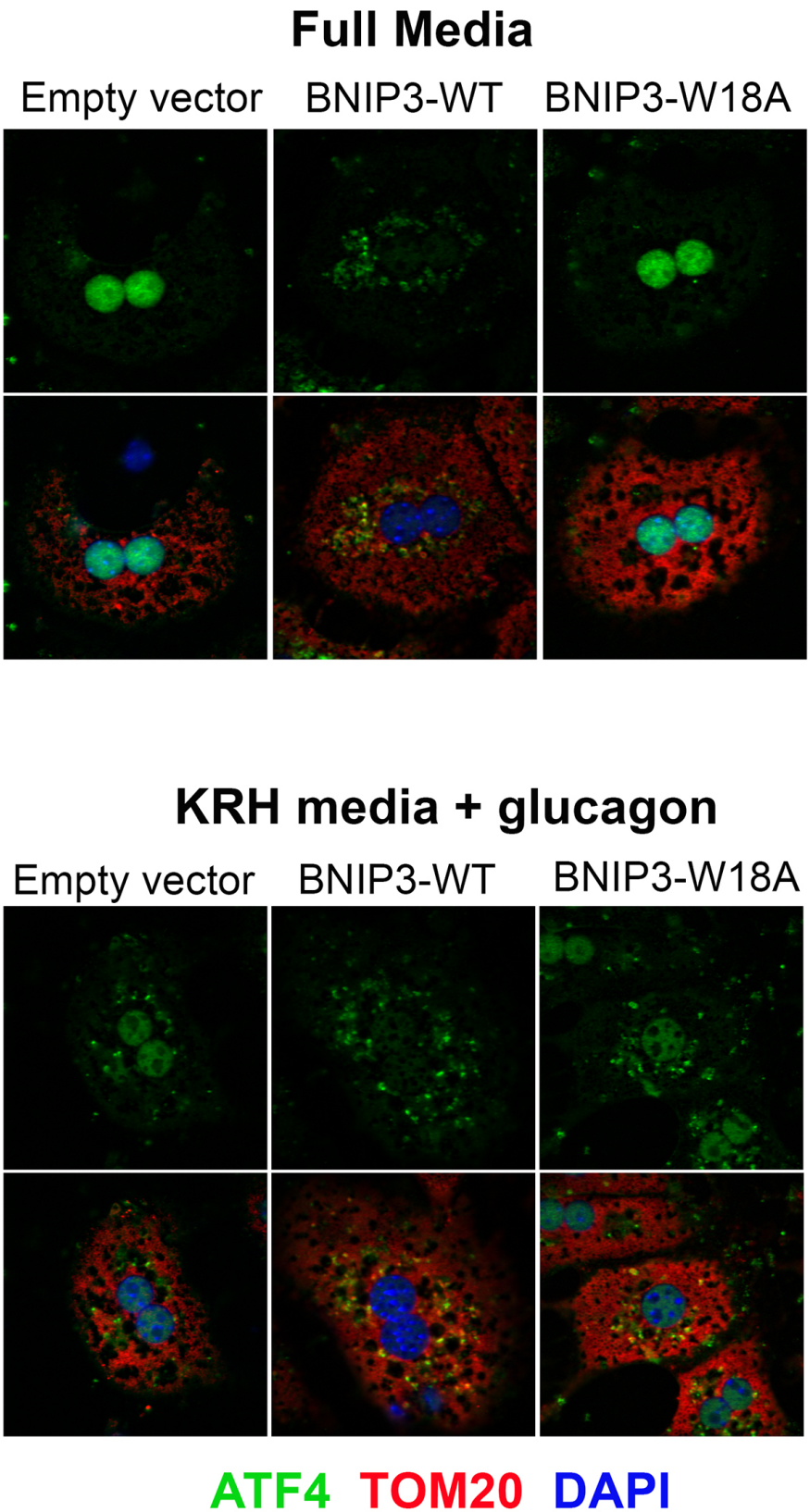

Figure 4.4 BNIP3 promotes the mitochondrial localization of ATF4 in a manner dependent on its ability to bind LC3 and/or ATF4. (continued on next page)

B

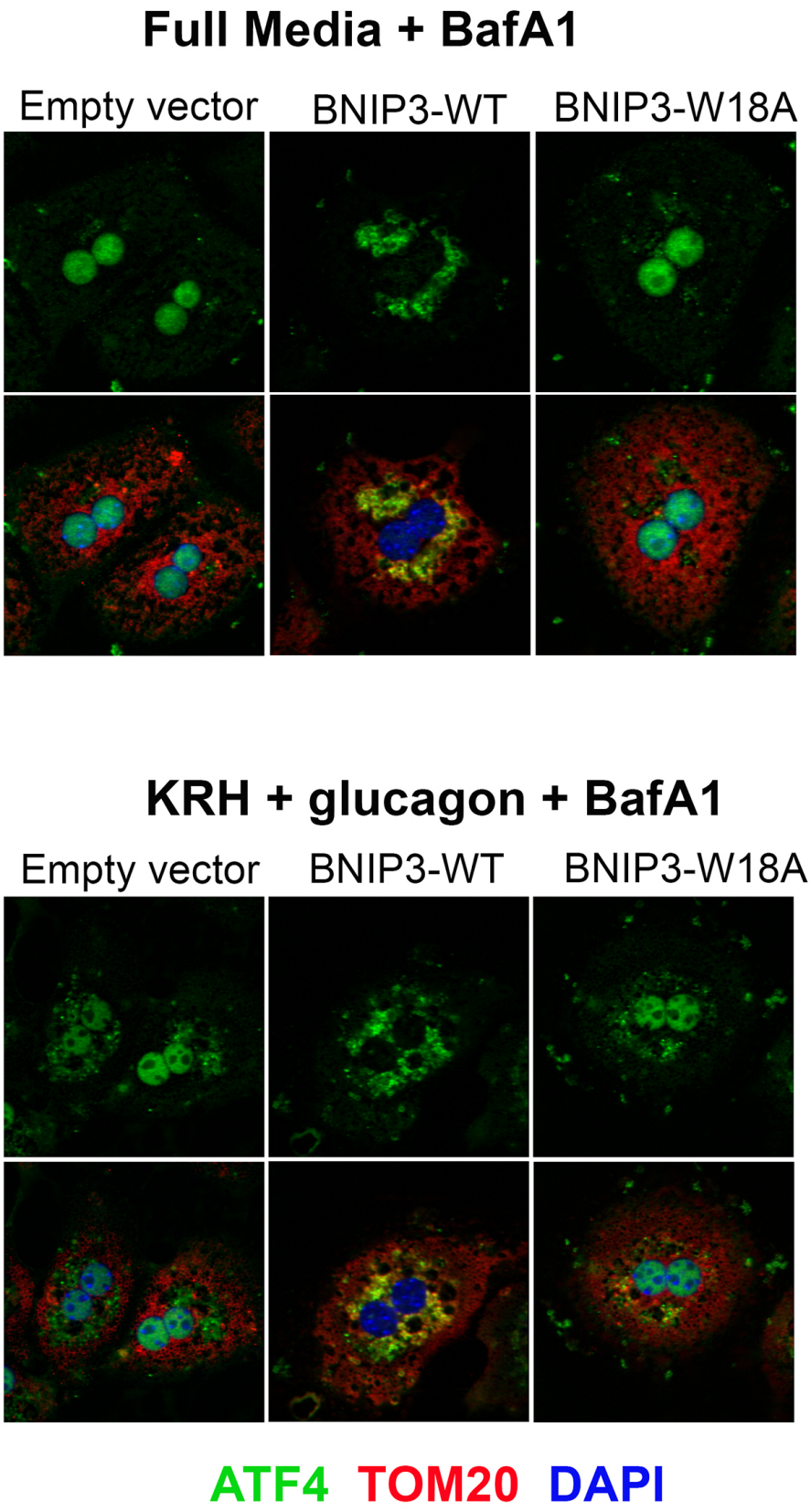

Figure 4.4 BNIP3 promotes the mitochondrial localization of ATF4 in a manner dependent on its ability to bind LC3 and/or ATF4. (continued on next page)

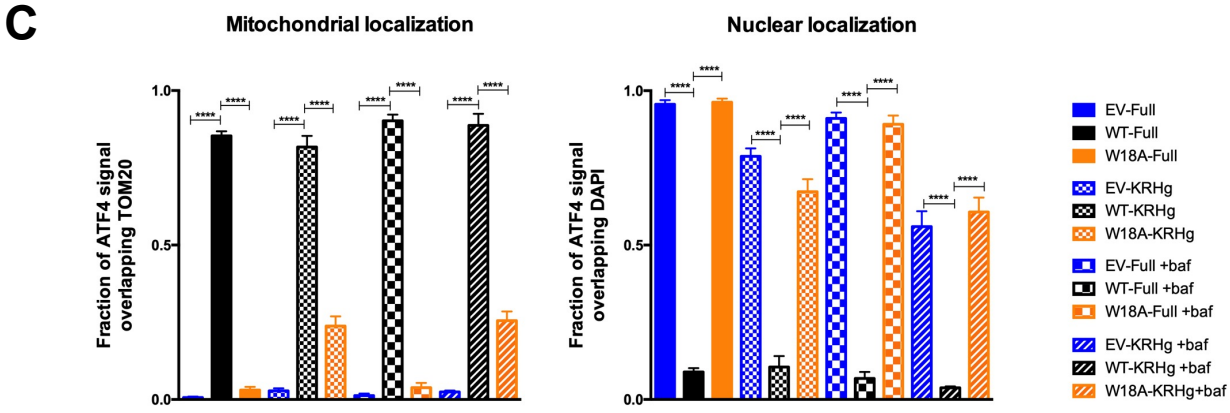

Figure 4.4 BNIP3 promotes the mitochondrial localization of ATF4 in a manner dependent on its ability to bind LC3 and/or ATF4. A) Representative immunofluorescence images of endogenous ATF4 (green) and mitochondrial TOM20 (red) in BNip3 null hepatocytes infected with EV, BNIP3-WT, or BNIP3-W18A adenoviruses, and following incubation in ± KRHg for 6 hours, and B) following treatment with 100 nM BafA1 for 4 hrs. C) Quantification of mitochondrial overlap between ATF4 and TOM20 signals and nuclear overlap between ATF4 and DAPI. Each condition represents the mean ± SEM of 8-10 images.

BNIP3 suppresses ATF4 target gene expression in a manner dependent on its ability to bind LC3 and/or ATF4

We next sought to investigate the downstream functional consequences of the BNIP3-ATF4 interaction for ATF4-dependent gene expression. In primary BNip3 null hepatocytes, overexpression of BNIP3-WT significantly suppressed expression of the ATF4 targets *Asns, Atf3, Fgf21,* and *Ppargc1α* in response to starvation compared to the same cells infected with EV as a control (Figure 4.5) By contrast, over-expression of BNIP3-W18A that cannot bind ATF4 or LC3, failed to show any significant decrease in ATF4 target gene expression compared to EV control infected cells (Figure 4.5). Together, these data indicate that BNip3 suppresses the expression of ATF4 target genes during starvation by sequestering ATF4 at mitochondria, and that this mechanism is dependent on a functional LIR motif in BNIP3.

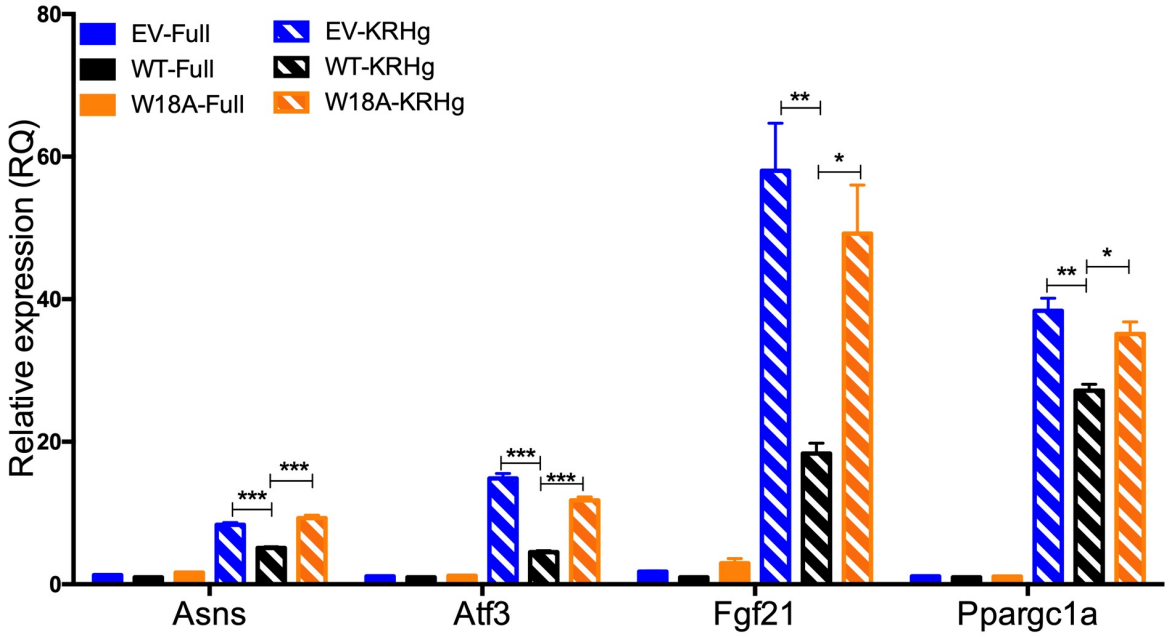

Figure 4.5 BNIP3 promotes suppression of ATF4 target gene expression in fasted hepatocytes in a manner dependent on its ability to bind LC3 and/or ATF4.
Quantitative PCR of ATF4 target genes on cDNA from primary BNip3 null hepatocytes infected with EV or overexpressing BNIP3-WT or BNIP3-W18A, ± KRHg for 16 hrs. Normalized to levels of mouse β-actin. Gene expression was relative to WT-Full. (*p<0.05, **p<0.01, ***p<0.001)

To determine whether these findings obtained in primary hepatocytes might be relevant in transformed cells, we repeated key experiments in the human HepG2 hepatocellular carcinoma cell line. This cell line was selected due to its liver origin, its Hepatitis B- and C-negative status, and because it expresses high levels of endogenous BNIP3 under basal conditions. HepG2-ΔBNIP3 cells over-expressing BNIP3-WT or BNIP3-W18A were generated and analyzed compared to control transfected cells expressing empty vector only (EV). As observed in primary hepatocytes, HepG2-ΔBNIP3 cells overexpressing BNIP3-WT exhibited significantly decreased gene expression of ATF4 gene targets (*ASNS, PPARGC1A, FGF21*) under nutrient stress compared to control EV cells, while overexpression of BNIP3-W18A failed to suppress these genes (Figure 4.6A-B).

Interestingly, *PPARGC1A* encodes PGC1α, the transcriptional co-activator that regulates mitochondrial biogenesis and metabolism, was suppressed by BNIP3-WT nearly 5-fold in the absence of nutrient starvation (Figure 4.6A). This finding was not observed in the primary hepatocytes under full media, and could indicate a potential role for BNIP3 in the coupling of mitophagy to mitochondrial biogenesis and mitochondrial function under basal growth conditions specifically in cancer cells. Indeed, increased PGC1α activity is linked to tumor cell proliferation and metastasis, including liver cancer.[162–164] For the metabolic regulator and stress hormone *FGF21*, KRHg-treated control EV cells and cells overexpressing BNIP3-W18A exhibited a striking 100-fold increase in expression relative to BNIP3-WT expressing cells, which only exhibited a 10-fold increase in expression under KRHg starvation (Figure 4.6B). FGF21 is highly expressed in the liver especially under starvation and as a hormone, is a regulator of systemic metabolism; the significance of its expression in cancer cells is unclear. The level of induction observed in HepG2s may be due to the fact that these cells are of hepatocellular origin, and reflective of the starvation response.

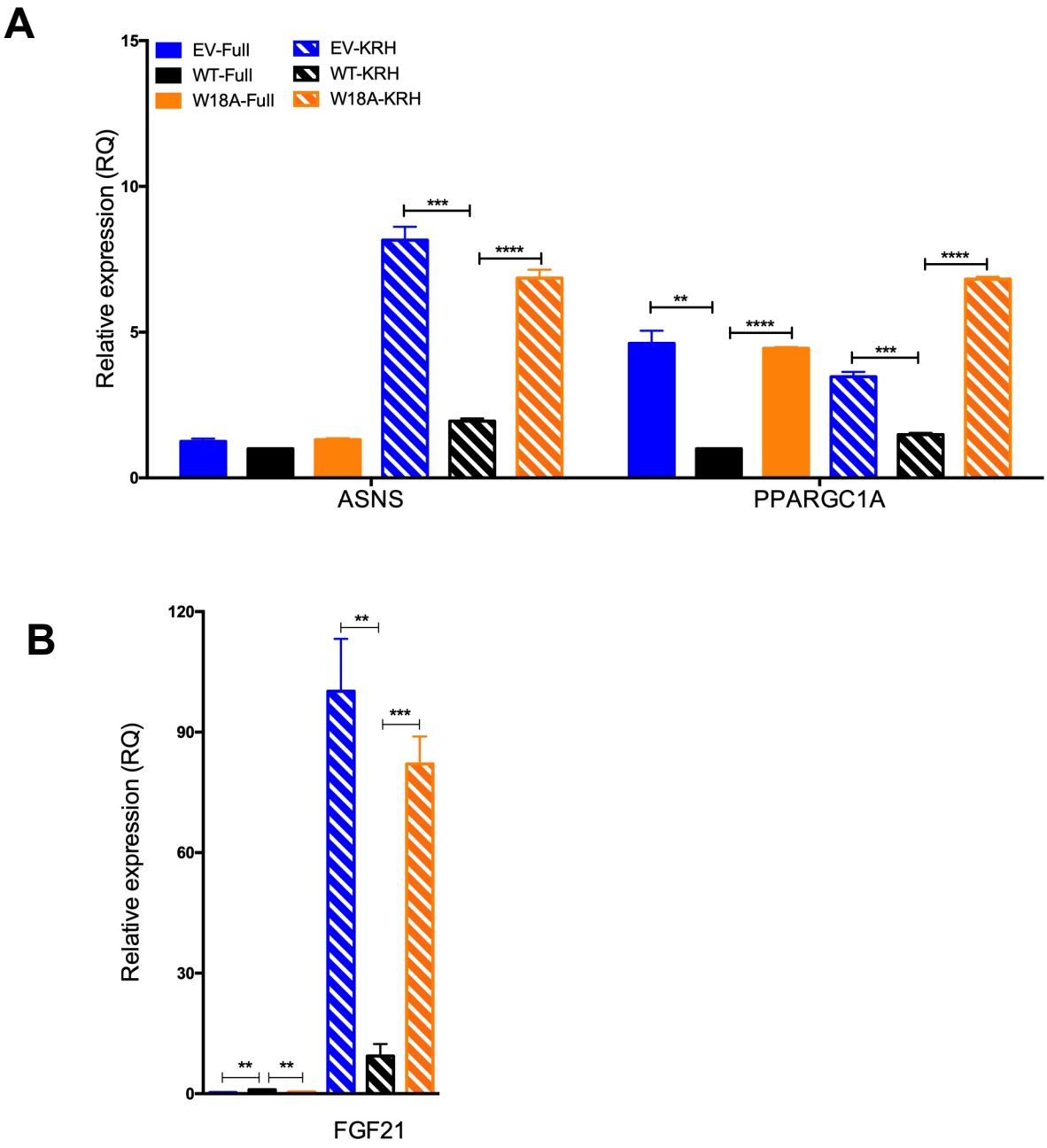

Figure 4.6 BNIP3 suppresses ATF4 target gene expression in human HepG2 cancer cells. A) Quantitative PCR of ASNS and PPARGC1A and B) FGF21, on cDNA from HepG2-ΔBNIP3 cells stably overexpressing EV, BNIP3-WT, or BNIP3-W18A and incubated in ± KRH buffer for 16 hrs. Normalized to levels of human β-actin. Gene expression was relative to WT-Full. (*p<0.05, **p<0.01, ***p<0.001, ****p<0.0001)

Conclusions

In this chapter, I have identified a novel mitochondrial interaction between BNIP3 and ATF4 with functional consequences for gene expression changes in response to nutrient stress. To investigate our prior findings that loss of BNIP3 resulted in significantly increased expression of amino acid biosynthesis genes in response to fasting in the mouse liver, we explored a possible interaction between BNIP3 and the ATF4 nuclear transcription factor, a key transcriptional regulator of the amino acid stress response. In wild-type and BNip3 null murine hepatocytes, ATF4 exhibits altered nuclear and mitochondrial localization patterns under fed and fasted conditions, with BNip3 expression appearing to drive mitochondrial localization of ATF4 under fasting. To our knowledge, this is the first description of mitochondrial ATF4 in mammalian cells. The literature describes ATF4 as a nuclear protein only that is rapidly upregulated at the translational level in response to acute nutrient stress.[86,87] However, our data suggests that high levels of ATF4 are present at basal conditions in hepatocytes and that ATF4 localization at mitochondria may be a specific response to nutrient stress mediated by the mitophagy receptor BNIP3. Given the exceptional metabolic demands of the liver and the greater biomass of mitochondria in hepatocytes, it is possible that this observation may be unique to the liver.

We also confirmed that exogenous HA-BNIP3 coimmunoprecipitates with ATF4-GFP and mapped the region of interaction to the amino terminus of BNIP3. Specifically, mutation of a critical tryptophan residue at position 18 to alanine (W18A) was sufficient to significantly reduce pull-down of BNIP3 with ATF4. Notably, this is the same mutation that ablates the interaction of BNIP3 and LC3, thereby inhibiting BNIP3-mediated mitophagy. In addition to our novel observation of ATF4 mitochondrial localization, this finding indicates a possible role for BNIP3 in the turnover of ATF4 by mitophagy. ATF4 is known to regulate autophagy as an adaptive response to prolonged stress, such as by transcriptional upregulation of ULK1 and LC3 in

cancer cells.[86,100,101,154] A direct role for ATF4 in mediating mitophagy or being turned over at mitophagosomes has not been described and will be addressed in the next chapter.

We observed that while ATF4 was nearly exclusively nuclear in BNip3 null hepatocytes, overexpression of BNIP3-WT was sufficient to prevent nuclear localization of ATF4, and ATF4 was predominantly observed at perinuclear mitochondria in both fed and fasted conditions. Colocalization of ATF4 and TOM20 at mitochondria was also significantly increased following treatment with the lysosomal inhibitor, BafA1. BNIP3-W18A expressing cells exhibited a similar phenotype to control cells, consistent with the abrogation of the interaction between ATF4 and BNIP3 limiting the perinuclear mitochondrial localization of ATF4. The functional consequences of altered sub-cellular localization of ATF4 for ATF4 target gene expression were addressed in both primary mouse hepatocytes and in human HepG2 liver cancer cells, with ATF4 target gene expression suppressed by expression of BNIP3-WT but not by BNIP3-W18A in both systems. Together, these data demonstrate the functional significance of ATF4 sequestration away from the nucleus to the mitochondria, specifically in response to nutrient starvation, for both dividing and non-dividing cells. In the next chapter, we will further investigate the consequences of this BNIP3-ATF4 interaction for cellular stress responses, cellular metabolism and cell growth.

CHAPTER 5

THE INTERACTION OF BNIP3, ATF4, AND LC3 IN MITOPHAGY, MITOCHONDRIAL STRESS RESPONSES, AND METABOLISM

Introduction

In the previous chapter, we described our novel finding that ATF4 localizes to the mitochondria in a BNIP3-dependent manner. We also showed that BNIP3 interacts with ATF4 at mitochondria in a manner dependent on a functional LIR motif in BNIP3, and that this interaction is crucial for promoting mitochondrial localization of ATF4, and suppression of ATF4 target gene transcription in the nucleus, in response to nutrient starvation. These findings indicated a possible function for ATF4 and BNIP3 in autophagy, and more specifically, mitophagy, in response to nutrient deprivation.

Given its emerging role in mitochondrial stress, it is possible that ATF4 is linked to the role of BNIP3 in mitophagy and maintaining mitochondrial fitness in response to stress, including nutrient deprivation. In addition to their role in respiration and production of ATP, mitochondria also serve as biosynthetic factories, producing macromolecules such as nucleotides and amino acids that are crucial for maintaing cellular homeostasis, and thus cell survival and proliferation.[165,166] A recent study has implicated ATF4 in mediating the mitochondrial stress response in mammalian cells, involving a mechanism that activates amino acid biosynthesis genes.[124] Our investigation of the BNIP3-ATF4 interaction could shed light on whether BNIP3-dependent mitophagy controls ATF4-mediated cellular stress responses to nutrient deprivation and explain how cells switch from deriving amino acids by *de novo* synthesis to via autophagy.

In this chapter, we examined the significance of the BNIP3-ATF4 interaction for cellular adaptation and survival under nutrient replete and starvation conditions, both in non-dividing primary mouse hepatocytes and in human HepG2 liver cancer cells. We examined the

consequences of disrupting the BNIP3-ATF4 interaction for rates of mitophagy, mitochondrial metabolism, cancer cell proliferation, amino acid biosynthesis, and mitochondrial stress. Finally, we identified two different molecular weight forms of ATF4 that localize to either the nucleus or the mitochondria, and examined their expression in primary human tumor sections.

The interaction of HA-BNIP3 with ATF4-GFP is enhanced upon inhibition of autophagy

Our prior coimmunoprecipitation studies elucidated a novel interaction between BNIP3 and ATF4 that is significantly decreased upon mutation of tryptophan 18 to alanine, which also disrupts the interaction between BNIP3 and LC3, thereby inhibiting BNIP3-dependent mitophagy. In order to determine the relevance of the BNIP3-ATF4 interaction for rates of autophagy, we performed coimmunoprecipitation experiments in the presence or absence of BafA1. Given that BNIP3 is turned over by mitophagy, we expected to see increased levels of HA BNIP3-WT when autophagy is inhibited. Indeed, increased levels of input HA- BNIP3-WT were detected in the presence of BafA1, resulting in increased pulldown of BNIP3-WT with ATF4-GFP (Figure 5.1, lane 1 vs. 2, lane 5 vs. 6). BafA1 treatment had no effect on BNIP3-W18A, which did not coimmunoprecipitate with ATF4-GFP despite increased input levels relative to HA-BNIP3-WT, consistent with our previous pulldown experiments (Figure 5.1, lane 3 vs. 4, lane 7 vs. 8). This result indicates that the BNIP3-ATF4 complex is turned over by autophagy.

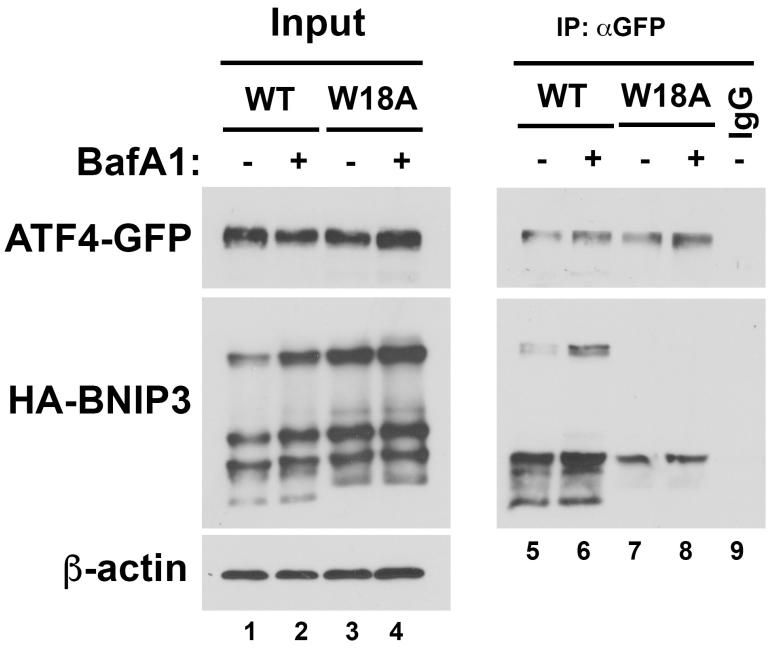

Figure 5.1 The interaction of HA-BNIP3 with ATF4-GFP is enhanced by autophagy inhibition. Coimmunoprecipitation in 293T-ΔBNIP3 cells stably over-expressing ATF4-GFP, transiently over-expressing HA-BNIP3-WT or HA-BNIP3-W18A, ± 100 nM BafA1 for 4 hrs.

BNIP3, ATF4, and LC3 interact in a tri-molecular complex that is turned over by autophagy

Having established that ATF4 localizes to the mitochondria and binds to BNIP3 in a manner dependent on the LC3-interacting region of BNIP3, we next sought to establish a link between ATF4 and other components of the autophagy machinery. In order to investigate whether ATF4 interacts with LC3 as well as BNIP3, we performed coimmunoprecipitation and western blot analysis in 293T-ΔBNIP3 cells overexpressing ATF4-GFP, DsRed-LC3, and HA-BNIP3-WT or HA- BNIP3-W18A, in the presence or absence of BafA1. We also included a condition with EV in lieu of HA-BNIP3, to test whether BNIP3 is required for the interaction between ATF4 and LC3. We observed increased input levels of ATF4 in the EV condition relative to the WT and W18A conditions, indicating that expression of BNIP3 may act to decrease ATF4 protein, potentially via mitophagy (Figure 5.2). We also found that DsRed-LC3 coimmmunoprecipitated with ATF4-GFP regardless of whether BNIP3 was co-expressed and in a manner that increased with autophagy inhibition. We observed the greatest pull-down of DsRed-LC3 with co-expression of HA- BNIP3-WT, while expression of HA- BNIP3-W18A resulted in an intermediate pulldown that was unaffected by BafA1 treatment (Figure 5.2). These findings demonstrated that while BNIP3 is not required for the interaction between LC3 and ATF4, expression of BNIP3-WT promotes this interaction significantly and that this in turn promotes ATF4 turnover by autophagy since levels of the LC3-ATF4 complex are markedly increased in the presence of BNIP3-WT when autophagy is inhibited. Taken together, these data indicate that BNIP3, ATF4, and LC3 interact in a tri-molecular complex that is turned over by autophagy. Given that BNIP3 is exclusively mitochondrial and that ATF4 localized to mitochondria in a BNIP3-dependent manner, this further indicates that ATF4 is being turned over specifically by mitophagy and that ATF4 localizes specifically to mitophagosomes (autophagosomes engaged predominantly in mitophagy).

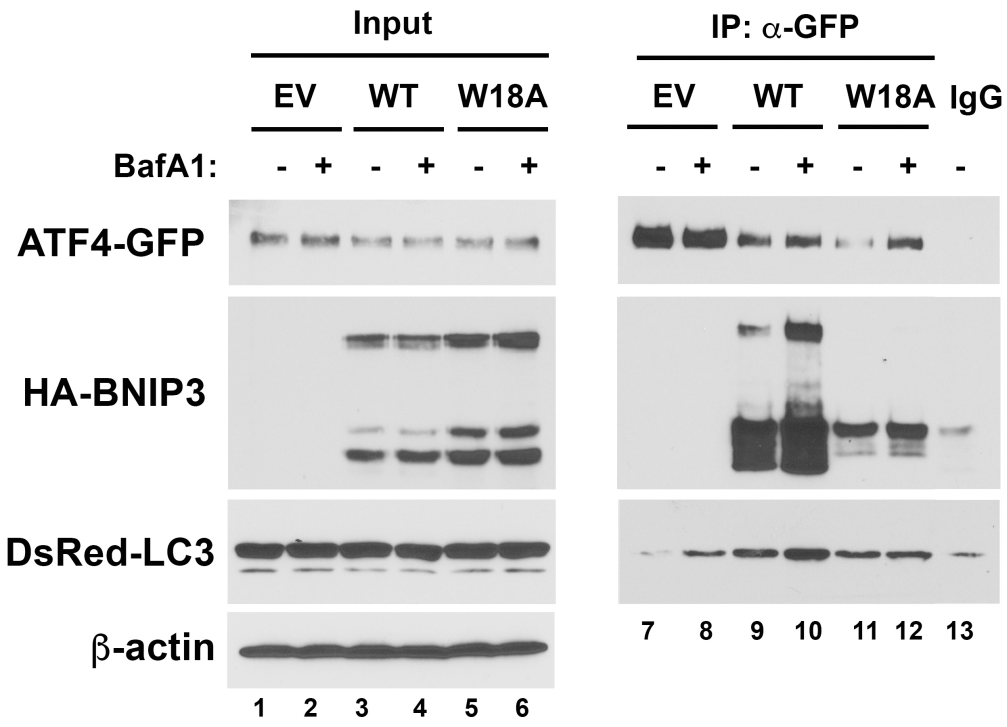

Figure 5.2 BNIP3 is not required for but is sufficient to promote the interaction of LC3 with ATF4. Coimmunoprecipitation in 293T-ΔBNIP3 cells stably over-expressing ATF4-GFP and transiently over-expressing DsRed-LC3 and either HA-BNIP3-WT, HA-BNIP3-W18A, or EV, ± 100 nM BafA1 for 4 hrs.

ATF4 localizes to mitophagosomes in a BNIP3-dependent manner

Using immunofluorescence and confocal microscopy, we next investigated how BNIP3 expression affected the interaction of endogenous LC3 and ATF4 in BNip3 null primary mouse hepatocytes overexpressing BNIP3-WT, or BNIP3-W18A and following treatment in full media or KRHg starvation buffer, in the presence of absence of BafA1 (Figure 5.3 A-D). Unexpectedly, we observed striking differences in LC3 localization and protein expression. Under full media conditions, LC3 was detected primarily in the nucleus in control EV cells or in cells expressing BNIP3-W18A, while overexpression of BNIP3-WT markedly induced cytosolic localization of LC3 (Figure 5.3A). This result indicates that BNIP3-WT is sufficient to promote trafficking of LC3 to puncta outside of the nucleus under fed conditions. LC3 has been previously observed in the nucleus in an acetylated form that redistributes to the cytoplasm in response to nutrient deprivation as a result of its de-acetylation.[167] Our results indicate that overexpression of BNIP3-WT phenocopies the effects of nutrient deprivation on LC3 localization, independent of nutrient conditions.

Following BafA1 treatment, the localization of LC3 to the cytoplasm was further enhanced (Figure 5.3B). Specifically, treatment of cells with BafA1 (Figure 5.3B, lower panel) increased the amount of cytosolic LC3 detected when BNIP3-WT was over-expressed, suggesting that LC3 was being effectively turned over by autophagy in response to BNIP3-WT over-expression. This effect was not seen in control EV cells or when BNIP3-W18A was over-expressed indicating that the ability of BNIP3 to interact with LC3 was required for its effect on the cytoplasmic localization of LC3. Interestingly, the overall levels of LC3 were less when BNIP3-W18A was expressed for reasons that will be discussed below.

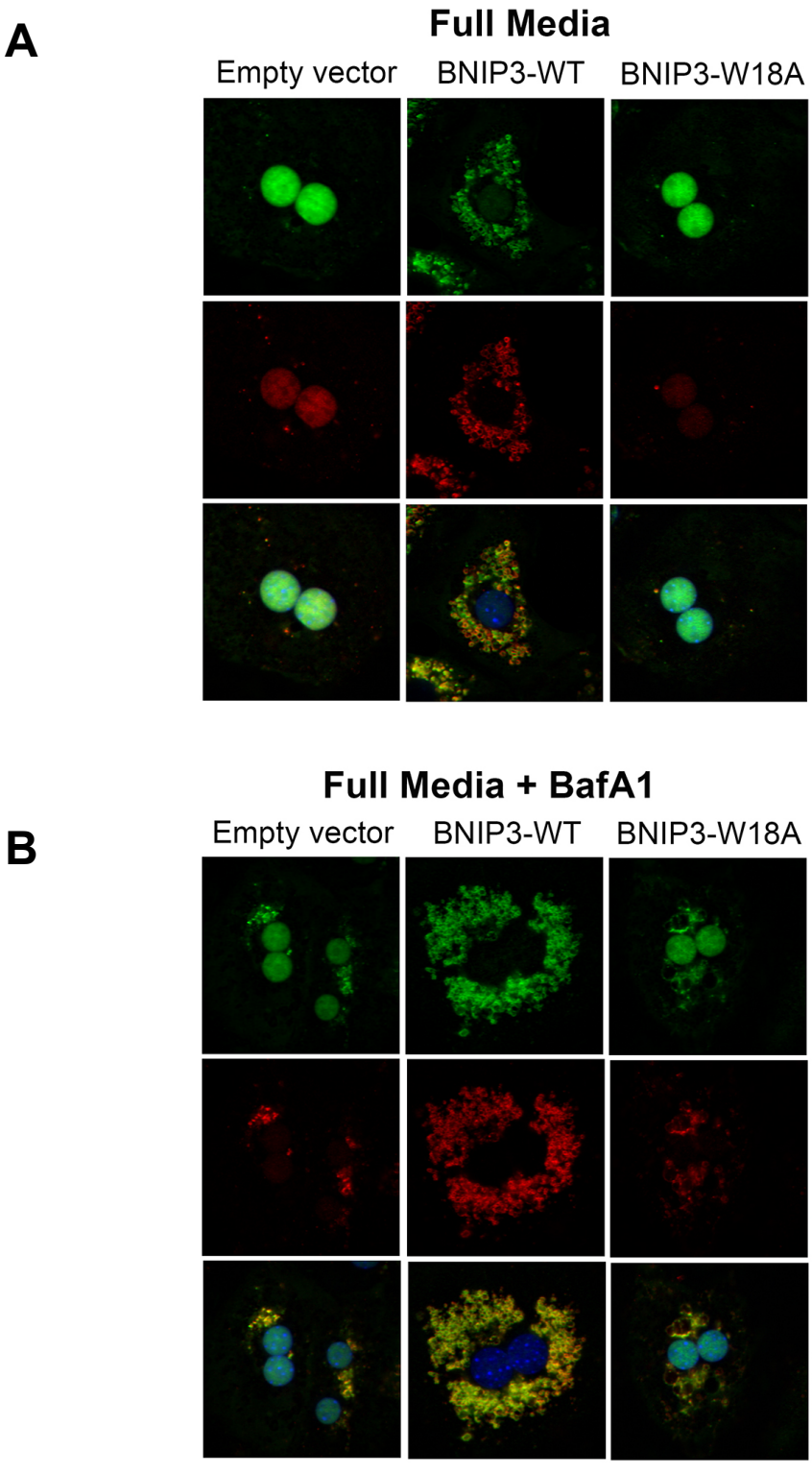

Figure 5.3 ATF4 localizes to mitophagosomes in a BNIP3-dependent manner in primary mouse hepatocytes. (Continued below)

Nutrient deprivation (KRHg conditions in Figure 5.3 C-D) induced cytosolic localization of LC3 independent of BNIP3, with fasted control EV cells showing a significant increase in cytosolic LC3 compared to EV cells under fed conditions (Figure 5.3 A). Expression of BNIP3-WT increased the amount of LC3 detected in the cytosol in response to nutrient deprivation that was further increased by treatment with BafA1 (Figure 5.3 D). This result indicated that while BNIP3 was not required for LC3 trafficking to the cytosol in response to nutrient deprivation, it did promote LC3 turnover and mitophagy in response to nutrient deprivation (Figure 5.3 C-D). The effect of BafA1 was less striking when BNIP3-W18A was expressed consistent with mitophagy requiring the interaction between LC3 and BNIP3.

When we examined how BNIP3-WT or BNIP3-W18A affected ATF4 and LC3 sub-cellular localization, we observed increased overlap between ATF4 and LC3 in the cytoplasm when BNIP3-WT was expressed compared to EV control cells, with almost no nuclear ATF4 detected when BNIP3-WT was expressed, as described previously in Chapter 4. Also as described in Chapter 4, ATF4 remained predominantly nuclear when BNIP3-W18A was over-expressed and unlike BNIP3-WT, BNIP3-W18A failed to induce mitochondrial localization of ATF4 (Figure 5.3 A). Most significantly here, statistical colocalization analysis showed an almost perfect overlap of all cytosolic ATF4 with LC3 staining in the cytosol when BNIP3-WT was expressed but not with BNIP3-W18A over-expression, which was further enhanced by treatment with BafA1 (Figure 5.3 E). This indicates that ATF4 is localizing with LC3 specifically to mitochondria that are undergoing mitophagy and that this is dependent on BNIP3-WT and the ability of BNIP3-WT to interact with ATF4 and/or LC3 via its conserved LIR motif.

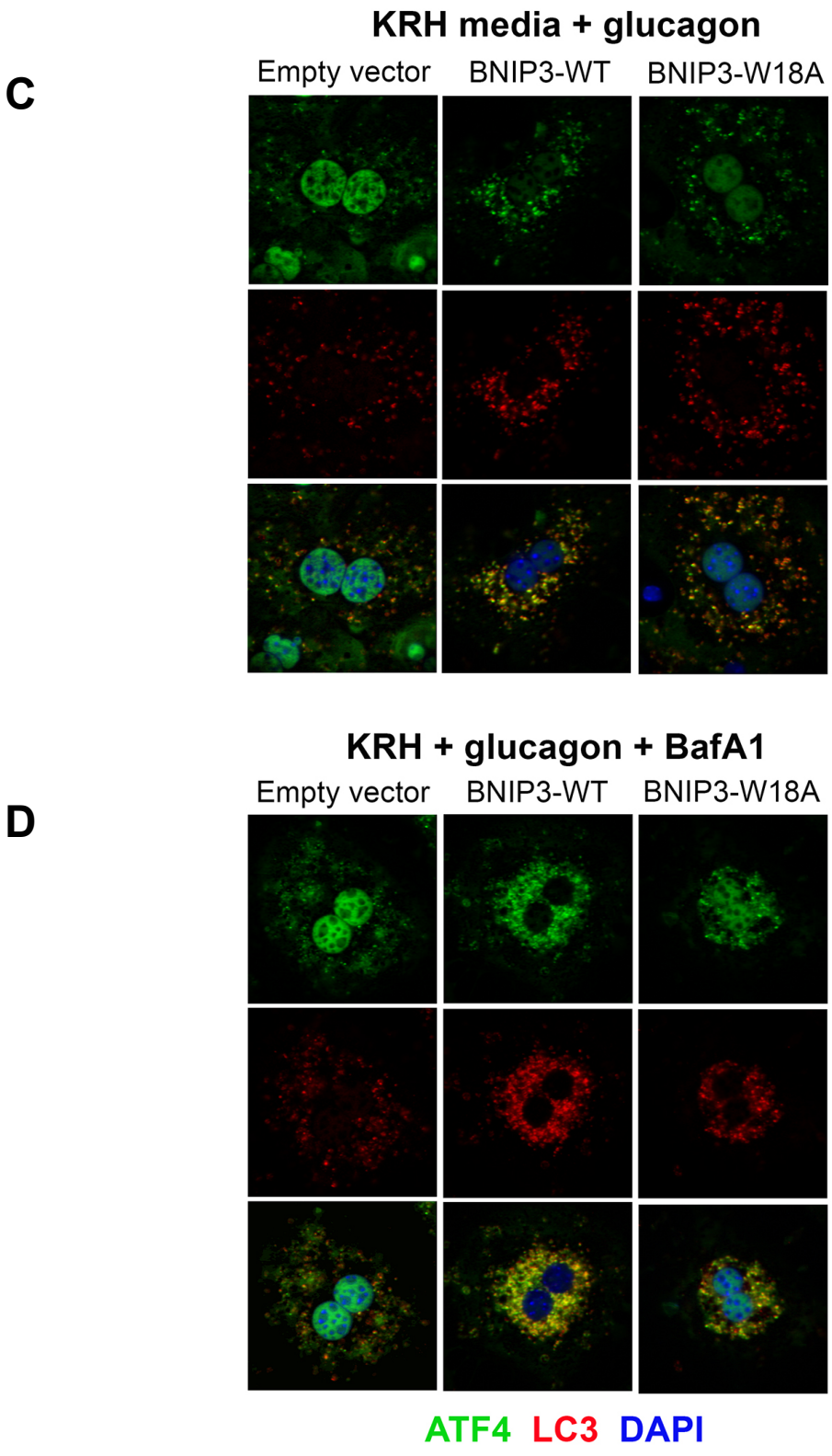

Figure 5.3 ATF4 localizes to mitophagosomes in a BNIP3-dependent manner in primary mouse hepatocytes. (Continued below)

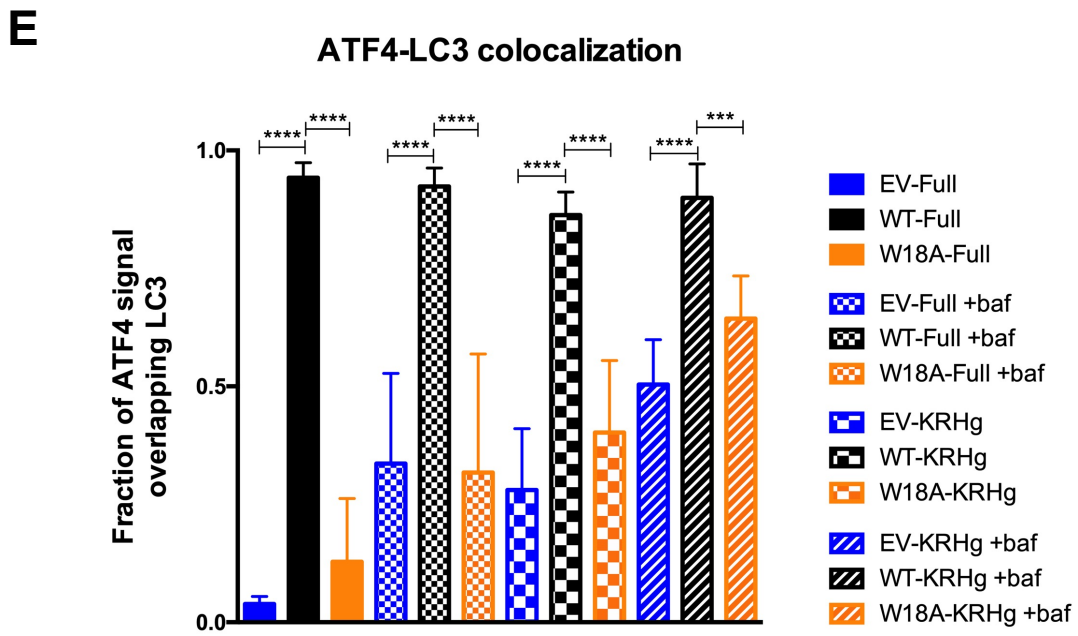

Figure 5.3 ATF4 localizes to mitophagosomes in a BNIP3-dependent manner in primary mouse hepatocytes. (Continued below)

Next, we performed a complementary analyses in which ATF4 and Lamp1, a lysosomal marker, were assessed by immunofluorescence under the same treatment conditions (Figure 5.3 F-I). Colocalization analysis revealed a statistically significant overlap between ATF4 and Lamp1 (Figure 5.3J). We observed approximately 60% of the total ATF4 is signal in BNIP3-WT-expressing cells was colocalized to LAMP1 (Figure 5.3 F-I), in contrast to control EV and BNIP3-W18A-expressing cells, which only exhibited increased signal overlap (20-60%) upon starvation ± BafA1 treatment (Figure 5.3 H-I). This increase in overlap under these conditions indicates that ATF4 was being turned over by autophagy at the lysosome in a manner that did not require BNIP3-WT but was significantly enhanced by it (Figure 5.3 J).

Taken together with the LC3 interaction studies and our studies showing overlap of ATF4 with TOM20 at mitochondria in Chapter 4, our findings indicate that ATF4 localizes to mitophagosomes in a BNIP3-dependent manner. While BNIP3 is not essential for ATF4 localization at mitophagosomes, as ATF4 can co-localize with LC3 and LAMP1 in response to nutrient deprivation ± in control EV cells that lack BNIP3, it does markedly increase their co-localization and the number of mitophagosomes detected.

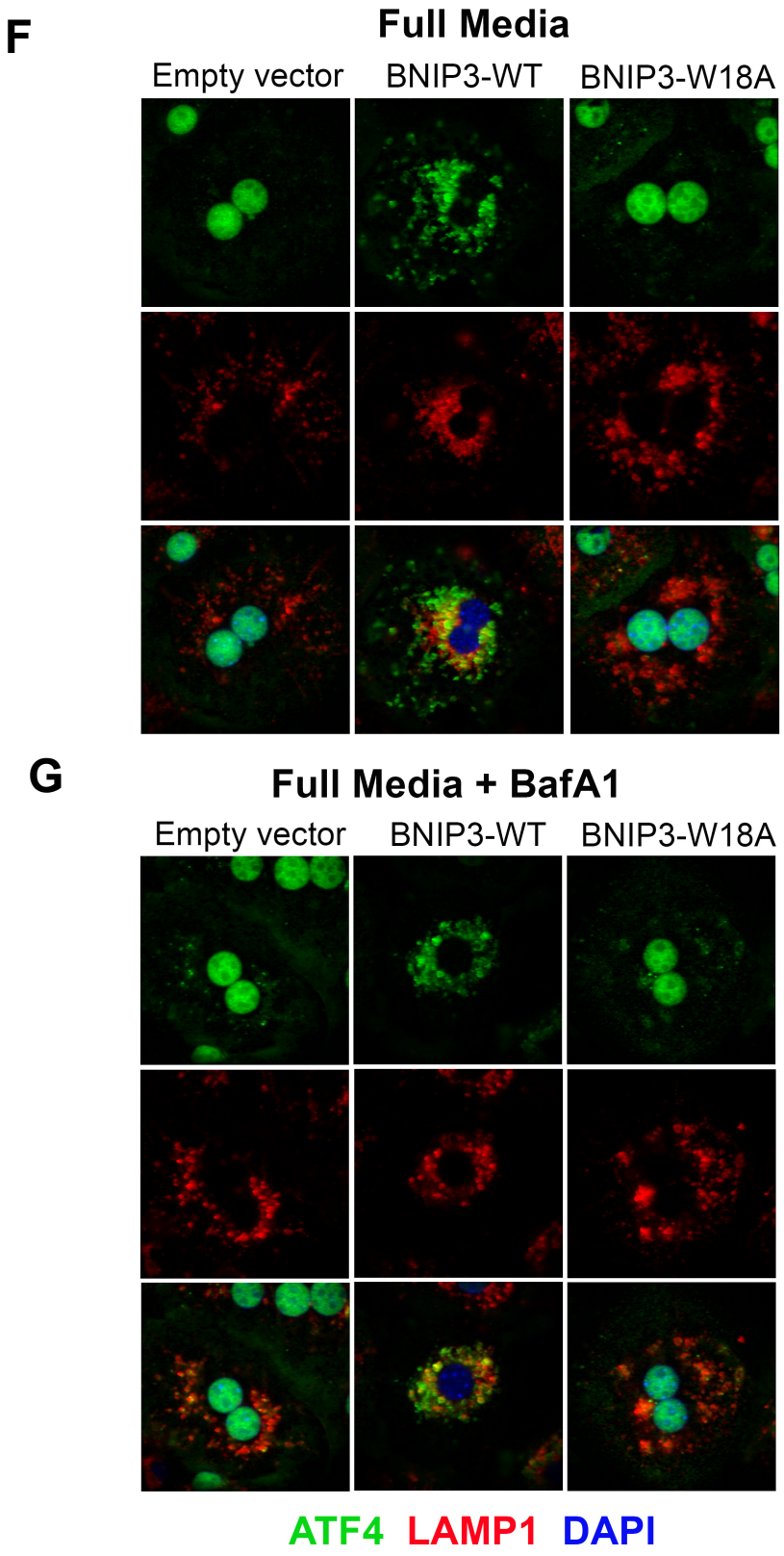

Figure 5.3 ATF4 localizes to mitophagosomes in a BNIP3-dependent manner in primary mouse hepatocytes. (Continued below)

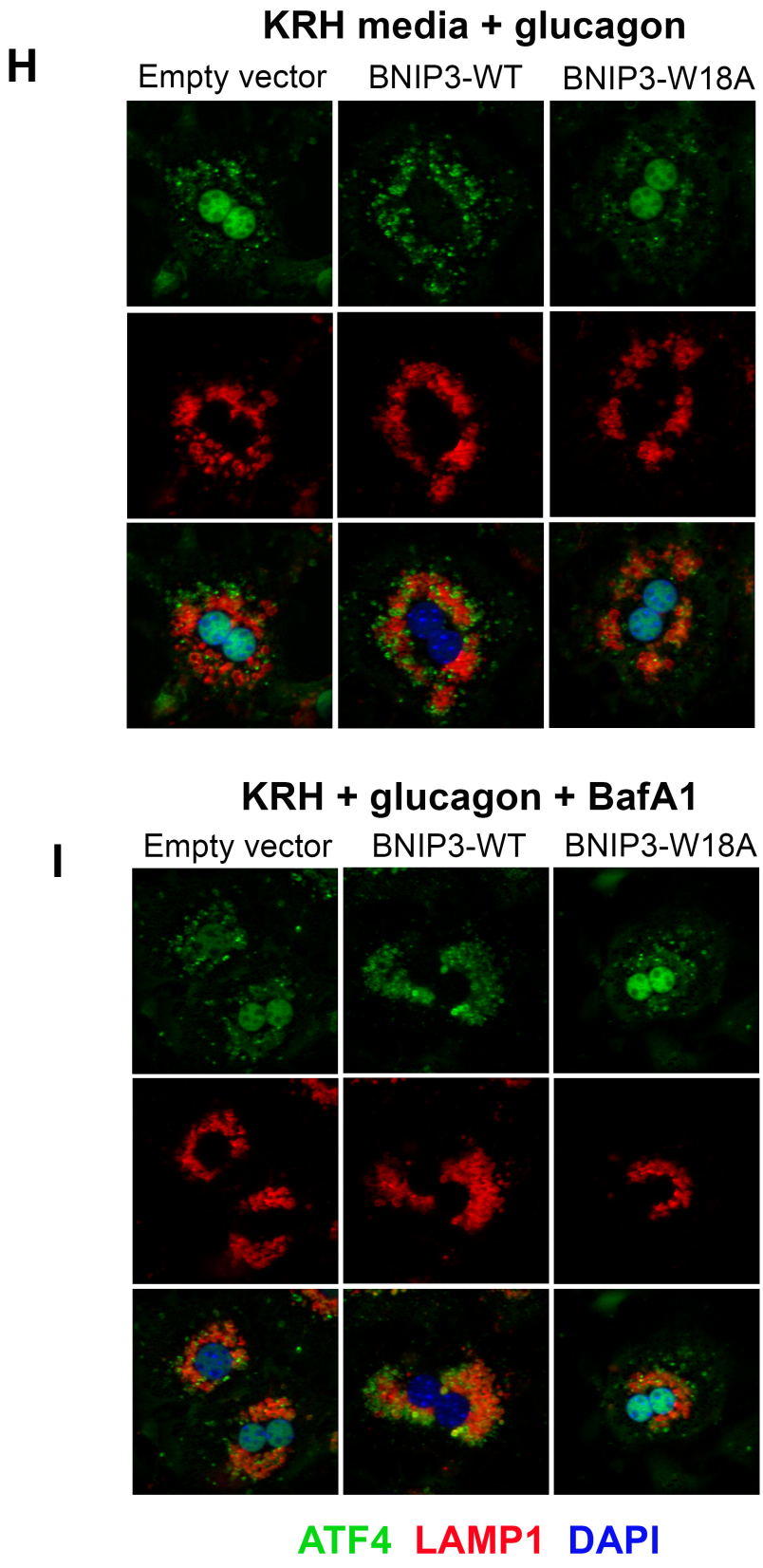

Figure 5.3 ATF4 localizes to mitophagosomes in a BNIP3-dependent manner in primary mouse hepatocytes. (Continued below)

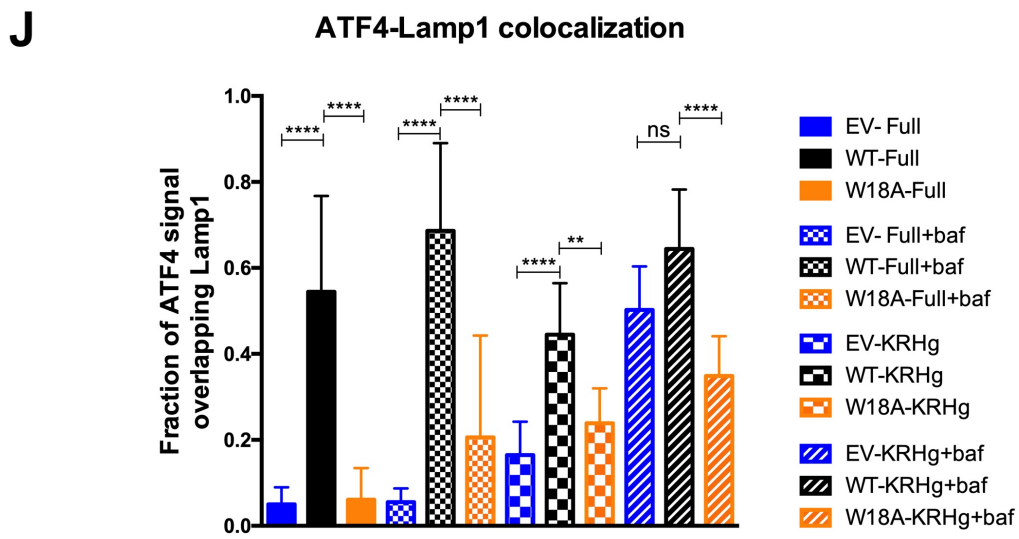

Figure 5.3 ATF4 localizes to mitophagosomes in a BNIP3-dependent manner in primary mouse hepatocytes. Representative immunofluorescence images of endogenous ATF4 (green) and LC3 (red) in BNip3 null hepatocytes infected with EV, BNIP3-WT, or BNIP3-W18A adenoviruses, and following incubation in A) full media, B) full media + 100nM BafA1 for 4 hrs, C) KRHg starvation media for 6 hours, and D) KRHg + 100 nM BafA1. E) Quantification of mitochondrial overlap between ATF4 and LC3 signals. F-I) Representative images of ATF4 (green) and LAMP1 (red) in above conditions, and J) Quantification of lysosomal overlap (Lamp1) and ATF4. Each condition represents the mean ± SEM of 8-10 images. (**p<0.01, ****p<0.0001)

LC3 is not required for the interaction of BNIP3 and ATF4

BNIP3 is a small 21.4 kDa protein with defined functional domains at its amino and carboxy termini. Given that the function of its LIR motif has been well-established in the field and in our own studies, we considered the possibility that BNIP3 cannot bind both ATF4 and LC3 at the same time and that BNIP3 may not be directly binding to ATF4. Instead, we speculated that their interaction may be indirectly mediated by separate interactions with LC3 (ATF4 with LC3, and BNIP3 with LC3) with LC3 being the central protein mediating complex formation, which would also explain the abrogated pulldown of BNIP3-W18A with ATF4. To assess the requirement for LC3 in the interaction between BNIP3 and ATF4, we performed a coimmunoprecipitation in parental 293T cells or 293T cells genetically deleted for LC3 via CRISPR-mediated gene editing (293T-ΔLC3). We found that in cells lacking LC3, HA-BNIP3 was still able to effectively co-immunoprecipitate with ATF4-GFP (Figure 5.4, lanes 7&8). However, overall levels of HA-BNIP3 and ATF4-GFP were increased in 293T-ΔLC3 cells, indicating that these proteins are accumulating in LC3-deficient cells due to a blockage in autophagy (Figure 5.4, lanes 1&2 vs. lanes 3&4). Overall, these results indicate that while we have observed a novel interaction between LC3 and ATF4, LC3 is not required for the BNIP3-ATF4 interaction, although LC3 is required for turning these proteins over through mitophagy. In summary, BNIP3 can interact with ATF4 independent of LC3, and LC3 can interact with ATF4 independent of BNIP3, but BNIP3 strongly promotes the ATF4-LC3 interaction, BNIP3 promotes cytoplasmic localization of ATF4 and LC3, and both BNIP3 and LC3 are required for the turnover of ATF4 by mitophagy.

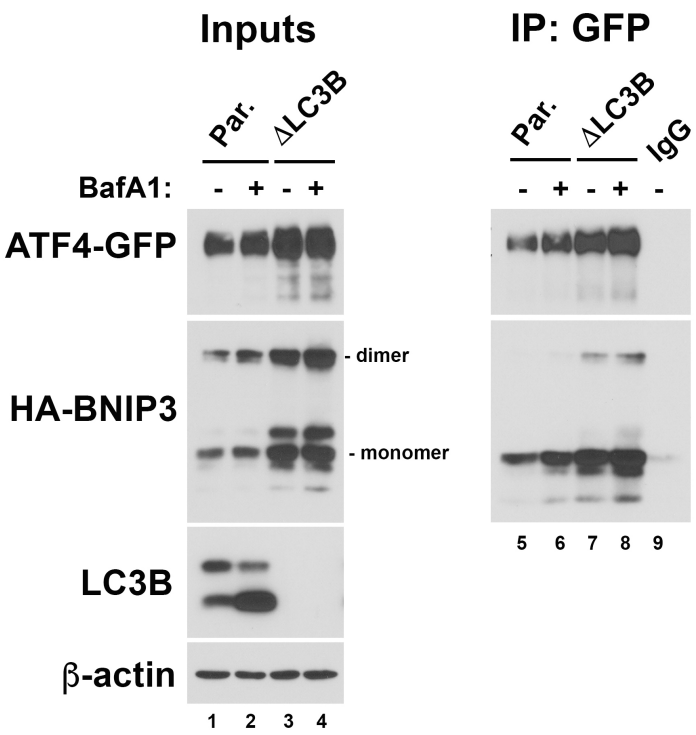

Figure 5.4 LC3 is not required for the interaction of BNIP3 and ATF4.
Coimmunoprecipitation in parental 293T cells or 293TΔLC3 cells stably over-expressing ATF4-GFP and transiently over-expressing HA-BNIP3-WT, ± 100 nM BafA1 for 4 hrs.

Overexpression of BNIP3 suppresses oxygen consumption and extracellular acidification rates in HepG2 cancer cells

Given the function of BNip3 in reducing mitochondrial mass via mitophagy, we next examined the downstream effects on mitochondrial function by measuring oxygen consumption rates (OCR) in human HepG2-ΔBNIP3 cancer cells overexpressing BNIP3-WT or BNIP3-W18A in comparison to control EV cells. Over-expressing BNIP3-WT suppressed basal OCR by approximately 2-fold in HepG2-ΔBNIP3 cells compared to control EV HepG2-ΔBNIP3 (Figure 5.5 A-B). Cells expressing BNIP3-WT also exhibited a 2-fold reduction in the maximal OCR compared to control EV cells (Figure 5.5 A, C). The reduced maximal OCR observed in BNIP3-WT expressing cells is consistent with a reduction in mitochondrial mass due to BNIP3-dependent mitophagy in line with our previous work examining OCR in primary hepatocytes from wild-type and BNip3 null mice.[38]

Expression of exogenous BNIP3-W18A did not suppress either basal or maximal OCR to the same extent as exogenous BNIP3-WT but did have a statistically significant (<2-fold) effect on basal OCR in particular, compared to control EV HepG2-ΔBNIP3 (Figure 5.5A-C). This suggests that BNIP3-W18A, while defective for LC3 and ATF4 binding, maintains residual functional activity unrelated to the role of BNIP3 in LC3 binding and mitophagy, or indeed control of ATF4 binding and turnover. This could involve interactions of BNIP3 with other mitochondrial proteins, including NIX, Bcl-x_L, Bcl-2, Rheb, VDAC, and OPA1.[41,44,168,169]

To complement our measurement of mitochondrial respiration rates, we also examined the extracellular acidification rates (ECAR) due to proton release. This is an indirect measure of lactate production and rates of glycolysis, which we previously found altered in primary BNip3 null mammary tumor cells.[28] We found that over-expressing BNIP3-WT in HepG2-ΔBNIP3 cells significantly reduced lactate production compared to control EV HepG2-ΔBNIP3 cells, consistent with our previous findings that BNIP3 limits lactate production by promoting

mitochondrial oxidation of glucose-derived carbon substrates. Surprisingly, over-expressing BNIP3-W18A in HepG2-ΔBNIP3 cells also reduced lactate production compared to control EV HepG2-ΔBNIP3 cells, with no statistical difference between the effect of BNIP3-WT and BNIP3-W18A on ECAR observed (Figure 5.5D). These results suggest that BNIP3 can reduce lactate production in a manner independent of its role in LC3-mediated mitophagy.

These data contrast with previously published work from our laboratory in primary mammary tumor lines, in which BNIP3-WT expression significantly increased oxygen consumption compared to BNip3 null cells.[28] In that study, BNIP3 reduced mitochondrial mass and limited the accumulation of damaging ROS and the Warburg effect, thereby increasing overall mitochondrial fitness and efficiency of oxidative metabolism compared to BNip3 null cells.[28] Our findings could be due to the unique dependence of the liver on aspects of mitochondrial metabolism and/or a phenotype that may be due to using a specific cell line, in this case HepG2 cells, which may have accumulated significant changes while in culture.

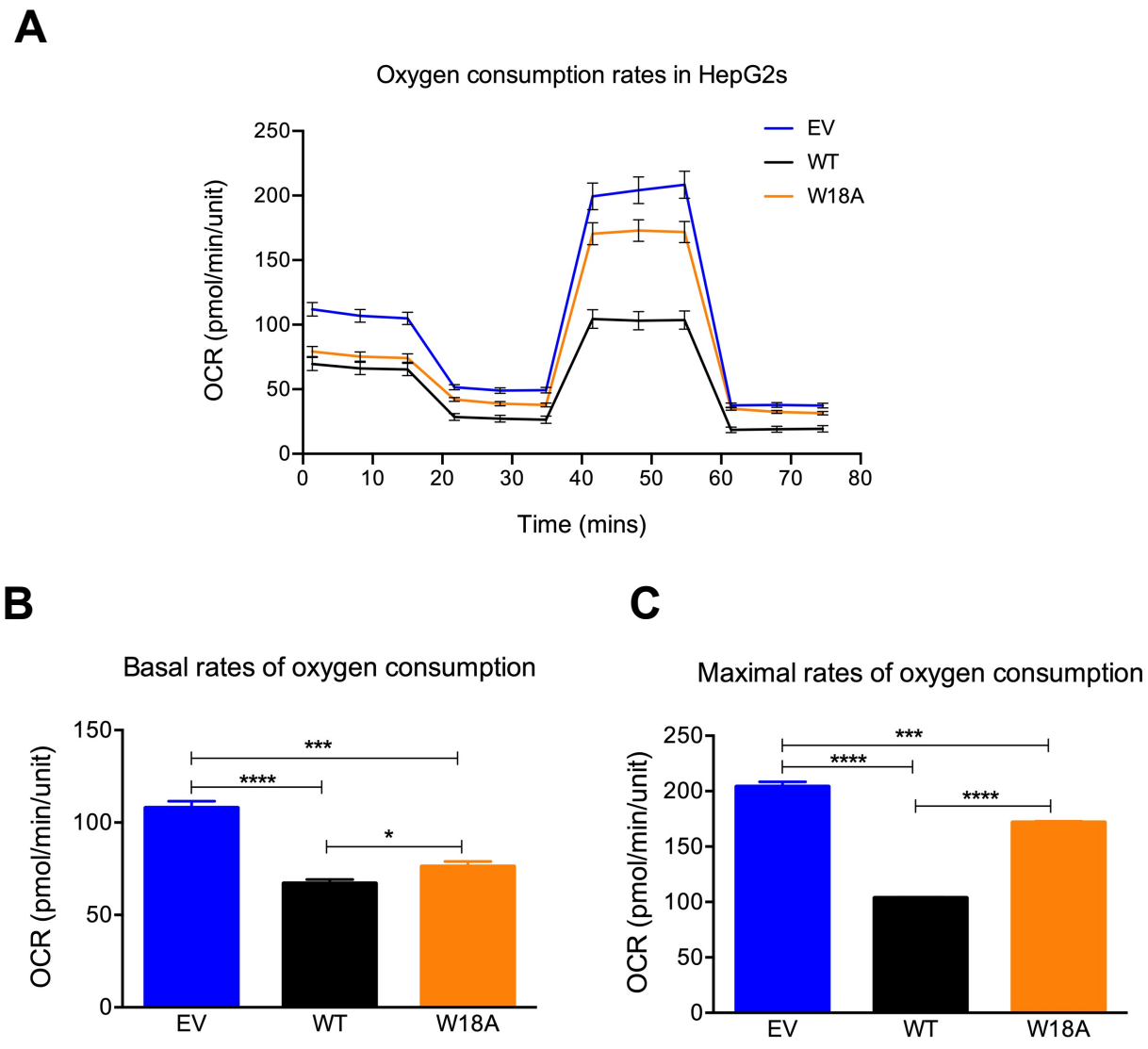

Figure 5.5 BNIP3-WT decreases oxygen consumption and extracellular acidification rates in HepG2 cancer cells. A) Oxygen consumption rate in EV-, HA-BNIP3-WT-, and HA-BNIP3-W18A-expressing HepG2-ΔBNIP3 cells, measured with the cell mito stress test on the XF-96 Seahorse Analyzer. B) Mean of the 3 basal reading and C) mean of the 3 maximal OCR readings. D)mean of 3 ECAR readings. (*p<0.05, **p<0.01, ***p<0.001, ****p<0.0001). Data in Panel A were generated in cooperation with Logan Poole.

D

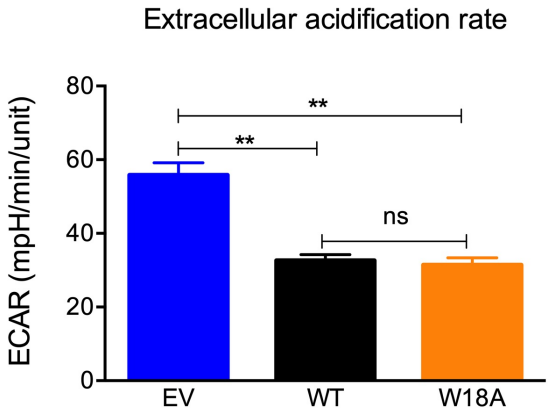

Figure 5.5 (continued)

BNIP3 suppresses growth of HepG2 tumor cells in manner partially dependent on its ability to bind LC3 and/or ATF4

Both published and unpublished work from our laboratory has established a growth suppressive function for BNIP3 in cell lines *in vitro* and mouse tumor models *in vivo*.[28] However, it is unclear to what extent the role of BNIP3 in mitophagy plays in its growth suppressive activity. Cancer cells exhibit unique metabolic demands as a result of the scarce resources encountered in the tumor microenvironment, which may be insufficient to support their rapid proliferation. ATF4 has emerged as a driver of tumor-promoting processes, specifically mediating the adaptive responses to amino acid limitation, oxidative stress, and ER stress.[143,152,155,157,170–174] Having established that BNIP3 suppresses ATF4 target genes in HepG2 cancer cells in response to starvation, we next investigated whether this interaction was necessary to suppress proliferation in HepG2-ΔBNIP3 tumor cells under basal growth conditions. We overexpressed BNIP3-WT or HA-BNIP3-W18A in HepG2-ΔBNIP3 tumor cells and examined log-phase growth over 7 days in comparison to control HepG2-ΔBNIP3 tumor cells stably transfected with EV.

Consistent with our previous observations in other systems, we observed a significant 7-fold decrease in growth in cells overexpressing BNIP3-WT compared to control EV cells (Figure 5.6). Interestingly, exogenous BNIP3-W18A also suppressed cell growth by approximately 2-fold compared to EV control cells, which while not as marked as the effect of BNIP3-WT, was statistically significant (Figure 5.6). These results indicate that BNIP3 plays a growth suppressive effect on tumor cell growth in a manner dependent on its ability to bind LC3 and/or ATF4 but also in a way that is independent of either of these activities. These data demonstrate that BNIP3 is sufficient to suppress growth of HepG2 tumor cells, in a manner partially dependent on its interaction with ATF4 and/or intact mitophagy. In line with the effects of WT and W18A on OCR and ECAR described above, we postulate that the intermediate growth

suppressive phenotype of BNIP3-W18A-expressing cells may be explained by interactions of BNIP3 with other binding partners that are involved in the regulation of cell death, such as Bcl-X_L or Bcl-2. Due to the involvement of W18 in the interaction of BNIP3 with both ATF4 and LC3, we cannot currently separate their roles in modulating cell growth properties.

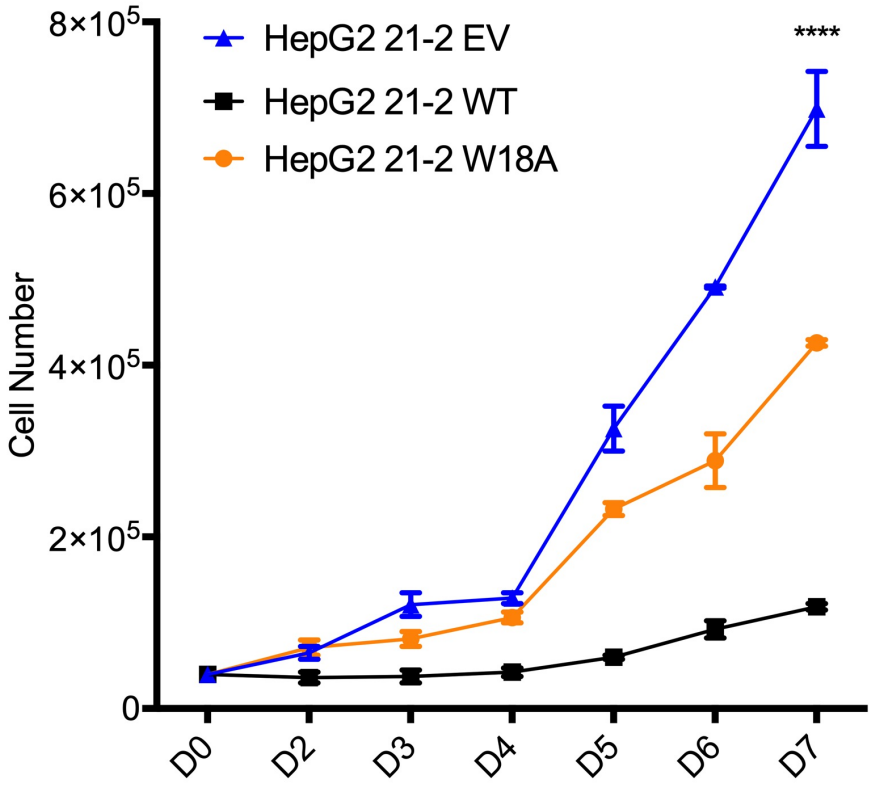

Figure 5.6 Overexpression of BNIP3-WT suppresses growth of HepG2, while BNIP3-W18A exhibits an intermediate growth suppressive effect. Growth curves of HepG2-ΔBNIP3 cells overexpressing EV, HA-BNIP3-WT, or HA-BNIP3-W18A. Cells were seeded at a density of $4x10^4$ cells and counted in duplicate for 6 days (****p<0.0001).

BNIP3 suppresses de novo serine and glycine biosynthesis

Our studies thus far have indicated a role for BNIP3 in suppressing ATF4-mediated transcriptional responses to metabolic stress by sequestering ATF4 at the mitochondria and promoting its turnover by mitophagy. However, BNIP3 over-expression is able to suppress growth of HepG2 tumor cells (and other cell types) in nutrient replete conditions suggesting that the functional consequences of the BNIP3-ATF4 interaction on cell growth are not dependent on nutrient deprivation. Since ATF4 is known to promote cell survival and tumor growth by promoting *de novo* amino acid biosynthesis and BNIP3 suppresses both cell growth and ATF4 target gene expression, we hypothesized that BNIP3 was in part suppressing tumor cell growth by limiting de novo amino acid biosynthesis. To test this hypothesis, we performed unbiased metabolomic glucose and glutamine carbon flux analysis on HepG2-ΔBNIP3 cells overexpressing BNIP3-WT or BNIP3-W18A under steady state conditions and compared incorporation of labeled carbon into different amino acids and other metabolites compared to control EV HepG2-ΔBNIP3 cells. Cells were grown in uniformly ^{3}C-labeled carbon sources, [U-^{13}C] D-glucose and [U-^{13}C] L-glutamine. Relative incorporation of ^{13}C derived from either ^{13}C-glucose or ^{13}C-glutamine was assessed by mass spectrometry in a collaboration with the UT Southwestern Medical Center Metabolomics Facility.

BNIP3-WT-expressing cells exhibited reduced flux of glucose-derived carbon to the TCA cycle, consistent with the reduction in mitochondrial respiration that we previously observed in these cells. However, the most significant differences were observed in the flux of labeled carbon from glucose to the amino acids serine and glycine, which was suppressed in cells expressing BNIP3-WT cells compared to control EV cells or to cells expressing BNIP3-W18A, which exhibited comparable levels of ^{13}C enrichment into serine and glycine to control EV cells (Figure 5.7). Serine and glycine are non-essential amino acids which are generated in cells by *de novo* biosynthesis from glycolytic intermediates.[113] In addition, *de novo* serine and glycine biosynthesis generates essential precursors for the synthesis of other cellular components, such

as nucleotides, lipids, and proteins, the production of which are crucial for sustaining the proliferation of cancer cells.[113,175,176] Of interest to our work, *de novo* serine biosynthesis is an ATF4-regulated process that involves transcription of several key metabolic enzymes, several of which have been shown to be upregulated or amplified in cancer (see Chapter 1).[116,150,151,177] Our findings indicate that BNIP3 may act to suppress tumor cell growth under basal conditions by suppressing the biosynthesis of serine and glycine. Furthermore, such a mechanism could underlie the observed epigenetic silencing or gene deletion of BNIP3 in advanced stages of various cancers.

A

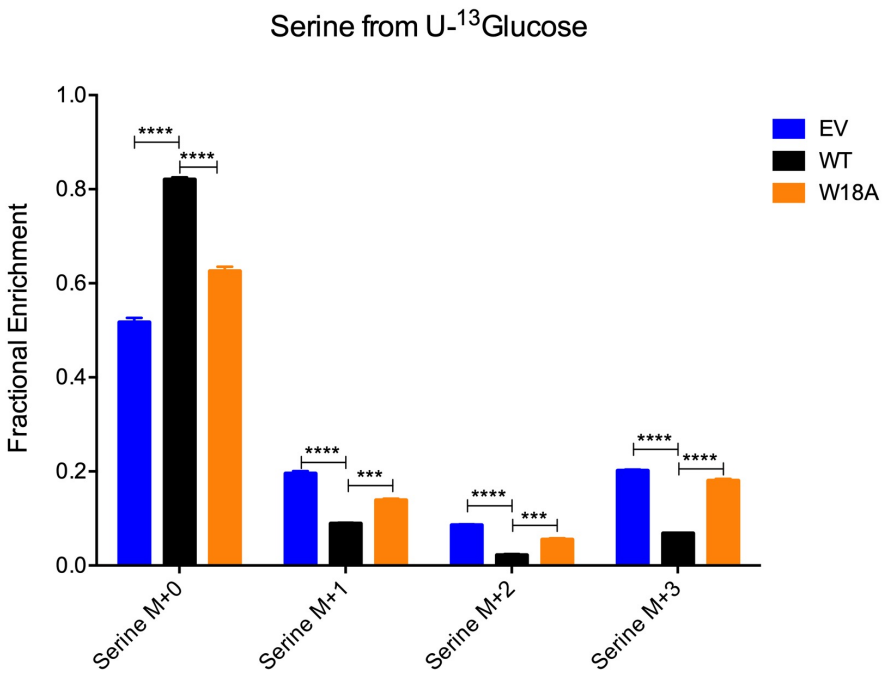

B

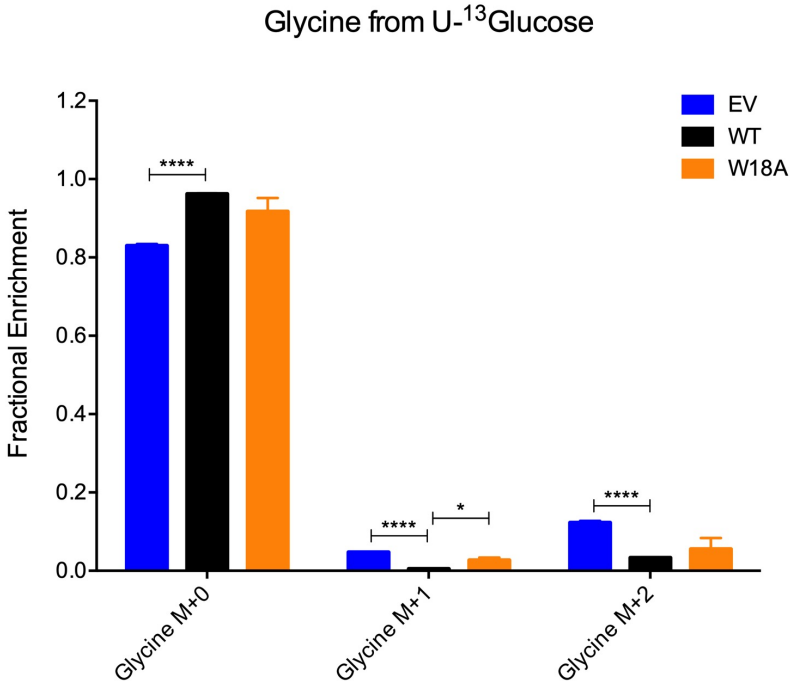

Figure 5.7 Overexpression of BNIP3-WT suppresses glucose-derived carbon flux to serine and glycine. Fractional enrichment of [U-^{13}C] D-glucose flux to A) serine and B) glycine in HepG2-ΔBNIP3 cells stably overexpressing EV, BNIP3-WT, or BNIP3-W18A. Each cell line was plated in triplicate. (*p<0.05, ***p<0.001, ****p<0.0001)

To determine whether the observed reduction in glucose-derived carbon flux to serine and glycine was linked to altered ATF4 target gene expression patterns, we performed qPCR on cDNA derived from RNA extracted from HepG2 cells grown under full media or under starvation conditions. We measured expression levels of ATF4 target genes encoding metabolic enzymes functioning in serine synthesis (*PSAT1, PHGDH,* and *PSPH*), conversion of serine to glycine (SHMT2), as well as those involved in the related pathways of mitochondrial folate/1C metabolism, cysteine biosynthesis, and redox homeostasis (*MTHFD2, CTH,* and *xCT*). For all of these targets, BNIP3-WT-expressing cells significantly suppressed expression compared to control EV HepG2-ΔBNIP3 cells to those cells expressing exogenous BNIP3-W18A (Figure 5.8). In contrast to our previous findings for other ATF4 target genes, this suppressive effect of BNIP3 on ATF4 target gene expression was independent of nutrient stress, with BNIP3-WT suppressing these biosynthetic genes under both basal full media and under nutrient deprivation with KRH (Figure 5.8). In cells lacking BNIP3 or expressing BNIP3-W18A, *PHGDH,* which encodes the rate-limiting enzyme for serine synthesis and is amplified in human cancers, exhibited a 3-fold and 5-fold induction under full media and starvation compared to BNIP3-WT-expressing cells, respectively (Figure 5.8). In addition to corroborating the findings from the carbon tracing studies, these findings suggests that in HepG2 liver cancer cells, BNIP3 functions to suppress the expression of metabolic enzymes that would otherwise ensure biosynthesis of amino acids and other macromolecules, such as nucleotides, and antioxidants. This effect was even more pronounced under nutrient starvation conditions, particularly in the expression of *MTHFD2*, *CTH,* and *xCT,* which were suppressed by approximately 3-, 5-, and 4-fold in BNIP3-WT cells, respectively (Figure 5.8). These genes are involved in the generation of nucleotides, cysteine, and glutathione and play particularly important functions for cell survival.[117,165,174,175,178] These are mitochondrial pathways that may also induce mitochondrial stress and impact cell function under prolonged nutrient stress. It is possible that this process is

negatively regulated by BNIP3 and mitophagy to limit mitochondrial proteostasis and/or as part of a mitochondrial stress response.

Complementary qPCR analysis on primary hepatocytes showed similar results, with BNIP3-WT suppressing expression some ATF4 target genes involved in serine and glycine biosynthesis and transport, under fasted conditions only (Figure 5.9). Specifically, statistically significant differences were observed for *PSPH, PHGDH, MTHFD2*, and *CTH,* with BNIP3-WT-expressing cells showing a 1.5-2-fold decrease in expression compared to control EV-cells and BNIP3-W18A-expressing cells (Figure 5.9). These differences were less substantial than those observed in HepG2s. Also in contrast to the HepG2s, BNIP3-WT did not appear to suppress serine biosynthesis genes under fed conditions. This is most likely explained by the fact that primary hepatocytes are non-transformed and non-dividing cells that are less dependent on *de novo* synthesis of amino acids, while tumor cells require metabolic reprogramming, including upregulation of *de novo* amino acid synthesis to meet their proliferative demands, regardless of extracellular nutrient status.[176,177]

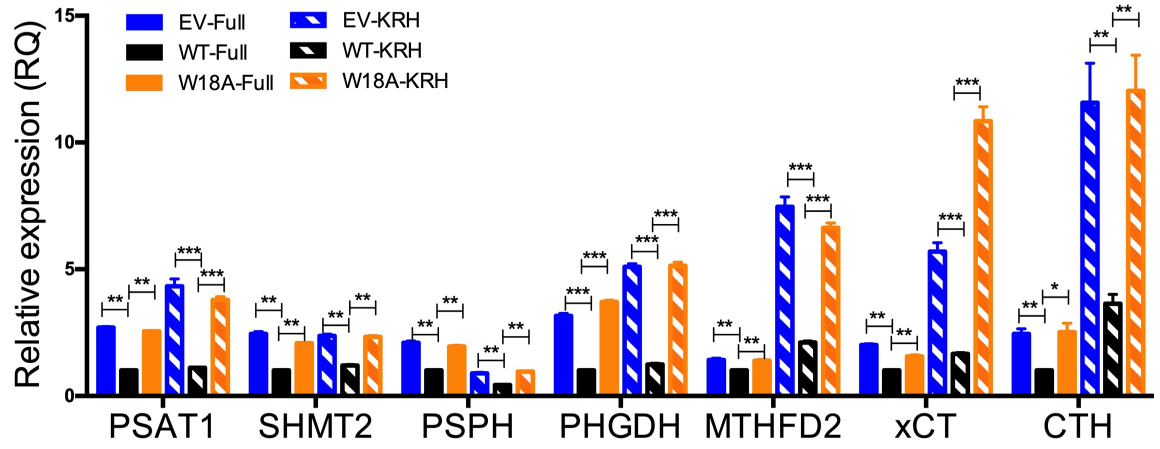

Figure 5.8 BNIP3-WT suppresses expression of genes involved in *de novo* serine and glycine synthesis in HepG2 cancer cells independent of nutrient status. Quantitative PCR of serine/glycine synthesis pathway genes on cDNA from HepG2-ΔBNIP3 cells stably overexpressing EV, BNIP3-WT, or BNIP3-W18A in full or KRH starvation buffers for 16hrs. Normalized to levels of human β-actin. Gene exprerelative to WT-Full. (*p<0.05, **p<0.01, ***p<0.001)

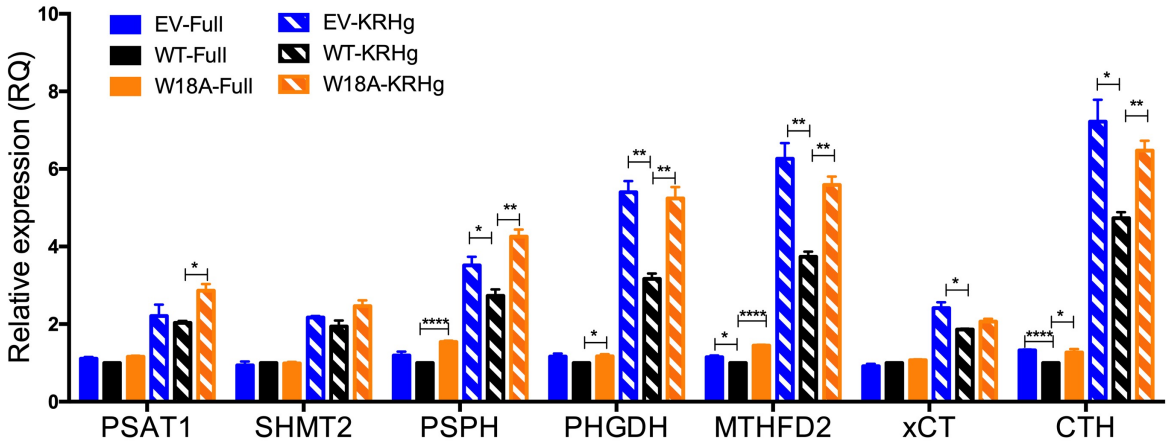

Figure 5.9 BNIP3-WT suppresses expression of genes involved in *de novo* serine and glycine synthesis in fasted primary murine hepatocytes. Quantitative PCR of ATF4 target genes on cDNA from primary BNip3 null hepatocytes infected with EV or overexpressing BNIP3-WT or BNIP3-W18A, ± KRHg for 16 hrs. Normalized to levels of mouse β-actin. Gene expression was relative to WT-Full. (*p<0.05, **p<0.01, ***p<0.001, ****p<0.0001)

BNIP3 plays a role in suppressing the mitochondrial stress response in the fasted mouse liver and in human HepG2 cancer cells

Thus far, our studies have largely focused on the role of BNIP3 in suppressing the amino acid stress response mediated by ATF4 at a transcriptional level in the nucleus. Given the role of both BNIP3 and ATF4 in responding to cellular and microenvironmental stresses, and the emerging role of ATF4 in mediating the mitochondrial unfolded protein response (UPR^{mt}), we postulated that BNIP3 may also regulate the ATF4-mediated transcriptional response to mitochondrial stress. Our findings above suggest a particularly important function for BNIP3 in suppressing expression of genes involved biosynthetic pathways taking place in the mitochondria. In response to mitochondrial stress, ATF4 was shown to upregulate expression of genes involved in amino acid biosynthesis, the mitochondrial 1C pathway, and redox balance.[124,125,132] Furthermore, numerous studies have linked UPR^{mt} to amino acid deprivation.[120,124,166,179] As *bona fide* mitochondrial stress target genes have yet to be described as regulated by ATF4, we chose to examine the expression of the mammalian homologs of genes previously shown to be upregulated by *atfs-1* (the worm homolog of ATF4) during the UPR^{mt} in *C. elegans*: *Cox1/mtCO1, CytB, Hsp60, Uqcrc1, Atp5a1, Cox4i1, Hmox1, Sdha, Lonp1, Hspa9, Ndufs3, Slc25a15*[180]. We measured expression of these genes in livers from fed and fasted wild-type and BNip3 null mice. In response to starvation, we observed significantly increased expression (2-fold) of nearly all of these genes in BNip3 null livers compared to wild-type controls (Figure 5.10). No difference was observed under fed conditions, implying that loss of BNip3 does not induce a mitochondrial stress gene signature in the absence of nutrient deprivation.

In complementary studies, we examined the expression of mitochondrial stress response genes (*COX4I1, SDHA, HSPD1, TFAM, HMOX1, SLC25A15, HSPA9, MT-ND5, MT-CO1, MT-CYB*, and *ATP5A1*) in HepG2s overexpressing BNIP3-WT or BNIP3-W18A

compared to control EV cells, under basal conditions (Figure 5.11). We found significantly decreased levels of all mitochondrial stress genes tested in BNIP3-WT-expressing cells compared to control EV cells or to those expressing exogenous BNIP3-W18A (Figure 5.11). This result indicates that in the absence of an extrinsic stressor such as nutrient deprivation, these cells exhibit evidence of a mitochondrial stress response in the absence of BNIP3 and BNIP3-mediated interaction with LC3 and/or ATF4. Mitochondrial stress and dysfunction induced by mitochondrial toxins have been shown to activate mitophagy in a manner involving the UPR^{mt} and ATFS-1 in worms and ATF4 in mammalian cells.[125,127] Ablation of *dct-1*, a homolog of BNIP3, has been shown to abrogate this mitochondrial stress response in worms, indicating an essential role for mitophagy coordinating proper mitochondrial function.[127,129]

Although these mitochondrial stress response genes have not been defined as ATF4 targets in mammalian cells as yet, the suppression of their transcript levels by BNIP3 suggests a future set of experiments to determine whether ATF4 can be detected at these promoters and if ATF4 promoter occupancy is reduced by BNIP3 over-expression. Furthermore, three of the genes (*MT-ND5, MT-CO1, MT-CYB*) suppressed by BNIP3-WT in HepG2s are encoded in the mitochondrial genome. While this result could be due to reduced mitochondrial content as a function of BNIP3-mediated mitophagy, we cannot rule out that BNIP3 also suppresses the ability of ATF4 to bind mitochondrial gene promoters. As ATFS-1 has been shown to regulate mitochondrial gene transcription in worms, ATF4 may have a similar function in mammalian cells.[180] Given these data, we hypothesize that induction of ATF4 may be a response to mitochondrial stress caused by nutrient deprivation, and BNIP3-WT functions to dampen this mechanism via turnover of mitochondria and ATF4 through mitophagy. Alternatively, loss of BNIP3-WT may itself induce a mitochondrial stress signature that promotes nuclear localization and activation of ATF4, contributing to tumor cell proliferation.

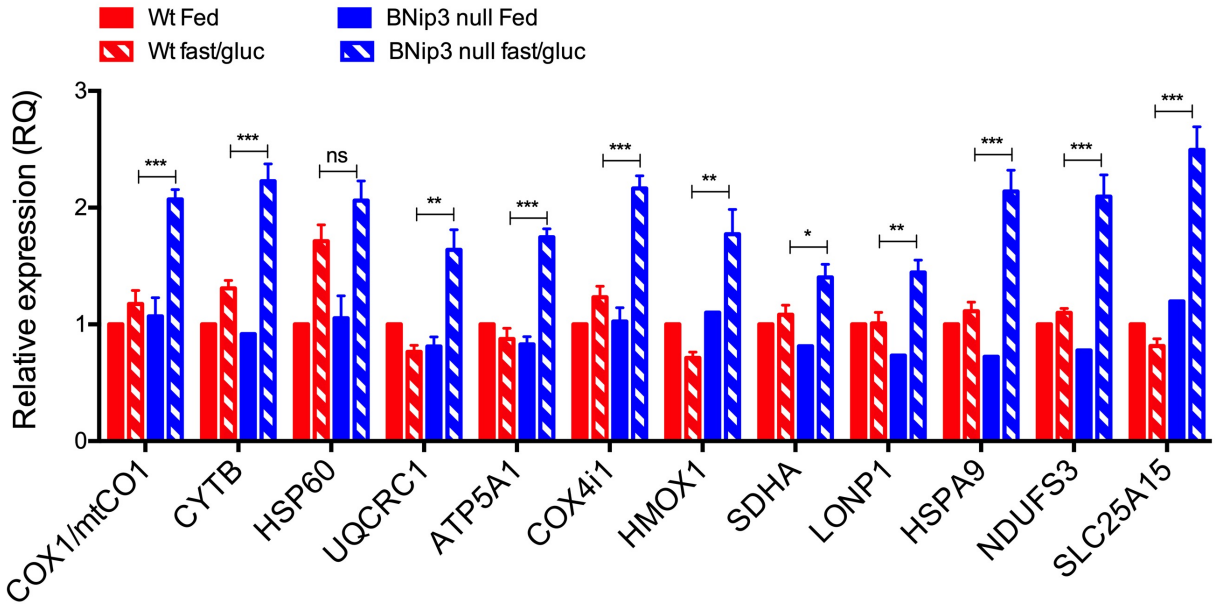

Figure 5.10 Mitochondrial stress genes are upregulated in the BNip3 null mouse liver following fasting. Quantitative PCR of mitochondrial stress genes on cDNA from livers of fed and 24h fasted/glucagon-injected wild-type or BNip3 null mice. Normalized to levels of β-actin. Gene expression was relative to WT Fed. (*p<0.05, **p<0.01, ***p<0.001)

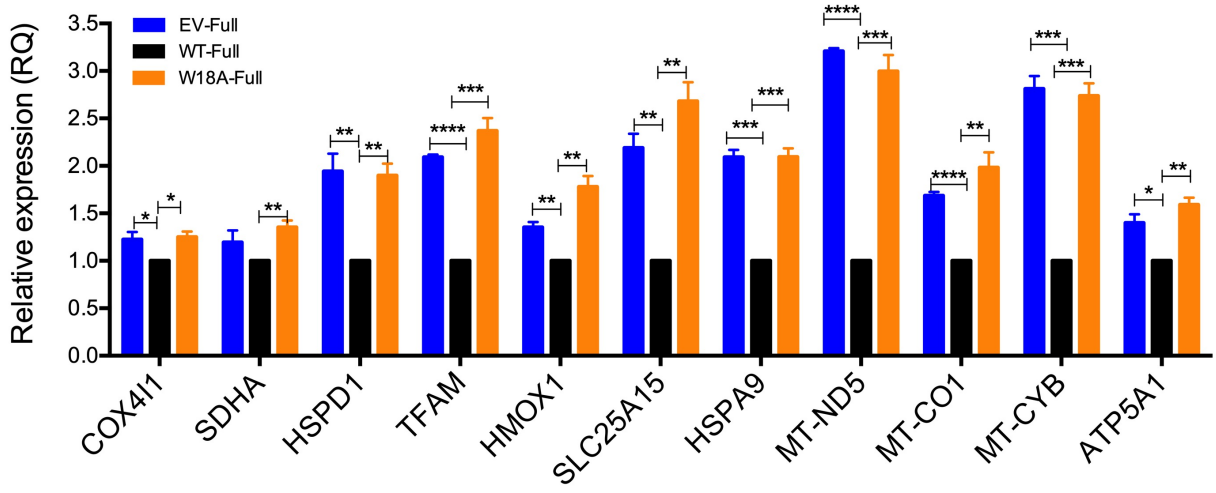

Figure 5.11 BNIP3 suppresses mitochondrial stress response genes in HepG2 cells under basal conditions. Quantitative PCR of mitochondrial stress genes on cDNA from HepG2-ΔBNIP3 cells stably overexpressing EV, BNIP3-WT, or BNIP3-W18A and incubated in ± KRH for 16 hrs. Normalized to levels of human β-actin. Gene exprerelative to WT-Full. (*p<0.05, **p<0.01, ***p<0.001, ****p<0.0001)

Subcellular localization of ATF4 in primary human tumors

Our data reveal a novel interaction between ATF4, BNIP3, and LC3 occurring at perinuclear mitochondria undergoing turnover by mitophagy (Chapter 4 and 5). While it is possible that our findings are tissue-specific and reflect the unique architecture of the mitochondria-rich liver, we sought to determine what the underlying basis of the altered localization of ATF4 to the nucleus or mitochondria. We compared the Cell Signaling Technology (CST) ATF4 antibody (cat# 11815S) primarily used for our studies to another commercially available antibody from Abcam (cat# ab184909). According to the manufacturers, the CST antibody recognizes a region at the C-terminus of ATF4, centered near the isoleucine residue at position 338, while the Abcam antibody recognizes an epitope within the first 85 amino acids at the N-terminus (Figure 5.12 A).

We exogenously overexpressed WT-ATF4-GFP in 293T cells transiently overexpressing EV, Full length WT-ATF4-GFP, ATF4 Δ10-85, or ATF4ΔN334-351 and performed western blot analyses, probing for GFP and with both the CST and Abcam ATF4 antibodies. Consistent with information provided by the manufacturers, the Abcam antibody failed to recognize the form of ATF4 carrying an amino-terminal truncation, and conversely, the CST antibody did not recognize the C-terminus truncation mutant (Figure 5.12 B). As expected, the GFP antibody recognized the WT and truncated versions of ATF4. Furthermore, only the GFP and CST antibodies recognized two different molecular weight bands of ATF4 while the Abcam antibody recognized the higher molecular weight band (Figure 5.12 B). From these data, we concluded that the Abcam antibody preferentially recognizes the full-length form of ATF4 while the CST antibody is able to recognize both the full-length form of ATF4 and a form of ATF4 not seen by the Abcam antibody that is likely missing its amino terminus. As the WT-ATF4-GFP plasmid encodes one ATF4 cDNA and displays two bands by western blot, the modification is likely the result of either proteolytic cleavage of ATF4 located between amino acids 10 and 85 or due to an alternative translational initiation of ATF4 downstream of amino acid 85.

Given that the Abcam antibody exclusively recognizes the nuclear form of ATF4 while the CST antibody recognizes the mitochondrial form of ATF4, we realized the opportunity to exploit these antibodies to assess the significance of nuclear versus mitochondrial ATF4 in vivo for human tumor progression. Initially, we tested this hypothesis using a test Tumor Microarray (TMA) that included representative cases of breast, prostate, lung, bladder and colorectal cancers. Consistent with our prior observations in hepatocytes, the CST ATF4 antibody exhibited a predominantly mitochondrial staining pattern in representative sections of breast cancer and CRC (Figure 5.12 C). In contrast, the Abcam ATF4 antibody almost exclusively stained the nuclei in these samples (Figure 5.12 C). Of note, some mitochondrial staining was detectable in the CRC tumor section probed with the Abcam ATF4 antibody, and likewise some nuclear staining was observed with the CST antibody (Figure 5.12 C).. However, the subcellular localization of ATF4 appeared more dichotomous in the breast cancer sample, with little to no staining of the mitochondria by the Abcam antibody or of the nucleus by the CST antibody (Figure 5.12 C). This observation may be due to tissue specific differences and/or clinical characteristics such as tumor stage/grade. Additionally, there may be molecular characteristics impacting the ATF4 staining patterns observed, such as loss of BNIP3.

These observations indicate that these two different forms of ATF4 are indeed detectable in human tumors and may be indicative of a functional role for each form in disease characteristics. Of particular importance, this finding bears clinical relevance in human tumors, in which the predominant localization of ATF4 could inform prognosis and treatment strategies.

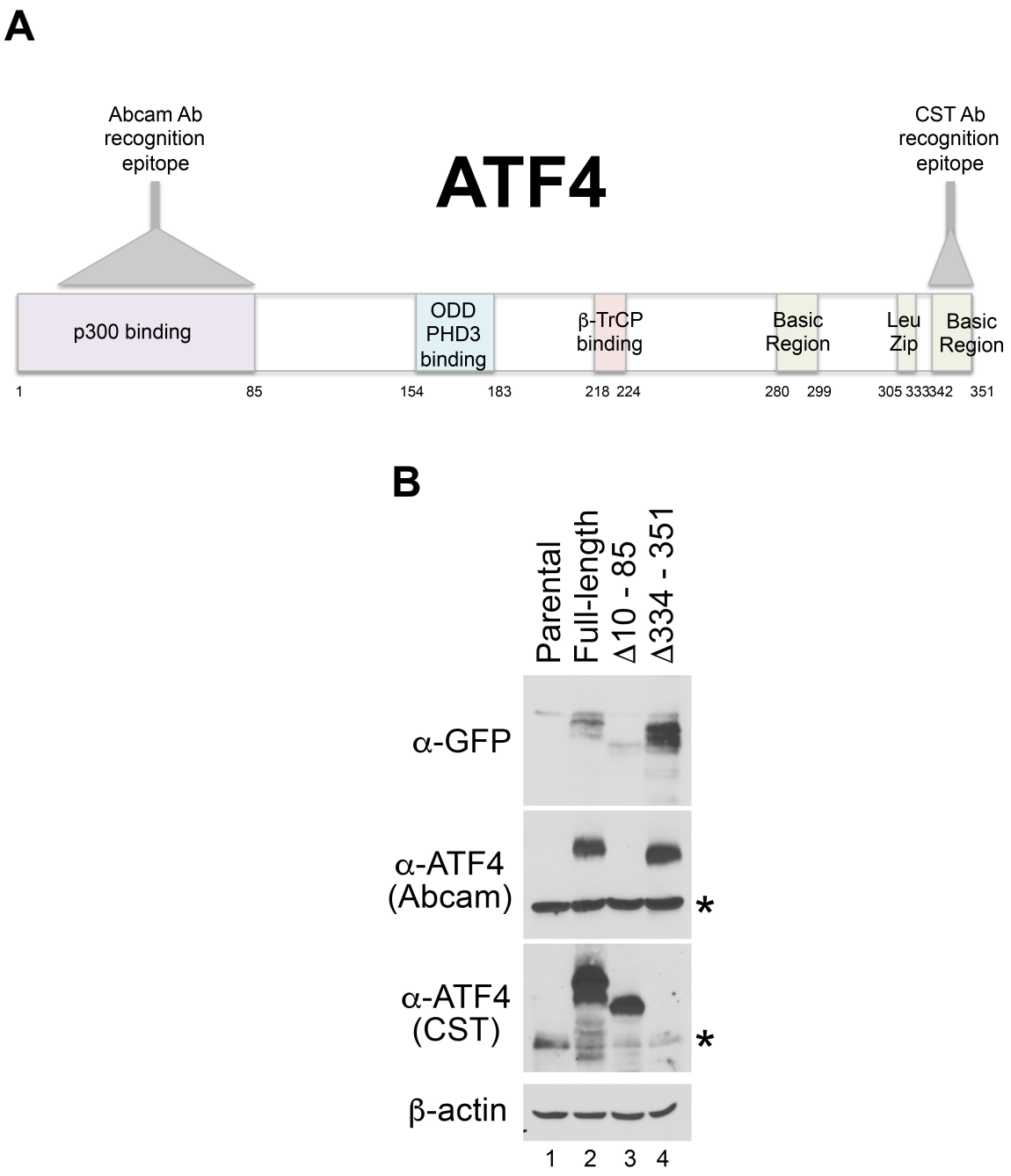

Figure 5.12 Subcellular localization of ATF4 in human tumors: comparison of two commercially available antibodies. A) Schematic of ATF4 structure with known domains and epitopes recognized by ATF4 antibodies from Abcam and Cell Signaling Technology (CST). B) Western blot analysis of 293T cells transiently overexpressing EV, Full length ATF4-GFP, ATF4 Δ10-85, or ATF4ΔN334-351 and probed with antibodies against GFP and ATF4. C) Immunohistochemistry comparing Abcam ATF4 and CST ATF4 antibodies in patient samples of breast and colorectal cancer.

C

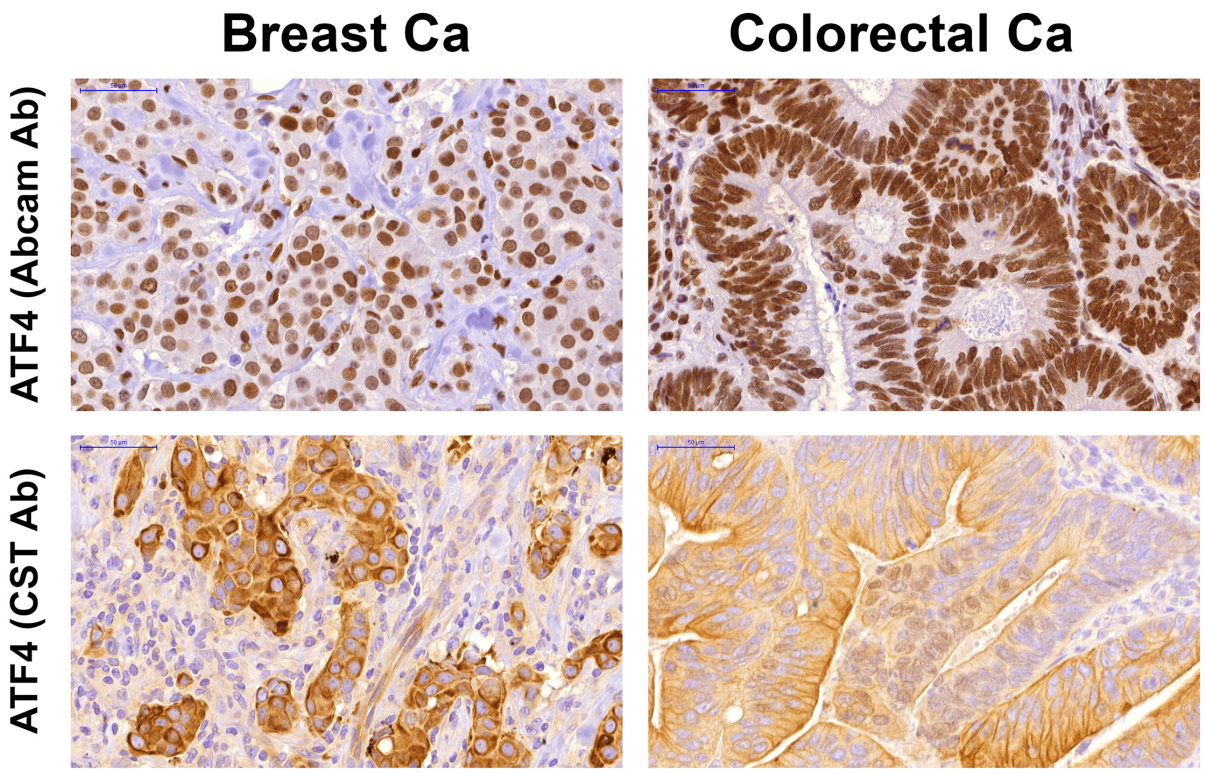

Figure 5.12 (continued).

Conclusions

In this chapter, we interrogated the BNIP3-ATF4 interaction and its consequences for mitochondrial function, metabolism, and tumor cell growth. Our initial experiments focused on further characterizing the interaction of BNIP3 and ATF4 through pulldown assays in 293T cells. Treatment with BafA1 resulted in an increased pulldown of BNIP3 with ATF4, potentially due to accumulation of input BNIP3. This result could also indicate that BNIP3-ATF4 complexes are turned over by autophagy. To investigate a potential function in autophagy, we examined whether LC3 mediated the interaction of ATF4 with BNIP3, given that the W18A mitophagy mutant ablates the interaction of BNIP3 with both proteins. LC3 did indeed coimmunoprecipitate with ATF4 in a manner that increased upon autophagy inhibition. LC3 pulldown was greatest with co-expression of BNIP3-WT and BafA1 treatment. Furthermore, we found that overexpression of BNIP3-WT was sufficient to decrease input levels of ATF4 relative to cells expressing no BNIP3 (EV). Thus, while BNIP3 is not required for the interaction of ATF4 and LC3, it is sufficient to promote their interaction and may also be involved in mediating the turnover of ATF4 at mitophagosomes.

In complementary immunofluorescence studies, primary mouse hepatocytes exhibited colocalization of endogenous LC3 with ATF4, and of ATF4 with Lamp1, which is significantly enhanced when BNIP3-WT is overexpressed and under conditions of starvation and/or autophagy inhibition. Furthermore, while BNIP3-WT was not required for LC3 trafficking to the cytosol in response to nutrient deprivation, it did promote LC3 turnover and mitophagy in response to nutrient deprivation. In conjunction with our previous findings of BNIP3-mediated mitochondrial localization of ATF4, these data indicate that BNIP3-WT, but not EV or BNIP3-W18A, is sufficient to significantly promote the localization of ATF4 at mitophagosomes. Specifically, these mitophagosomes reside in the perinuclear region of the cell, which may bear functional relevance. For example, ROS produced at perinuclear mitochondria have been linked to hypoxia-induced nuclear gene transcription.[181] As BNIP3 is a hypoxia-inducible gene target,

this could function as a feed-forward mechanism to promote the continued expression of BNIP3 under conditions of nutrient stress. Additionally, the specific turnover of perinuclear mitochondria could be a mechanism to counteract the unrestrained accumulation of damaging ROS at these mitochondria. We assessed levels of ATF4 autophagy gene targets (*ATG5, ULK1*, and *LC3*) and found no differences in control EV, BNIP3-WT-, or BNIP3-W18A-expressing cells under starvation, indicating that the BNIP3-mediated increase in mitophagy is occurring at the post-translational level (data not shown).

While we found that ATF4, BNIP3, and LC3 may interact together in a tri-molecular complex, pulldown assays in 293TΔLC3 cells revealed that LC3 is dispensable for the interaction between ATF4 and BNIP3. We cannot exclude the possibility that another LC3-family protein, such as GABARAP or GATE-16, can compensate for loss of LC3 and form a complex with ATF4 and BNIP3. Absence of LC3 did result in increased levels of total ATF4 and BNIP3 input protein, confirming that these proteins are indeed turned over by autophagy.

Our remaining functional studies focused primarily on the significance of the BNIP3-ATF4 interaction to cancer cell growth properties. In HepG2s, we found that BNIP3-WT suppressed oxygen consumption rates (OCR) relative to cells expressing EV or BNIP3-W18A, with BNIP3-W18A-expressing cells exhibiting an intermediate OCR. EV-expressing cells exhibited significantly increased extracellular acidification rates relative to both WT- and BNIP3-W18A. BNIP3-WT dramatically suppressed cell growth, consistent with prior work in our laboratory supporting a tumor suppressor function for BNIP3. Again, BNIP3-W18A had an intermediate growth phenotype. These findings are most likely explained by intact interactions of BNIP3 with other proteins, which could be enhanced or diminished in the absence of interactions with LC3 and ATF4.

Other factors contributing to the cell growth phenotype may be related to the effects of ATF4 on amino acid biosynthesis. Indeed, in HepG2s, glucose-derived carbon flux to serine and glycine was suppressed in BNIP3-WT-expressing cells compared to EV or BNIP3-W18A. ATF4

gene targets encoding metabolic enzymes involved in *de novo* serine and glycine synthesis and other mitochondrial biosynthetic pathways were suppressed in BNIP3-WT-expressing cells, independent of nutrient status. In contrast, starvation was required to observe the same phenotype in primary hepatocytes, which may be due to the fact that cancer cells are transformed and rapidly proliferating. Similarly, BNIP3-dependent mitochondrial stress gene signatures were observed only under fasted conditions in mouse livers, while this phenotype was present in HepG2 cancer cells under basal growth conditions.

Our studies have defined a novel function for ATF4 at the mitochondria, in contrast to the literature indicating that ATF4 localizes primarily to the nucleus. Our comparison of ATF4 truncation mutants with probing by two different antibodies indicate that there may be two forms of ATF4 resulting from proteolysis or some other post-translational modification. This finding bore clinical significance in primary human tumors, in which immunohistochemical staining showed predominantly nuclear staining by one antibody and mitochondrial staining by the other. We postulate that a specific, modified form of ATF4 is sequestered at mitochondria by BNIP3, where it also interacts with LC3 at mitophagosomes. Given that our studies have consistently shown in the absence of BNIP3-WT, ATF4 is almost exclusively nuclear, BNIP3 is likely involved in the modification of ATF4. We predict that this interaction dampens the adaptive functions of ATF4 as a nuclear transcription factor in response to nutrient deprivation and mitochondrial stress, thereby suppressing tumor growth.

CHAPTER 6

DISCUSSION

Summary and significance

The work presented in this thesis demonstrates a previously unknown function for ATF4 at mitochondria and reveal that it interacts with LC3 and BNIP3 in a tri-molecular complex that is turned over by autophagy. In addition to the novel functions we have identified for ATF4, we provide new mechanistic insight into the tumor suppressive functions of BNIP3. We identify a role for BNIP3 and mitophagy in modulating amino acid homeostasis, suppressing critical biosynthetic pathways that would otherwise fuel cell growth and survival. Our findings also suggest a link between BNIP3-mediated mitophagy and the suppression of mitochondrial stress responses, likely mediated by ATF4.

BNIP3 is highly expressed in metabolic tissues such as the liver, where our laboratory has previously established a crucial function for BNIP3 in regulating mitophagy and lipid metabolism. In Chapter 3, we investigated a broader role for BNIP3 in modulating metabolism with unbiased transcriptome profiling of livers from fed and fasted BNip3 null and wild-type mice. We identified a role for BNip3 in the suppression of genes involved in amino acid biosynthesis in the fasted state, finding that several of the most significantly upregulated genes in livers from BNip3 null fasted mice were targets of the nuclear transcription factor ATF4. Using both *ex vivo* and *in vitro* systems, we demonstrated that BNIP3 was both necessary and sufficient to suppress ATF4 target gene expression specifically in response to starvation. Furthermore, we observed that loss of BNip3 plays a role in modulating the promoter occupancy of known ATF4 target genes in the liver.

In Chapter 4, we sought to identify the mechanism by which BNip3 modulated ATF4 transcriptional activity. In primary mouse wild-type hepatocytes, we observed mitochondrial localization of endogenous ATF4, a novel finding. By contrast, BNip3 null hepatocytes exhibited

predominantly nuclear ATF4, indicating that BNip3 suppresses the localization of ATF4 at the nucleus through sequestration at mitochondria. This was supported by further studies indicating that BNIP3 coimmunoprecipitates with ATF4 in a manner dependent on a functional LIR motif, with mutation of W18 to alanine abrogating this interaction. Overexpression of WT-BNIP3 in BNip3 null hepatocytes suppressed nuclear localization and promoted mitochondrial localization of ATF4, while control EV cells and BNIP3-W18A-expressing cells exhibited nearly exclusive nuclear ATF4. Consistent with the inhibition of ATF4 nuclear localization, qPCR analysis revealed that only WT-BNIP3 promoted the suppression of ATF4 target genes in fasted hepatocytes. Given the significance of ATF4 in the promotion of growth and BNIP3 in the suppression of growth, we sought to extend these findings to cancer cells. Indeed, HepG2 liver cancer cells also exhibited significantly decreased expression of ATF4 target genes in a manner that depended on BNIP3-WT, under starvation conditions. Together, these data demonstrated the functional significance of ATF4 sequestration away from the nucleus to the mitochondria, in response to nutrient starvation.

In Chapter 5, we interrogated the functional consequences of this BNIP3-ATF4 interaction for mitophagy, cellular metabolism, and cell growth. Coimmunoprecipitation experiments revealed that ATF4 also interacted with LC3 in a manner that did not require BNIP3, but was enhanced by BNIP3-WT and not BNIP3-W18A. Thus, BNIP3, ATF4, and LC3 interact in a tri-molecular complex that is turned over by autophagy. Consistent with this finding, we confirmed that ATF4 colocalizes to LC3 and LAMP1, and thus mitophagosomes, in a BNIP3-dependent manner and that BNIP3 promotes the cytosolic trafficking of ATF4 and LC3 independent of nutrient stress. Further analysis of mitochondrial function in HepG2 cancer cells indicated that BNIP3 suppressed oxygen consumption and extracellular acidification rates. BNIP3 significantly attenuated the growth of HepG2 tumor cells in manner partially dependent on its ability to bind LC3 and/or ATF4. Supporting this growth suppressive function for BNIP3, carbon-tracing analysis revealed that HepG2ΔBNIP3 cells overexpressing BNIP3-WT exhibited

significantly reduced glucose-derived carbon flux to the amino acids serine and glycine. Gene expression analysis further corroborated this finding, indicating that BNIP3 suppresses expression of metabolic enzymes (established ATF4 target genes) involved in *de novo* serine/glycine biosynthesis, 1C metabolism, and redox homeostasis in a manner dependent on its ability to bind LC3 and/or ATF4. Furthermore, BNIP3 plays a role in suppressing the mitochondrial stress response in human HepG2 cancer cells under basal conditions, thus linking mitophagy, and possibly its interaction with ATF4, to the mitochondrial stress response in tumor cell proliferation. Finally, we challenge the prevailing notion that ATF4 is solely a nuclear protein and provide evidence that there are two forms of ATF4 that localize predominantly to either the nucleus or mitochondria, and show that each form is detected in a human TMA.

Together, the above-described work provides evidence of a novel function for BNIP3 in the sequestration of ATF4 at mitochondria to limit *de novo* amino acid biosynthesis in response to nutrient stress. This work expands our understanding of the mechanistic basis for the functions of BNIP3 and mitophagy in metabolism and cell proliferation. Furthermore, we describe a novel role for ATF4 at the mitochondria and the existence of a tri-molecular complex comprised of ATF4, BNIP3, and LC3 at mitophagosomes that has functional consequences for rates of mitophagy, mitochondrial function, cellular metabolism, and cell growth. This work has led to the generation of a model depicting the relationship between BNIP3 and ATF4 during nutrient stress (Figure 6.1). This model involves the coordinated induction of ATF4 as a rapid response to nutrient stress followed by a delayed suppression of ATF4 via BNIP3. As part of the AAR, ATF4 is quickly upregulated at the translational level and induces the expression of metabolic enzymes involved in amino acid biosynthesis, and potentially proteins involved in the mitochondrial stress response. These genes promote metabolic adaptation through the *de novo* synthesis of amino acids and subsequent generation of macromolecules that fuel cell growth and survival. BNIP3 expression is delayed due to its transcriptional upregulation in response to stress and sequesters ATF4 at mitochondria through an as-yet unknown mechanism, where it

binds BNIP3 and LC3 in a tri-molecular complex. This limits the AAR response during prolonged nutrient stress, instead promoting growth arrest and eventually, cell death. Of note, ATF4 activity is often increased in human tumors and associated with growth promotion, while BNIP3 has putative tumor suppressor functions and is silenced in progression to invasive cancer. Thus, loss of BNIP3 in cancer would confer a greater capacity for metabolic adaption and a growth advantage through the uncontrolled ATF4-mediated stress response.

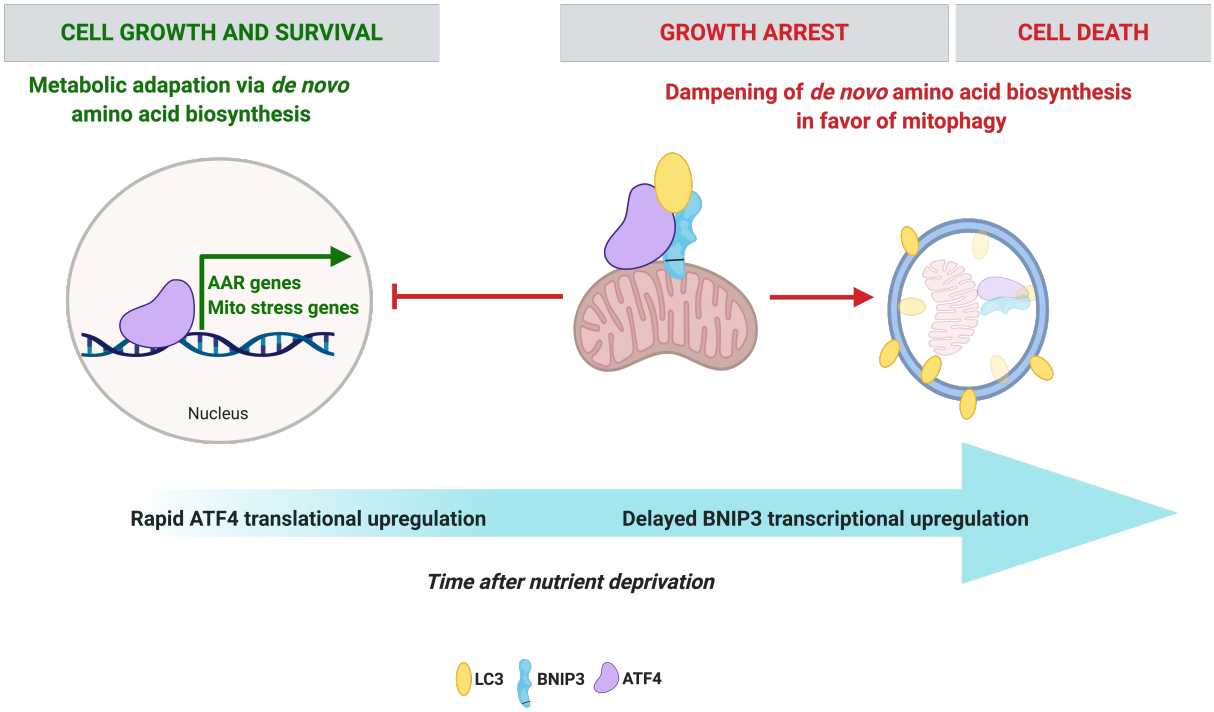

Figure 6.1 Proposed model for role of BNIP3 in modulating ATF4 localization and activity in response to nutrient stress. ATF4 is rapidly translationally upregulated in response to nutrient deprivation and induces the transcription of genes involved in the amino acid response and mitochondrial stress response. These genes promote metabolic adaptation through the *de novo* synthesis of amino acids and generation of macromolecules that fuel cell growth and survival. BNIP3 expression is delayed due to its transcriptional upregulation in response to stress and sequesters ATF4 at mitochondria through an as-yet unknown mechanism, where it binds BNIP3 and LC3 in a trimolecular complex and is targeted for degradation via mitophagy. This limits the AAR response during prolonged nutrient stress, instead promoting growth arrest and eventually, cell death. Thus, loss of BNIP3 in cancer would confer a greater capacity for metabolic adaption and a growth advantage through the uncontrolled ATF4 stress response.

How does BNIP3-mediated turnover of ATF4 at mitophagosomes contribute to overall energetic homeostasis?

In addition to implications for tumor biology, our model suggests a critical homeostatic function for BNIP3 in normal physiology. We postulate that during prolonged nutrient deprivation in non-dividing cells such as hepatocytes in the liver, BNIP3 dampens the *de novo* synthesis of macromolecules in favor of the more energetically favorable mechanism of autophagy. In Chapter 5, we described the unexpected finding that BNIP3 promotes increased protein levels and cytosolic trafficking of LC3. In conjunction with other preliminary work from our laboratory, this indicates that in addition to its function as a mitophagy receptor, BNIP3 may play a broader role in promoting general autophagy. In this way, the functions of BNIP3 are three-fold: 1) to reduce mitochondrial mass, 2) to sequester ATF4 at mitochondria and turn off the nuclear response to stress, and 3) to rapidly generate amino acids and maintain energy homeostasis through the catabolic processes of mitophagy/autophagy. To test this hypothesis, a future experiment could utilize pulse-chase metabolite tracing experiments using isotype-labeled nutrients (glucose and amino acids) in HepG2ΔBNIP3 cells overexpressing BNIP3-WT or BNIP3-W18A, compared to control EV cells. These studies would involve labeling cells in media containing ^{13}C and ^{15}N- uniformly labeled amino acids and ^{13}C-labeled glucose, followed by chasing in cold media and starvation in KRH buffer or full nutrient media in the presence or absence of the autophagy inhibitor BafA1. We would then analyze incorporation of labeled nutrients into amino acids using mass spectrometry to determine if BNIP3 is affecting the replenishment of amino acids via autophagy vs. *de novo* synthesis through ATF4.

What is the function of ATF4 at mitochondria?

The findings we present here support a growing body of literature proposing that ATF4 is a mammalian homolog of ATFS-1, mediating a cytoprotective transcriptional program in response to mitochondrial stress.[124,125,132] In *C. elegans*, this mechanism involves mitochondrial-

to-nuclear communication to coordinate the metabolic rewiring required to cope with mitochondrial proteotoxic stress (Chapter 1). In addition to its function as a nuclear transcription factor, ATFS-1 localizes to the mitochondria via a mitochondrial target sequencing that when cleaved in the mitochondria, initiates its proteolytic degradation; the efficiency of mitochondrial targeting of ATFS-1 dictates the extent of its nuclear functions.[126,180] However, ATFS-1 was also shown to exert transcriptional regulation of mtDNA to repress the expression of OXPHOS genes.[180] We observed that ATF4 localizes to both the nucleus and the mitochondria, and that there may exist two different molecular weight forms of ATF4 that are detectable in cells and in human tumors. It is possible that ATF4 also maintains a conserved function in the transcriptional regulation of mtDNA that involves a modified form of the protein, but this has yet to be demonstrated in the literature.

Other nuclear proteins and transcription factors have been recently shown to regulate mitochondrial DNA synthesis, replication, and transcription, such as p53 and MDM2.[182,183] Of interest to our work, in response to oxidative stress and serine deprivation, MDM2 is recruited to chromatin independently of p53 where it interacts with ATF4 to promote transcription of genes involved in amino acid and redox homeostasis.[184] More recently, MDM2 was also shown to localize to the mitochondrial matrix where it represses transcription of the complex I subunit MT-ND6, inhibiting mitochondrial respiration.[182] Furthermore, enhancing the levels of mitochondrial MDM2 in tumor cells increased their motility and invasiveness.[182]

Given the increasingly broad array of functions for nuclear proteins in mediating cellular stress responses at mitochondria, it is possible that ATF4 also possesses a similar function. This would be a further example of mitochondrial-to-nuclear signaling in mammalian cells. This hypothesis could be tested in primary mouse hepatocytes as well as HepG2 cells with chromatin immunoprecipitation of ATF4-bound mtDNA using the CST ATF4 antibody under conditions of nutrient deprivation, followed by sequencing of the mtDNA fragments that are pulled down. The regulation of the OXPHOS genes *MT-ND5, MT-CO1,* and *MT-CYB* is of

particular interest, as we observed that they were significantly suppressed by BNIP3-WT in HepG2s (Chapter 5). While this result could be due to reduced mitochondrial content as a function of BNIP3-mediated mitophagy, we cannot rule out that BNIP3 also suppresses the ability of ATF4 to bind to these specific mitochondrial gene promoters. This could indicate that similar to ATFS-1 in worms, ATF4 may act as a transcriptional repressor of OXPHOS genes in response to stress, and that BNIP3-WT sequesters ATF4 at mitochondria to promote this second function. This would be consistent with the significant decrease in oxygen consumption rates that we observed in BNIP3-WT-expressing cells (Chapter 5). If ATF4 does not act as part of the mitochondrial transcription machinery, it is possible that it plays a role in mtDNA quality control and repair, synthesis, replication, or apoptosis, as has been shown for p53.[183]

What is the function of ATF4 in autophagy?

In Chapter 5, we described our finding that ATF4 is turned over by autophagy in a manner that is dependent on BNIP3. While the proteasomal degradation of ATF4 is well-established in the literature, it has not been shown to be turned over by autophagy until now. Furthermore, we did not observe differences in gene expression of autophagy target genes (*ULK1, ATG5, LC3*) previously shown to be transcriptionally regulated by ATF4, although this could be an artifact of the timepoint used for starvation. Our surprising finding that ATF4 interacts with LC3 may be indicative of an additional function for ATF4 in regulating autophagy that also serves as a negative feedback mechanism to turn off the ISR. In addition, it is possible that like BNIP3, ATF4 acts as a cargo adaptor and may itself be facilitating the interaction between BNIP3 and LC3, and their subsequent turnover through autophagy. Furthermore, because it lacks a mitochondrial targeting sequence, the localization of ATF4 may be a consequence of its interaction with a mitochondrial protein (BNIP3) and LC3.

A search of the iLIR Database, a web resource which uses an *in silico* algorithm to predict LIR motifs based on protein sequence, indicates that ATF4 possesses two predicted LIR

motifs within its amino terminus at residues 35-40 (amino acid sequence DDYLEV) and residues 59-64 (SEWLAV).[185] The presence of these predicted motifs at the amino terminus is significant, as this is the portion of ATF4 that we hypothesize is modified in order to localize to mitochondria (where it is recognized by the CST ATF4 antibody, as described in Chapter 5). Mutation of the tyrosine or tryptophan residues in these motifs and subsequent pulldown assays with LC3 would allow us to determine whether one or both are a *bona fide* LIR motif and address whether ATF4 may be an autophagy cargo adaptor. It would then be necessary to address whether the ability of ATF4 to bind LC3 is required for the interaction of BNIP3 with LC3, and BNIP3 with ATF4.

How does BNIP3 regulate the mitochondrial-nuclear shuttling of ATF4?

The colocalization studies described in Chapter 5 revealed striking differences in LC3 and ATF4 trafficking that was dependent on overexpression of BNIP3-WT. BNIP3-WT was sufficient to promote trafficking of LC3 and ATF4 to puncta outside of the nucleus under fed conditions. Our results indicated that overexpression of BNIP3-WT under basal conditions phenocopies the effects of nutrient deprivation on LC3 localization, in a manner that promotes the colocalization with ATF4. In addition to implications for functions of ATF4 and BNIP3 in general autophagy, this finding is suggestive of a possible mechanism for the nucleocytoplasmic shuttling of ATF4 via LC3. LC3 has been previously observed in the nucleus in an acetylated form that redistributes to the cytoplasm in response to nutrient deprivation as a result of its de-acetylation by the nuclear deacetylase Sirt1.[167] This shuttling of LC3 depends on its interaction with the nuclear protein DOR (also known as TP53INP2).[167] Intriguingly, BNIP3 expression and subsequent mitophagy have also been shown to be promoted through the deacetylation of FOXO3, albeit by Sirt3, in response to oxidative stress.[186]

Further studies examining the acetylation of LC3 in the presence or absence of BNIP3 would determine whether BNIP3 is required to promote the de-acetylation of LC3, thereby

promoting its cytoplasmic shuttling. Sirtuins are NAD^+-dependent, and as NAD^+ pools are increased during energy stress such as starvation, the deacetylase activity of sirtuins is tightly attuned to the energy status of the cell.[187,188] Mitophagy is also induced by replenishment of NAD+, including expression of the BNIP3 homolog *dct-1* in worms.[130,189] It is possible that BNIP3 is itself induced by increased NAD^+ pools and acts in a positive feedback mechanism to maintain high NAD^+ under nutrient starvation through modulation of metabolic pathways, such as the TCA cycle. In this manner, BNIP3 could impact the deacetylation of LC3, regulate its transport to the cytoplasm, and promote autophagy. If BNIP3 does in fact regulate this shuttling, it may explain how ATF4 traffics to mitophagosomes, particularly if the interaction of ATF4 and LC3 is mediated by a functional LIR motif, as discussed above.

One of the limitations from this work is in our use of exogenous overexpression of BNIP3 to study effects on endogenous ATF4. As BNIP3 is constitutively expressed in this setting, the effects we observed on ATF4 localization and suppression of target gene expression likely do not reflect the kinetics of this mechanism under actual physiological conditions. A timecourse study examining the induction of ATF4 target gene expression and mitophagosomal localization in wild-type primary hepatocytes (expressing endogenous BNip3) compared to BNip3 null hepatocytes would shed light on how BNIP3 mediates its effects on ATF4. Such an experiment would involve KRH starvation for shorter timepoints (i.e. 30 minutes-1 hr) and extended timepoints (i.e. 12 hrs-24 hrs). We would expect to see nuclear localization of ATF4 at early timepoints of starvation, with a gradual shift towards mitochondrial localization during prolonged starvation due to the delayed transcriptional upregulation of BNip3.

Are the growth suppressive functions of BNIP3 dependent on ATF4?

As discussed in Chapter 1, the majority of studies in the field have indicated a tumor-promoting function for ATF4. This is largely due to its function in *de novo* amino acid biosynthesis of amino acids such as asparagine, serine, and glycine, which also aid in the

generation of the macromolecules required to sustain rapidly proliferating tumors under microenvironmental stress.[87,143] Conversely, we and others have observed growth suppressive properties BNIP3, previously thought to be due to a function in promoting cell death, but more recently established to involve its role as a mitophagy receptor.[28] Our finding that BNIP3 interacts with ATF4 at mitochondria to dampen *de novo* amino acid biosynthesis suggests another mechanism by which BNIP3 limits cell proliferation. In addition, we have also identified two putative forms of ATF4 that predominantly localize to either the nucleus or mitochondria in a manner depending on BNIP3. We propose that BNIP3 dampens the pro-growth functions of ATF4 by sequestering a specific form of ATF4 at mitochondria and turning it over by mitophagy. As discussed earlier, we also do not exclude the possibility that ATF4 may possess tumor-suppressive functions at the mitochondria, such as in the transcriptional repression of OXPHOS genes in mtDNA. Evidence for such a function exists in the literature, with opposing oncogenic nuclear and apoptotic mitochondrial functions described for the related protein ATF2.[161,190]

In order to test the hypothesis that BNIP3 regulates tumor growth in a manner dependent on its interaction with mitochondrial ATF4, we propose the generation of ATF4 mutants specifically targeted to the mitochondria or nucleus through deletion of the amino terminus or the carboxy terminus as described in Chapter 5. These constructs would then be overexpressed in HepG2ΔBNIP3ΔATF4 cells lacking both endogenous BNIP3 and ATF4. If the putative ATF4 LIR motifs described earlier prove to be functional and promote mitochondrial localization, this construct could be used in place of a larger amino terminus deletion. Subsequent overexpression of BNIP3-WT or BNIP3-W18A would then allow us to determine whether the growth-suppressive effects of BNIP3 are due to its interaction with ATF4 at the mitochondria, and whether this is dependent on the function of BNIP3 as a mitophagy receptor. We would expect overexpression of a nuclear-specific form of ATF4 to prevent the growth-suppressive functions of BNIP3. In addition, separating the nuclear and mitochondrial forms of

ATF4 could allow us to tease apart the function of BNIP3 in mitophagy from its interaction with ATF4, which remains a limitation of the work presented here.

Does BNIP3 regulate an ATF4-mediated mitochondrial stress response?

In Chapter 5, we identified a putative function for endogenous BNIP3 in suppressing the expression of mitochondrial stress response genes in the liver in response to fasting, and for exogenous BNIP3 in HepG2 liver cancer cells under basal conditions. This was an unexpected finding, as mitophagy has been shown to be induced alongside the UPR^{mt}, although the majority of this work was performed in worms.[129,130,180] However, this could be explained by induction of a negative feedback loop to turn off the UPR^{mt} and/or could be a reflection of disrupted kinetics due to our use of exogenous overexpression (in the case of the HepG2s). In non-pathological settings, such as in the liver, activating cytoprotective mechanisms such as the UPR^{mt} would be beneficial for preserving proper homeostatic function and health. However, evidence suggests that prolonged basal activation of the UPR^{mt} and mitophagy is tumor-promoting, enabling cancer cells to continuously cope with oxidative stress and metastasize.[191–193] In contrast, we and others have shown that mitophagy can function to promote turnover of mitochondria in response to stress, thereby limiting the excess accumulation of otherwise damaging ROS, and slowing tumor progression.[28,51] These two opposing functions for mitophagy in the regulation of mitochondrial stress in cancer may be explained by tissue specific differences, the specific oncogenes involved, and other genetic differences. Given the delayed transcriptional induction of BNIP3, we expect that while BNIP3-mediated mitophagy might initially be upregulated in response to stress, its interaction with ATF4 may also function as a negative feedback mechanism to restrain the continued activation of the UPR^{mt}. If ATF4 does indeed function similarly to ATFS-1, with nuclear and mitochondrial roles in transcriptional regulation, BNIP3 would disrupt the mitonuclear communication needed to maintain a sustained UPR^{mt}.

Similar to our hypothesis that BNIP3 functions in a delayed manner to dampen the nuclear functions of ATF4, we propose that BNIP3 acts in a similar manner to dampen the mitochondrial stress response in cancer cells. To test this hypothesis, we must first establish whether ATF4 transcriptionally regulates the putative UPR^{mt} genes examined in Chapter 5. These include both nuclear- and mitochondrial-encoded transcripts and could be accomplished using chIP-seq. Leveraging the mitochondrial- and nuclear-targeted ATF4 constructs described above would enable us to determine whether the mitochondrial interaction of ATF4 with BNIP3 is able to suppress the expression of UPR^{mt} genes in response to a variety of mitochondrial toxins, such as uncoupling agents and mitochondrial translation inhibitors. Elucidating such a mechanism would provide further evidence that ATF4 is a mammalian homolog for ATFS- that elicits unrestrained cytoprotective tumor-promoting stress responses in the context of BNIP3 loss.

REFERENCES

1. Kroemer, G., Mariño, G. & Levine, B. Autophagy and the integrated stress response. *Mol. Cell* **40**, 280–293 (2010).

2. Weidberg, H., Shvets, E. & Elazar, Z. Biogenesis and cargo selectivity of autophagosomes. *Annu. Rev. Biochem.* **80**, 125–156 (2011).

3. Kuma, A. *et al.* The role of autophagy during the early neonatal starvation period. *Nature* **432**, 1032–1036 (2004).

4. Komatsu, M. *et al.* Impairment of starvation-induced and constitutive autophagy in Atg7-deficient mice. *J. Cell Biol.* **169**, 425–434 (2005).

5. Green, D. R. & Levine, B. To be or not to be? How selective autophagy and cell death govern cell fate. *Cell* **157**, 65–75 (2014).

6. Russell, R. C. *et al.* ULK1 induces autophagy by phosphorylating Beclin-1 and activating VPS34 lipid kinase. *Nat. Cell Biol.* **15**, 741–750 (2013).

7. Mizushima, N. *et al.* A protein conjugation system essential for autophagy. *Nature* **395**, 395–398 (1998).

8. Youle, R. J. & Narendra, D. P. Mechanisms of mitophagy. *Nat. Rev. Mol. Cell Biol.* **12**, 9–14 (2011).

9. Tanida, I., Ueno, T. & Kominami, E. LC3 and Autophagy. *Methods Mol. Biol. Clifton NJ* **445**, 77–88 (2008).

10. Rabinowitz, J. D. & White, E. Autophagy and metabolism. *Science* **330**, 1344–1348 (2010).

11. Bowman, E. J., Siebers, A. & Altendorf, K. Bafilomycins: a class of inhibitors of membrane ATPases from microorganisms, animal cells, and plant cells. *Proc. Natl. Acad. Sci. U. S. A.* **85**, 7972–7976 (1988).

12. Galluzzi, L. *et al.* Autophagy in malignant transformation and cancer progression. *EMBO J.* **34**, 856–880 (2015).

13. Roy, S. & Debnath, J. Autophagy and Tumorigenesis. *Semin. Immunopathol.* **32**, 383–396 (2010).

14. Mathew, R. *et al.* Autophagy suppresses tumor progression by limiting chromosomal instability. *Genes Dev.* **21**, 1367–1381 (2007).

15. Liang, X. H. *et al.* Induction of autophagy and inhibition of tumorigenesis by beclin 1. *Nature* **402**, 672–676 (1999).

16. Yue, Z., Jin, S., Yang, C., Levine, A. J. & Heintz, N. Beclin 1, an autophagy gene essential for early embryonic development, is a haploinsufficient tumor suppressor. *Proc. Natl. Acad. Sci. U. S. A.* **100**, 15077–15082 (2003).

17. Karantza-Wadsworth, V. *et al.* Autophagy mitigates metabolic stress and genome damage in mammary tumorigenesis. *Genes Dev.* **21**, 1621–1635 (2007).

18. Takamura, A. *et al.* Autophagy-deficient mice develop multiple liver tumors. *Genes Dev.* **25**, 795–800 (2011).

19. Fung, C., Lock, R., Gao, S., Salas, E. & Debnath, J. Induction of autophagy during extracellular matrix detachment promotes cell survival. *Mol. Biol. Cell* **19**, 797–806 (2008).

20. Sharifi, M. N. *et al.* Autophagy Promotes Focal Adhesion Disassembly and Cell Motility of Metastatic Tumor Cells through the Direct Interaction of Paxillin with LC3. *Cell Rep.* **15**, 1660–1672 (2016).

21. White, E., Mehnert, J. M. & Chan, C. S. Autophagy, Metabolism, and Cancer. *Clin. Cancer Res.* **21**, 5037–5046 (2015).

22. Guo, J. Y. *et al.* Autophagy suppresses progression of K-ras-induced lung tumors to oncocytomas and maintains lipid homeostasis. *Genes Dev.* **27**, 1447–1461 (2013).

23. Strohecker, A. M. & White, E. Autophagy promotes BrafV600E-driven lung tumorigenesis by preserving mitochondrial metabolism. *Autophagy* **10**, 384–385 (2014).

24. Yang, S. *et al.* Pancreatic cancers require autophagy for tumor growth. *Genes Dev.* **25**, 717–729 (2011).

25. Perera, R. M. *et al.* Transcriptional control of autophagy-lysosome function drives pancreatic cancer metabolism. *Nature* **524**, 361–365 (2015).

26. Rosenfeldt, M. T. *et al.* p53 status determines the role of autophagy in pancreatic tumour development. *Nature* **504**, 296–300 (2013).

27. Amaravadi, R. K., Kimmelman, A. C. & Debnath, J. Targeting Autophagy in Cancer: Recent Advances and Future Directions. *Cancer Discov.* **9**, 1167–1181 (2019).

28. Chourasia, A. H. *et al.* Mitophagy defects arising from BNip3 loss promote mammary tumor progression to metastasis. *EMBO Rep.* **16**, 1145–1163 (2015).

29. Humpton, T. J. *et al.* Oncogenic KRAS Induces NIX-Mediated Mitophagy to Promote Pancreatic Cancer. *Cancer Discov.* **9**, 1268–1287 (2019).

30. Ahn, C. S. & Metallo, C. M. Mitochondria as biosynthetic factories for cancer proliferation. *Cancer Metab.* **3**, 1 (2015).

31. Madrigal-Matute, J. & Cuervo, A. M. Regulation of Liver Metabolism by Autophagy. *Gastroenterology* **150**, 328–339 (2016).

32. Chourasia, A. H., Boland, M. L. & Macleod, K. F. Mitophagy and cancer. *Cancer Metab.* **3**, 4 (2015).

33. Pickrell, A. M. & Youle, R. J. The roles of PINK1, parkin, and mitochondrial fidelity in Parkinson's disease. *Neuron* **85**, 257–273 (2015).

34. Drake, L. E., Springer, M. Z., Poole, L. P., Kim, C. J. & Macleod, K. F. Expanding perspectives on the significance of mitophagy in cancer. *Semin. Cancer Biol.* **47**, 110–124 (2017).

35. Sandoval, H. *et al.* Essential role for Nix in autophagic maturation of erythroid cells. *Nature* **454**, 232–235 (2008).

36. Vande Velde, C. *et al.* BNIP3 and genetic control of necrosis-like cell death through the mitochondrial permeability transition pore. *Mol. Cell. Biol.* **20**, 5454–5468 (2000).

37. Guo, K. *et al.* Hypoxia induces the expression of the pro-apoptotic gene BNIP3. *Cell Death Differ.* **8**, 367–376 (2001).

38. Glick, D. *et al.* BNip3 regulates mitochondrial function and lipid metabolism in the liver. *Mol. Cell. Biol.* **32**, 2570–2584 (2012).

39. Ney, P. A. Mitochondrial autophagy: Origins, significance, and role of BNIP3 and NIX. *Biochim. Biophys. Acta* **1853**, 2775–2783 (2015).

40. Springer, M. Z. & Macleod, K. F. In Brief: Mitophagy: mechanisms and role in human disease. *J. Pathol.* **240**, 253–255 (2016).

41. Ray, R. *et al.* BNIP3 Heterodimerizes with Bcl-2/Bcl-XL and Induces Cell Death Independent of a Bcl-2 Homology 3 (BH3) Domain at Both Mitochondrial and Nonmitochondrial Sites. *J. Biol. Chem.* **275**, 1439–1448 (2000).

42. Yasuda, M., Theodorakis, P., Subramanian, T. & Chinnadurai, G. Adenovirus E1B-19K/BCL-2 interacting protein BNIP3 contains a BH3 domain and a mitochondrial targeting sequence. *J. Biol. Chem.* **273**, 12415–12421 (1998).

43. Boyd, J. M. *et al.* Adenovirus E1B 19 kDa and Bcl-2 proteins interact with a common set of cellular proteins. *Cell* **79**, 341–351 (1994).

44. Landes, T. *et al.* The BH3-only Bnip3 binds to the dynamin Opa1 to promote mitochondrial fragmentation and apoptosis by distinct mechanisms. *EMBO Rep.* **11**, 459–465 (2010).

45. Sulistijo, E. S., Jaszewski, T. M. & MacKenzie, K. R. Sequence-specific dimerization of the transmembrane domain of the 'BH3-only' protein BNIP3 in membranes and detergent. *J. Biol. Chem.* **278**, 51950–51956 (2003).

46. Hanna, R. A. *et al.* Microtubule-associated protein 1 light chain 3 (LC3) interacts with Bnip3 protein to selectively remove endoplasmic reticulum and mitochondria via autophagy. *J. Biol. Chem.* **287**, 19094–19104 (2012).

47. Zhu, Y. *et al.* Modulation of serines 17 and 24 in the LC3-interacting region of Bnip3 determines pro-survival mitophagy versus apoptosis. *J. Biol. Chem.* **288**, 1099–1113 (2013).

48. Bruick, R. K. Expression of the gene encoding the proapoptotic Nip3 protein is induced by hypoxia. *Proc. Natl. Acad. Sci.* **97**, 9082–9087 (2000).

49. Tracy, K. *et al.* BNIP3 is an RB/E2F target gene required for hypoxia-induced autophagy. *Mol. Cell. Biol.* **27**, 6229–6242 (2007).

50. Shaw, J. *et al.* Antagonism of E2F-1 regulated Bnip3 transcription by NF-kappaB is essential for basal cell survival. *Proc. Natl. Acad. Sci. U. S. A.* **105**, 20734–20739 (2008).

51. Mammucari, C. *et al.* FoxO3 controls autophagy in skeletal muscle in vivo. *Cell Metab.* **6**, 458–471 (2007).

52. Kalas, W. *et al.* H-ras up-regulates expression of BNIP3. *Anticancer Res.* **31**, 2869–2875 (2011).

53. Wu, S.-Y. *et al.* Ras-related tumorigenesis is suppressed by BNIP3-mediated autophagy through inhibition of cell proliferation. *Neoplasia N. Y. N* **13**, 1171–1182 (2011).

54. Lee, J. M. *et al.* Nutrient-sensing nuclear receptors coordinate autophagy. *Nature* **516**, 112–115 (2014).

55. Shimizu, N. *et al.* A muscle-liver-fat signalling axis is essential for central control of adaptive adipose remodelling. *Nat. Commun.* **6**, 6693 (2015).

56. Cesari, R. *et al.* Parkin, a gene implicated in autosomal recessive juvenile parkinsonism, is a candidate tumor suppressor gene on chromosome 6q25-q27. *Proc. Natl. Acad. Sci. U. S. A.* **100**, 5956–5961 (2003).

57. Rui, L. Energy Metabolism in the Liver. *Compr. Physiol.* **4**, 177–197 (2014).

58. Czaja, M. J. *et al.* Functions of autophagy in normal and diseased liver. *Autophagy* **9**, 1131–1158 (2013).

59. Ezaki, J. *et al.* Liver autophagy contributes to the maintenance of blood glucose and amino acid levels. *Autophagy* **7**, 727–736 (2011).

60. Singh, R. *et al.* Autophagy regulates lipid metabolism. *Nature* **458**, 1131–1135 (2009).

61. Kaur, J. & Debnath, J. Autophagy at the crossroads of catabolism and anabolism. *Nat. Rev. Mol. Cell Biol.* **16**, 461–472 (2015).

62. Cholankeril, G., Patel, R., Khurana, S. & Satapathy, S. K. Hepatocellular carcinoma in non-alcoholic steatohepatitis: Current knowledge and implications for management. *World J. Hepatol.* **9**, 533–543 (2017).

63. Ni, H.-M., Williams, J. A. & Ding, W.-X. Mitochondrial dynamics and mitochondrial quality control. *Redox Biol.* **4**, 6–13 (2014).

64. Agnihotri, S. *et al.* PINK1 Is a Negative Regulator of Growth and the Warburg Effect in Glioblastoma. *Cancer Res.* **76**, 4708–4719 (2016).

65. Fujiwara, M. *et al.* Parkin as a tumor suppressor gene for hepatocellular carcinoma. *Oncogene* **27**, 6002–6011 (2008).

66. Zhang, C. *et al.* Parkin, a p53 target gene, mediates the role of p53 in glucose metabolism and the Warburg effect. *Proc. Natl. Acad. Sci.* **108**, 16259–16264 (2011).

67. Li, C. *et al.* PINK1 and PARK2 Suppress Pancreatic Tumorigenesis through Control of Mitochondrial Iron-Mediated Immunometabolism. *Dev. Cell* **46**, 441-455.e8 (2018).

68. Fei, P. *et al.* Bnip3L is induced by p53 under hypoxia, and its knockdown promotes tumor growth. *Cancer Cell* **6**, 597–609 (2004).

69. Manka, D., Spicer, Z. & Millhorn, D. E. Bcl-2/adenovirus E1B 19 kDa interacting protein-3 knockdown enables growth of breast cancer metastases in the lung, liver, and bone. *Cancer Res.* **65**, 11689–11693 (2005).

70. Tan, E. Y. *et al.* BNIP3 as a Progression Marker in Primary Human Breast Cancer; Opposing Functions in In situ Versus Invasive Cancer. *Clin. Cancer Res.* **13**, 467–474 (2007).

71. Koop, E. A. *et al.* Expression of BNIP3 in invasive breast cancer: correlations with the hypoxic response and clinicopathological features. *BMC Cancer* **9**, 175 (2009).

72. Sowter, H. M. *et al.* Expression of the cell death genes BNip3 and NIX in ductal carcinoma in situ of the breast; correlation of BNip3 levels with necrosis and grade. *J. Pathol.* **201**, 573–580 (2003).

73. Murai, M. *et al.* Aberrant methylation and silencing of the BNIP3 gene in colorectal and gastric cancer. *Clin. Cancer Res. Off. J. Am. Assoc. Cancer Res.* **11**, 1021–1027 (2005).

74. Murai, M. *et al.* Aberrant DNA methylation associated with silencing BNIP3 gene expression in haematopoietic tumours. *Br. J. Cancer* **92**, 1165–1172 (2005).

75. Okami, J., Simeone, D. M. & Logsdon, C. D. Silencing of the hypoxia-inducible cell death protein BNIP3 in pancreatic cancer. *Cancer Res.* **64**, 5338–5346 (2004).

76. Akada, M. *et al.* Intrinsic chemoresistance to gemcitabine is associated with decreased expression of BNIP3 in pancreatic cancer. *Clin. Cancer Res. Off. J. Am. Assoc. Cancer Res.* **11**, 3094–3101 (2005).

77. Erkan, M. *et al.* Loss of BNIP3 expression is a late event in pancreatic cancer contributing to chemoresistance and worsened prognosis. *Oncogene* **24**, 4421–4432 (2005).

78. Calvisi, D. F. *et al.* Mechanistic and prognostic significance of aberrant methylation in the molecular pathogenesis of human hepatocellular carcinoma. *J. Clin. Invest.* **117**, 2713–2722 (2007).

79. Abe, T. *et al.* Upregulation of BNIP3 by 5-aza-2'-deoxycytidine sensitizes pancreatic cancer cells to hypoxia-mediated cell death. *J. Gastroenterol.* **40**, 504–510 (2005).

80. Burton, T. R. *et al.* BNIP3 acts as transcriptional repressor of death receptor-5 expression and prevents TRAIL-induced cell death in gliomas. *Cell Death Dis.* **4**, e587–e587 (2013).

81. Milasta, S. *et al.* Apoptosis-inducing factor (AIF)-dependent mitochondrial function is required for T cell but not B cell function. *Immunity* **44**, 88–102 (2016).

82. Burton, T. R., Eisenstat, D. D. & Gibson, S. B. BNIP3 (Bcl-2 19 kDa interacting protein) acts as transcriptional repressor of apoptosis-inducing factor expression preventing cell death in human malignant gliomas. *J. Neurosci. Off. J. Soc. Neurosci.* **29**, 4189–4199 (2009).

83. Thompson, J. W. *et al.* Bnip3 Binds and Activates p300: Possible Role in Cardiac Transcription and Myocyte Morphology. *PLoS ONE* **10**, (2015).

84. Flick, K. & Kaiser, P. Protein Degradation and the Stress Response. *Semin. Cell Dev. Biol.* **23**, 515–522 (2012).

85. Ameri, K. & Harris, A. L. Activating transcription factor 4. *Int. J. Biochem. Cell Biol.* **40**, 14–21 (2008).

86. Wortel, I. M. N., van der Meer, L. T., Kilberg, M. S. & van Leeuwen, F. N. Surviving Stress: Modulation of ATF4-Mediated Stress Responses in Normal and Malignant Cells. *Trends Endocrinol. Metab. TEM* **28**, 794–806 (2017).

87. Kilberg, M. S., Shan, J. & Su, N. ATF4-dependent transcription mediates signaling of amino acid limitation. *Trends Endocrinol. Metab. TEM* **20**, 436–443 (2009).

88. Vattem, K. M. & Wek, R. C. Reinitiation involving upstream ORFs regulates ATF4 mRNA translation in mammalian cells. *Proc. Natl. Acad. Sci. U. S. A.* **101**, 11269–11274 (2004).

89. Lu, P. D., Harding, H. P. & Ron, D. Translation reinitiation at alternative open reading frames regulates gene expression in an integrated stress response. *J. Cell Biol.* **167**, 27–33 (2004).

90. Han, J. *et al.* ER-stress-induced transcriptional regulation increases protein synthesis leading to cell death. *Nat. Cell Biol.* **15**, 481–490 (2013).

91. Luo, S., Baumeister, P., Yang, S., Abcouwer, S. F. & Lee, A. S. Induction of Grp78/BiP by translational block: activation of the Grp78 promoter by ATF4 through and upstream ATF/CRE site independent of the endoplasmic reticulum stress elements. *J. Biol. Chem.* **278**, 37375–37385 (2003).

92. De Sousa-Coelho, A. L., Marrero, P. F. & Haro, D. Activating transcription factor 4-dependent induction of FGF21 during amino acid deprivation. *Biochem. J.* **443**, 165–171 (2012).

93. Wan, X. *et al.* ATF4- and CHOP-dependent induction of FGF21 through endoplasmic reticulum stress. *BioMed Res. Int.* **2014**, 807874 (2014).

94. Tezze, C., Romanello, V. & Sandri, M. FGF21 as Modulator of Metabolism in Health and Disease. *Front. Physiol.* **10**, (2019).

95. Dickhout, J. G. *et al.* Integrated stress response modulates cellular redox state via induction of cystathionine γ-lyase: cross-talk between integrated stress response and thiol metabolism. *J. Biol. Chem.* **287**, 7603–7614 (2012).

96. Dey, S. *et al.* ATF4-dependent induction of heme oxygenase 1 prevents anoikis and promotes metastasis. *J. Clin. Invest.* **125**, 2592–2608 (2015).

97. Suragani, R. N. V. S. *et al.* Heme-regulated eIF2α kinase activated Atf4 signaling pathway in oxidative stress and erythropoiesis. *Blood* **119**, 5276–5284 (2012).

98. Huggins, C. J. *et al.* C/EBPγ Is a Critical Regulator of Cellular Stress Response Networks through Heterodimerization with ATF4. *Mol. Cell. Biol.* **36**, 693–713 (2016).

99. Füllgrabe, J., Ghislat, G., Cho, D.-H. & Rubinsztein, D. C. Transcriptional regulation of mammalian autophagy at a glance. *J. Cell Sci.* **129**, 3059–3066 (2016).

100. Pike, L. R. G. *et al.* Transcriptional up-regulation of ULK1 by ATF4 contributes to cancer cell survival. *Biochem. J.* **449**, 389–400 (2013).

101. Rouschop, K. M. A. *et al.* The unfolded protein response protects human tumor cells during hypoxia through regulation of the autophagy genes *MAP1LC3B* and *ATG5*. *J. Clin. Invest.* **120**, 127–141 (2010).

102. B'chir, W. *et al.* The eIF2α/ATF4 pathway is essential for stress-induced autophagy gene expression. *Nucleic Acids Res.* **41**, 7683–7699 (2013).

103. Milani, M. *et al.* The Role of ATF4 Stabilization and Autophagy in Resistance of Breast Cancer Cells Treated with Bortezomib. *Cancer Res.* **69**, 4415–4423 (2009).

104. Guo, J. Y. *et al.* Autophagy provides metabolic substrates to maintain energy charge and nucleotide pools in Ras-driven lung cancer cells. *Genes Dev.* **30**, 1704–1717 (2016).

105. Fawcett, T. W., Martindale, J. L., Guyton, K. Z., Hai, T. & Holbrook, N. J. Complexes containing activating transcription factor (ATF)/cAMP-responsive-element-binding protein (CREB) interact with the CCAAT/enhancer-binding protein (C/EBP)-ATF composite site to regulate Gadd153 expression during the stress response. *Biochem. J.* **339 (Pt 1)**, 135–141 (1999).

106. Jiang, H.-Y. *et al.* Activating transcription factor 3 is integral to the eukaryotic initiation factor 2 kinase stress response. *Mol. Cell. Biol.* **24**, 1365–1377 (2004).

107. Pan, Y.-X., Chen, H., Thiaville, M. M. & Kilberg, M. S. Activation of the ATF3 gene through a co-ordinated amino acid-sensing response programme that controls transcriptional regulation of responsive genes following amino acid limitation. *Biochem. J.* **401**, 299–307 (2007).

108. Su, N. & Kilberg, M. S. C/EBP homology protein (CHOP) interacts with activating transcription factor 4 (ATF4) and negatively regulates the stress-dependent induction of the asparagine synthetase gene. *J. Biol. Chem.* **283**, 35106–35117 (2008).

109. Bröer, S. & Bröer, A. Amino acid homeostasis and signalling in mammalian cells and organisms. *Biochem. J.* **474**, 1935–1963 (2017).

110. Balasubramanian, M. N., Butterworth, E. A. & Kilberg, M. S. Asparagine synthetase: regulation by cell stress and involvement in tumor biology. *Am. J. Physiol. Endocrinol. Metab.* **304**, E789-799 (2013).

111. Chen, H., Pan, Y.-X., Dudenhausen, E. E. & Kilberg, M. S. Amino acid deprivation induces the transcription rate of the human asparagine synthetase gene through a timed program of expression and promoter binding of nutrient-responsive basic region/leucine zipper transcription factors as well as localized histone acetylation. *J. Biol. Chem.* **279**, 50829–50839 (2004).

112. Averous, J., Jousse, C., Maurin, A.-C., Bruhat, A. & Fafournoux, P. Chapter 20 - Adaptation to Amino Acid Availability: Role of GCN2 in the Regulation of Physiological

Functions and in Pathological Disorders**The authors have equally participated to this work. in *The Molecular Nutrition of Amino Acids and Proteins* (ed. Dardevet, D.) 289–303 (Academic Press, 2016). doi:10.1016/B978-0-12-802167-5.00021-9.

113. Amelio, I., Cutruzzolá, F., Antonov, A., Agostini, M. & Melino, G. Serine and glycine metabolism in cancer. *Trends Biochem. Sci.* **39**, 191–198 (2014).

114. Locasale, J. W. Serine, glycine and the one-carbon cycle: cancer metabolism in full circle. *Nat. Rev. Cancer* **13**, 572–583 (2013).

115. Gao, X. *et al.* Serine Availability Influences Mitochondrial Dynamics and Function through Lipid Metabolism. *Cell Rep.* **22**, 3507–3520 (2018).

116. DeNicola, G. M. *et al.* NRF2 regulates serine biosynthesis in non-small cell lung cancer. *Nat. Genet.* **47**, 1475–1481 (2015).

117. Ben-Sahra, I., Hoxhaj, G., Ricoult, S. J. H., Asara, J. M. & Manning, B. D. mTORC1 induces purine synthesis through control of the mitochondrial tetrahydrofolate cycle. *Science* **351**, 728–733 (2016).

118. D'Amico, D., Sorrentino, V. & Auwerx, J. Cytosolic Proteostasis Networks of the Mitochondrial Stress Response. *Trends Biochem. Sci.* **42**, 712–725 (2017).

119. Quirós, P. M., Mottis, A. & Auwerx, J. Mitonuclear communication in homeostasis and stress. *Nat. Rev. Mol. Cell Biol.* **17**, 213–226 (2016).

120. Baker, B. M., Nargund, A. M., Sun, T. & Haynes, C. M. Protective Coupling of Mitochondrial Function and Protein Synthesis via the eIF2α Kinase GCN-2. *PLOS Genet.* **8**, e1002760 (2012).

121. Melber, A. & Haynes, C. M. UPR mt regulation and output: a stress response mediated by mitochondrial-nuclear communication. *Cell Res.* **28**, 281–295 (2018).

122. Martinus, R. D. *et al.* Selective induction of mitochondrial chaperones in response to loss of the mitochondrial genome. *Eur. J. Biochem.* **240**, 98–103 (1996).

123. Zhao, Q. *et al.* A mitochondrial specific stress response in mammalian cells. *EMBO J.* **21**, 4411–4419 (2002).

124. Quirós, P. M. *et al.* Multi-omics analysis identifies ATF4 as a key regulator of the mitochondrial stress response in mammals. *J. Cell Biol.* **216**, 2027–2045 (2017).

125. Martínez-Reyes, I., Sánchez-Aragó, M. & Cuezva, J. M. AMPK and GCN2-ATF4 signal the repression of mitochondria in colon cancer cells. *Biochem. J.* **444**, 249–259 (2012).

126. Nargund, A. M., Pellegrino, M. W., Fiorese, C. J., Baker, B. M. & Haynes, C. M. Mitochondrial import efficiency of ATFS-1 regulates mitochondrial UPR activation. *Science* **337**, 587–590 (2012).

127. Sorrentino, V. *et al.* Enhancing mitochondrial proteostasis reduces amyloid-β proteotoxicity. *Nature* **552**, 187–193 (2017).

128. Beck, J. S., Mufson, E. J. & Counts, S. E. Evidence for Mitochondrial UPR Gene Activation in Familial and Sporadic Alzheimer's Disease. *Curr. Alzheimer Res.* **13**, 610–614 (2016).

129. Palikaras, K., Lionaki, E. & Tavernarakis, N. Coordination of mitophagy and mitochondrial biogenesis during ageing in C. elegans. *Nature* **521**, 525–528 (2015).

130. Fang, E. F. *et al.* NAD+ Replenishment Improves Lifespan and Healthspan in Ataxia Telangiectasia Models via Mitophagy and DNA Repair. *Cell Metab.* **24**, 566–581 (2016).

131. Fiorese, C. J. *et al.* The Transcription Factor ATF5 Mediates a Mammalian Mitochondrial UPR. *Curr. Biol. CB* **26**, 2037–2043 (2016).

132. Bao, X. R. *et al.* Mitochondrial dysfunction remodels one-carbon metabolism in human cells. *eLife* **5**, e10575 (2016).

133. Fusakio, M. E. *et al.* Transcription factor ATF4 directs basal and stress-induced gene expression in the unfolded protein response and cholesterol metabolism in the liver. *Mol. Biol. Cell* **27**, 1536–1551 (2016).

134. Maruyama, R., Shimizu, M., Li, J., Inoue, J. & Sato, R. Fibroblast growth factor 21 induction by activating transcription factor 4 is regulated through three amino acid response elements in its promoter region. *Biosci. Biotechnol. Biochem.* **80**, 929–934 (2016).

135. Münch, C. & Harper, J. W. Mitochondrial unfolded protein response controls matrix pre-RNA processing and translation. *Nature* **534**, 710–713 (2016).

136. Bouman, L. *et al.* Parkin is transcriptionally regulated by ATF4: evidence for an interconnection between mitochondrial stress and ER stress. *Cell Death Differ.* **18**, 769–782 (2011).

137. Qing, G. *et al.* ATF4 regulates MYC-mediated neuroblastoma cell death upon glutamine deprivation. *Cancer Cell* **22**, 631–644 (2012).

138. Csibi, A. *et al.* The mTORC1 pathway stimulates glutamine metabolism and cell proliferation by repressing SIRT4. *Cell* **153**, 840–854 (2013).

139. Ameri, K. *et al.* Anoxic induction of ATF-4 through HIF-1-independent pathways of protein stabilization in human cancer cells. *Blood* **103**, 1876–1882 (2004).

140. Bi, M. *et al.* ER stress-regulated translation increases tolerance to extreme hypoxia and promotes tumor growth. *EMBO J.* **24**, 3470–3481 (2005).

141. Ye, J. *et al.* The GCN2-ATF4 pathway is critical for tumour cell survival and proliferation in response to nutrient deprivation. *EMBO J.* **29**, 2082–2096 (2010).

142. Zhang, N. *et al.* Increased Amino Acid Uptake Supports Autophagy-Deficient Cell Survival upon Glutamine Deprivation. *Cell Rep.* **23**, 3006–3020 (2018).

143. Gwinn, D. M. *et al.* Oncogenic KRAS Regulates Amino Acid Homeostasis and Asparagine Biosynthesis via ATF4 and Alters Sensitivity to L-Asparaginase. *Cancer Cell* **33**, 91-107.e6 (2018).

144. Krall, A. S., Xu, S., Graeber, T. G., Braas, D. & Christofk, H. R. Asparagine promotes cancer cell proliferation through use as an amino acid exchange factor. *Nat. Commun.* **7**, 1–13 (2016).

145. Nakamura, A. *et al.* Inhibition of GCN2 sensitizes ASNS-low cancer cells to asparaginase by disrupting the amino acid response. *Proc. Natl. Acad. Sci. U. S. A.* **115**, E7776–E7785 (2018).

146. Knott, S. R. V. *et al.* Asparagine bioavailability governs metastasis in a model of breast cancer. *Nature* **554**, 378–381 (2018).

147. Toda, K. *et al.* Metabolic Alterations Caused by KRAS Mutations in Colorectal Cancer Contribute to Cell Adaptation to Glutamine Depletion by Upregulation of Asparagine Synthetase. *Neoplasia* **18**, 654–665 (2016).

148. Hettmer, S. *et al.* Functional genomic screening reveals asparagine dependence as a metabolic vulnerability in sarcoma. *Mol. Cell. Pediatr.* **2**, (2015).

149. Chen, S.-H. Asparaginase Therapy in Pediatric Acute Lymphoblastic Leukemia: A Focus on the Mode of Drug Resistance. *Pediatr. Neonatol.* **56**, 287–293 (2015).

150. Possemato, R. *et al.* Functional genomics reveal that the serine synthesis pathway is essential in breast cancer. *Nature* **476**, 346–350 (2011).

151. Locasale, J. W. *et al.* Phosphoglycerate dehydrogenase diverts glycolytic flux and contributes to oncogenesis. *Nat. Genet.* **43**, 869–874 (2011).

152. Zhao, E. *et al.* KDM4C and ATF4 Cooperate in Transcriptional Control of Amino Acid Metabolism. *Cell Rep.* **14**, 506–519 (2016).

153. Lassot, I. *et al.* ATF4 degradation relies on a phosphorylation-dependent interaction with the SCF(betaTrCP) ubiquitin ligase. *Mol. Cell. Biol.* **21**, 2192–2202 (2001).

154. Rzymski, T. *et al.* Regulation of autophagy by ATF4 in response to severe hypoxia. *Oncogene* **29**, 4424–4435 (2010).

155. Linares, J. F. *et al.* ATF4-Induced Metabolic Reprograming Is a Synthetic Vulnerability of the p62-Deficient Tumor Stroma. *Cell Metab.* **26**, 817-829.e6 (2017).

156. Hart, L. S. *et al.* ER stress-mediated autophagy promotes Myc-dependent transformation and tumor growth. *J. Clin. Invest.* **122**, 4621–4634 (2012).

157. Tameire, F. *et al.* ATF4 couples MYC-dependent translational activity to bioenergetic demands during tumour progression. *Nat. Cell Biol.* **21**, 889–899 (2019).

158. Wang, C. *et al.* Effects of ATF4 on PGC1α expression in brown adipose tissue and metabolic responses to cold stress. *Metabolism* **62**, 282–289 (2013).

159. Whitney, M. L., Jefferson, L. S. & Kimball, S. R. ATF4 is necessary and sufficient for ER stress-induced upregulation of REDD1 expression. *Biochem. Biophys. Res. Commun.* **379**, 451–455 (2009).

160. Lee, J. *et al.* Mitochondrial Cyclic AMP Response Element-binding Protein (CREB) Mediates Mitochondrial Gene Expression and Neuronal Survival. *J. Biol. Chem.* **280**, 40398–40401 (2005).

161. Lau, E. *et al.* PKCε regulates ATF2 availability to alter mitochondrial permeability following genotoxic stress. *Cell* **148**, 543–555 (2012).

162. Bhalla, K. *et al.* PGC1α promotes tumor growth by inducing gene expression programs supporting lipogenesis. *Cancer Res.* **71**, 6888–6898 (2011).

163. Vazquez, F. *et al.* PGC1α expression defines a subset of human melanoma tumors with increased mitochondrial capacity and resistance to oxidative stress. *Cancer Cell* **23**, 287–301 (2013).

164. Bost, F. & Kaminski, L. The metabolic modulator PGC-1α in cancer. *Am. J. Cancer Res.* **9**, 198–211 (2019).

165. Spinelli, J. B. & Haigis, M. C. The multifaceted contributions of mitochondria to cellular metabolism. *Nat. Cell Biol.* **20**, 745–754 (2018).

166. Johnson, M. A. *et al.* Amino Acid Starvation Has Opposite Effects on Mitochondrial and Cytosolic Protein Synthesis. *PLoS ONE* **9**, (2014).

167. Huang, R. *et al.* Deacetylation of nuclear LC3 drives autophagy initiation under starvation. *Mol. Cell* **57**, 456–466 (2015).

168. Zhang, X., Bian, X. & Kong, J. The Proapoptotic Protein BNIP3 Interacts with VDAC to Induce Mitochondrial Release of Endonuclease G. *PLOS ONE* **9**, e113642 (2014).

169. Li, Y. *et al.* Bnip3 mediates the hypoxia-induced inhibition on mammalian target of rapamycin by interacting with Rheb. *J. Biol. Chem.* **282**, 35803–35813 (2007).

170. Gao, S. *et al.* PSAT1 is regulated by ATF4 and enhances cell proliferation via the GSK3β/β-catenin/cyclin D1 signaling pathway in ER-negative breast cancer. *J. Exp. Clin. Cancer Res.* **36**, 179 (2017).

171. Pathria, G. *et al.* Targeting the Warburg effect via LDHA inhibition engages ATF4 signaling for cancer cell survival. *EMBO J.* **37**, e99735 (2018).

172. Shi, Z. *et al.* Activation of the PERK-ATF4 pathway promotes chemo-resistance in colon cancer cells. *Sci. Rep.* **9**, 1–8 (2019).

173. The Role of ATF4 Stabilization and Autophagy in Resistance of Breast Cancer Cells Treated with Bortezomib | Cancer Research. https://cancerres.aacrjournals.org/content/69/10/4415.short.

174. Daher, B. *et al.* Genetic Ablation of the Cystine Transporter xCT in PDAC Cells Inhibits mTORC1, Growth, Survival, and Tumor Formation via Nutrient and Oxidative Stresses. *Cancer Res.* **79**, 3877–3890 (2019).

175. Ye, J. *et al.* Pyruvate kinase M2 promotes de novo serine synthesis to sustain mTORC1 activity and cell proliferation. *Proc. Natl. Acad. Sci. U. S. A.* **109**, 6904–6909 (2012).

176. Dang, C. V. Essentiality of non-essential amino acids for tumour cells and tumorigenesis. *Nat. Metab.* **1**, 847–848 (2019).

177. Mattaini, K. R., Sullivan, M. R. & Vander Heiden, M. G. The importance of serine metabolism in cancer. *J. Cell Biol.* **214**, 249–257 (2016).

178. Diehl, F. F., Lewis, C. A., Fiske, B. P. & Heiden, M. G. V. Cellular redox state constrains serine synthesis and nucleotide production to impact cell proliferation. *Nat. Metab.* **1**, 861–867 (2019).

179. Harding, H. P. *et al.* An Integrated Stress Response Regulates Amino Acid Metabolism and Resistance to Oxidative Stress. *Mol. Cell* **11**, 619–633 (2003).

180. Nargund, A. M., Fiorese, C. J., Pellegrino, M. W., Deng, P. & Haynes, C. M. Mitochondrial and nuclear accumulation of the transcription factor ATFS-1 promotes OXPHOS recovery during the UPR(mt). *Mol. Cell* **58**, 123–133 (2015).

181. Al-Mehdi, A.-B. *et al.* Perinuclear Mitochondrial Clustering Creates an Oxidant-Rich Nuclear Domain Required for Hypoxia-Induced Transcription. *Sci. Signal.* **5**, ra47–ra47 (2012).

182. Arena, G. *et al.* Mitochondrial MDM2 Regulates Respiratory Complex I Activity Independently of p53. *Mol. Cell* **69**, 594-609.e8 (2018).

183. Park, J.-H., Zhuang, J., Li, J. & Hwang, P. M. p53 as guardian of the mitochondrial genome. *FEBS Lett.* **590**, 924–934 (2016).

184. Riscal, R. *et al.* Chromatin-Bound MDM2 Regulates Serine Metabolism and Redox Homeostasis Independently of p53. *Mol. Cell* **62**, 890–902 (2016).

185. Jacomin, A.-C., Samavedam, S., Promponas, V. & Nezis, I. P. iLIR database: A web resource for LIR motif-containing proteins in eukaryotes. *Autophagy* **12**, 1945–1953 (2016).

186. Tseng, A. H. H., Shieh, S.-S. & Wang, D. L. SIRT3 deacetylates FOXO3 to protect mitochondria against oxidative damage. *Free Radic. Biol. Med.* **63**, 222–234 (2013).

187. Haigis, M. C. & Guarente, L. P. Mammalian sirtuins--emerging roles in physiology, aging, and calorie restriction. *Genes Dev.* **20**, 2913–2921 (2006).

188. Cantó, C., Menzies, K. J. & Auwerx, J. NAD(+) Metabolism and the Control of Energy Homeostasis: A Balancing Act between Mitochondria and the Nucleus. *Cell Metab.* **22**, 31–53 (2015).

189. Jang, S., Kang, H. T. & Hwang, E. S. Nicotinamide-induced mitophagy: event mediated by high NAD+/NADH ratio and SIRT1 protein activation. *J. Biol. Chem.* **287**, 19304–19314 (2012).

190. Lau, E. *et al.* PKCε Promotes Oncogenic Functions of ATF2 in the Nucleus while Blocking Its Apoptotic Function at Mitochondria. *Cell* **148**, 543–555 (2012).

191. Kenny, T. C., Craig, A. J., Villanueva, A. & Germain, D. Mitohormesis Primes Tumor Invasion and Metastasis. *Cell Rep.* **27**, 2292-2303.e6 (2019).

192. Kenny, T. C., Manfredi, G. & Germain, D. The Mitochondrial Unfolded Protein Response as a Non-Oncogene Addiction to Support Adaptation to Stress during Transformation in Cancer and Beyond. *Front. Oncol.* **7**, (2017).

193. Kenny, T. C. *et al.* Selected mitochondrial DNA landscapes activate the SIRT3 axis of the UPR mt to promote metastasis. *Oncogene* **36**, 4393–4404 (2017).